SUSTech Southern University of Science and Technology

地球与空间科学系 DEPARTMENT OF EARTH AND SPACE SCIENCES

Crustal Structure

Constraints from seismic imaging technology

Speaker: Hejun Zhu

Nov 13, 2026

SIML SEISMIC IMAGING AND MONITORING LABORATORY

SUSTech Southern University of Science and Technology

Outline

- Seismology 101
- Seismic methods for crustal model building
- Global crustal structure
- Case study 1: Oklahoma crustal model (continent)
- Case study 2: Axial seamount imaging (ocean)

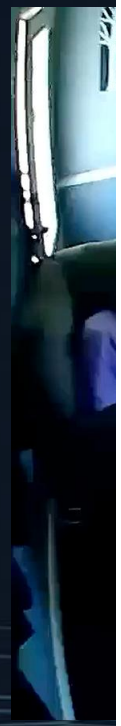


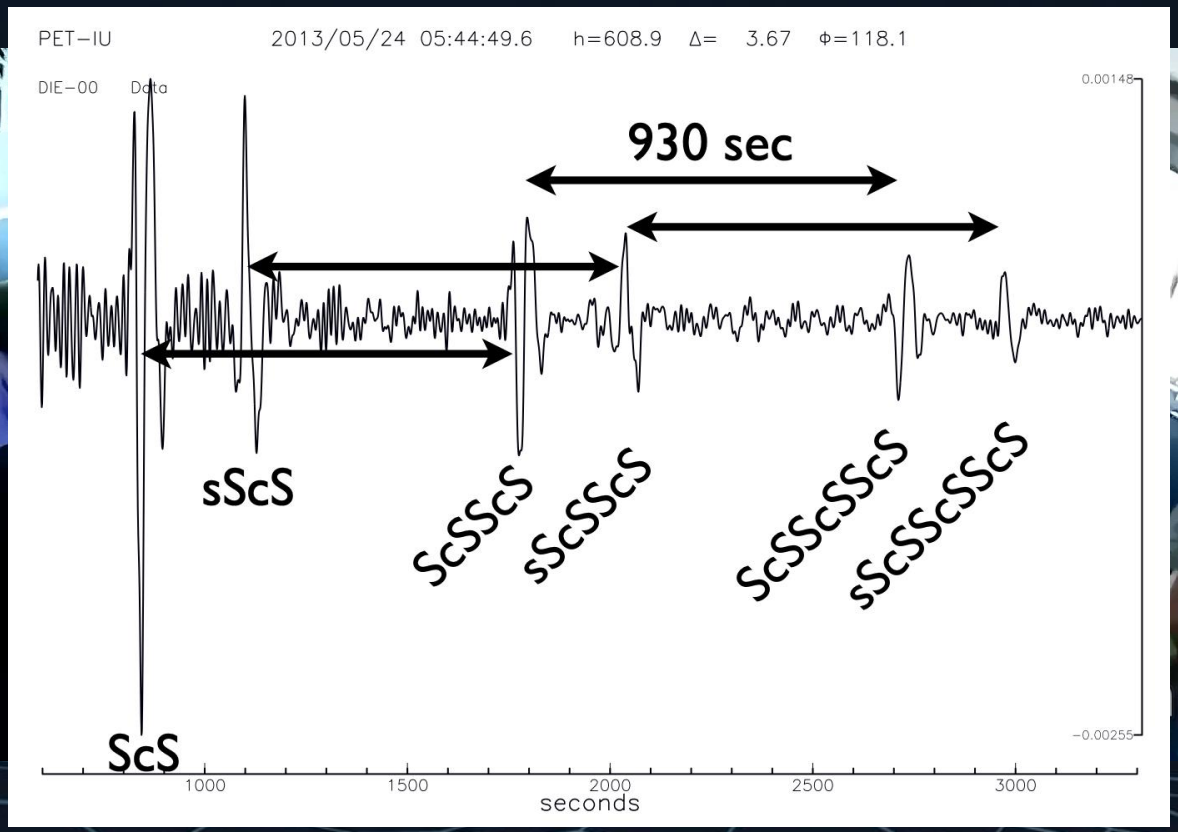
1. Seismology 101

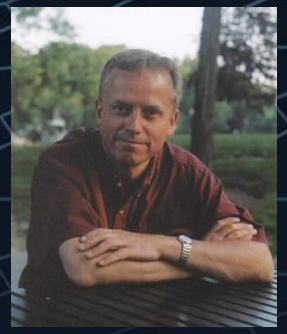
SUSTech Southern University of Science and Technology

Seismology for everyone









Goran Ekstrom

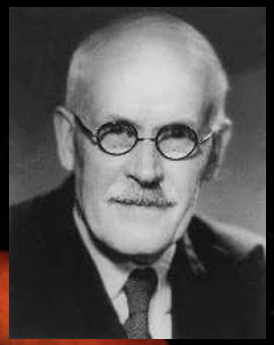
Average speed of the seismic wave through the mantle and crust 2×2891/930=6.21 km/s

Shear wave velocity of granite at 20 km depth ~3.5 km/s

A century of seismological studies of the Earth



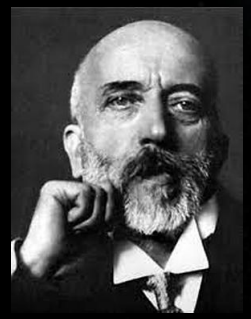
Beno Gutenberg (1889-1960)
1913 Discovery of the CMB



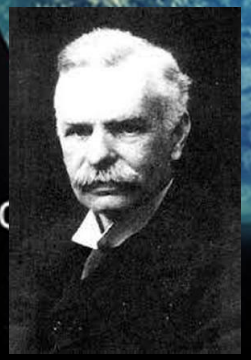
Harold Jeffreys (1891-1989)
1926 Discovery of liquid core



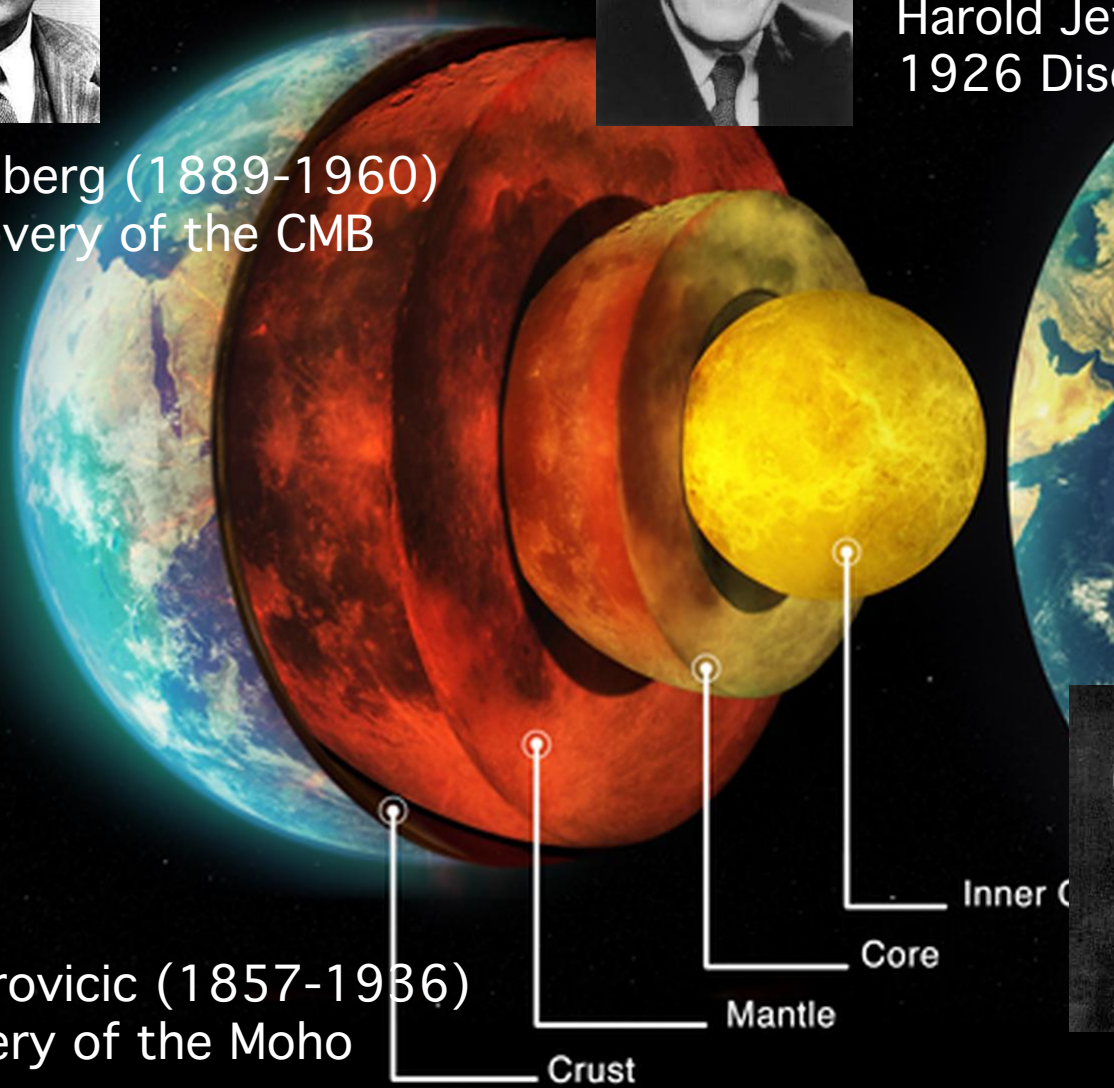
Inge Lehmann (1888-1993)
1936 Discovery of Earth's inner



Andrija Mohorovicic (1857-1936)
1910 Discovery of the Moho



Richard Oldham (1858-1936)
1906 Discovery of Earth's core



SUSTech Southern University of Science and Technology

Sources to generate seismic waves

Passive sources

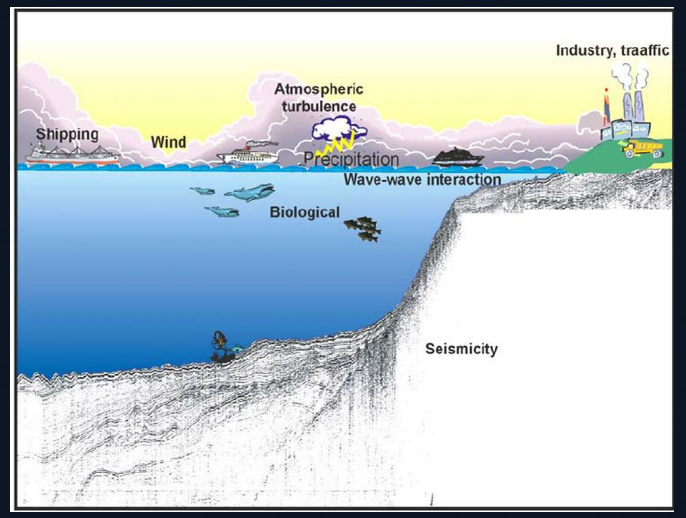
Earthquakes



Volcanoes



Environment



Active sources

Air guns



Vibrator trucks



Explosions

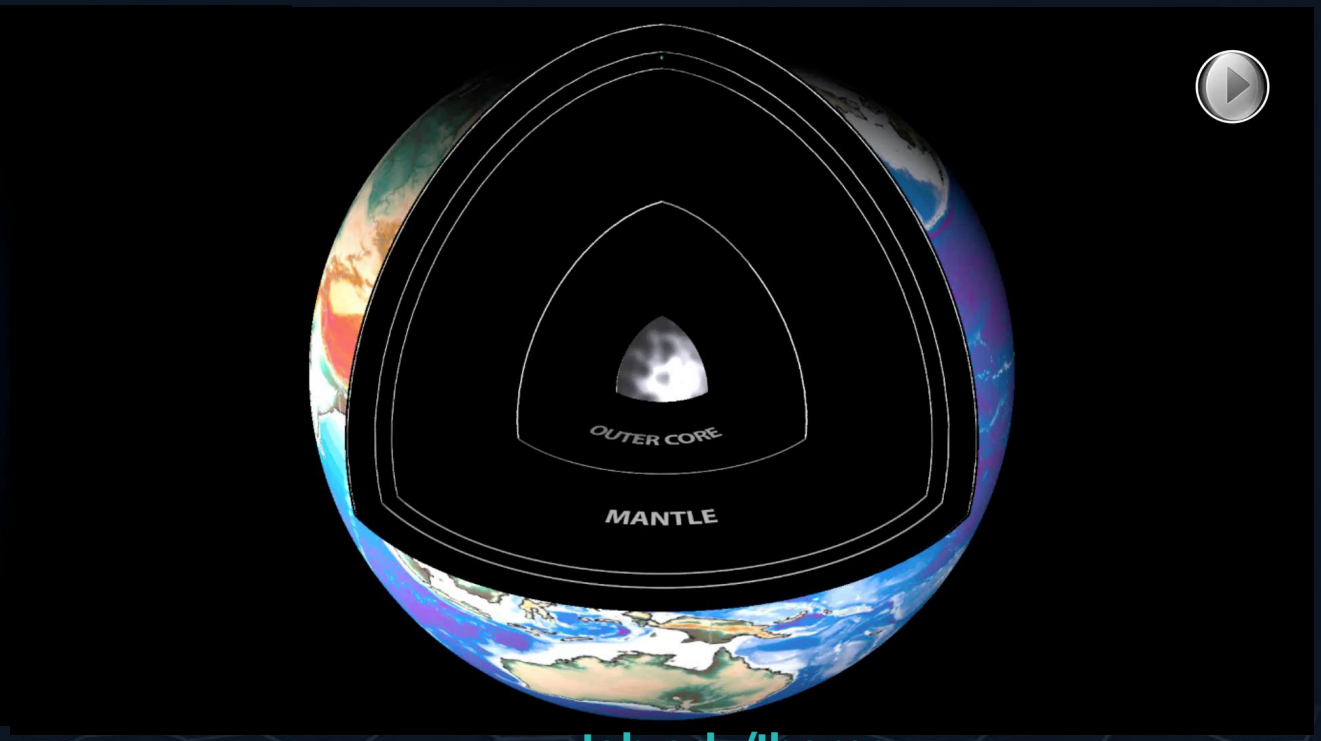


SUSTech Southern University of Science and Technology

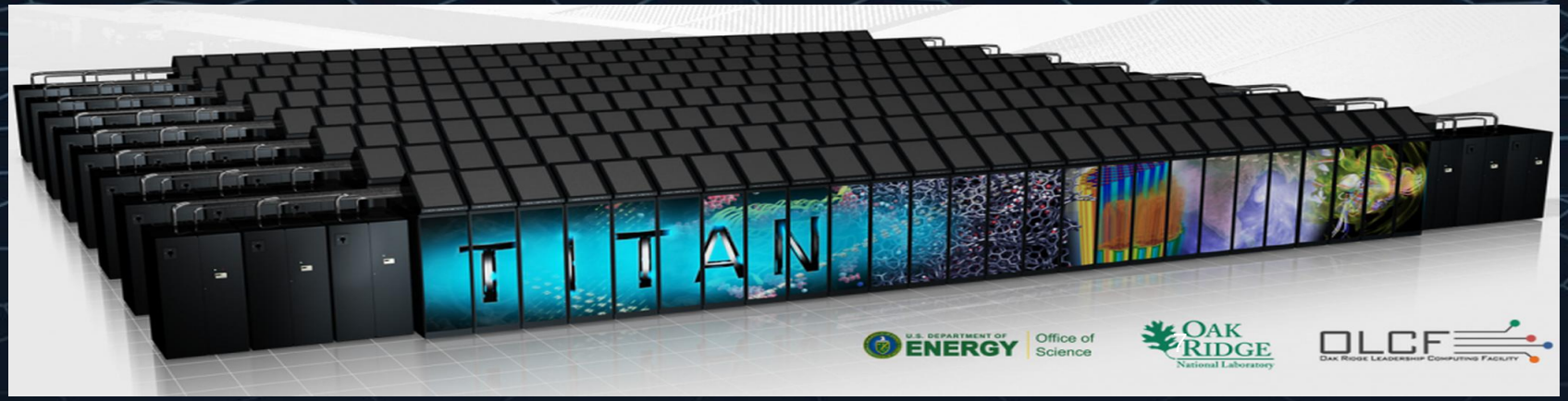
Seismic wavefields simulations



www.global.shakemovie.princeton.edu



www.utah.edu/thorne



Conservation of momentum

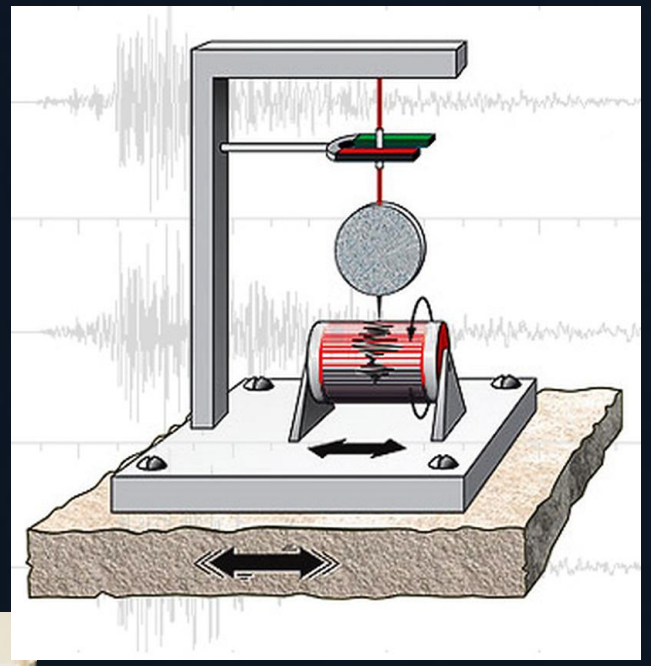
$$\rho\,\partial_t^2\mathbf{s} - \nabla\cdot\mathbf{T} = \mathbf{f}$$

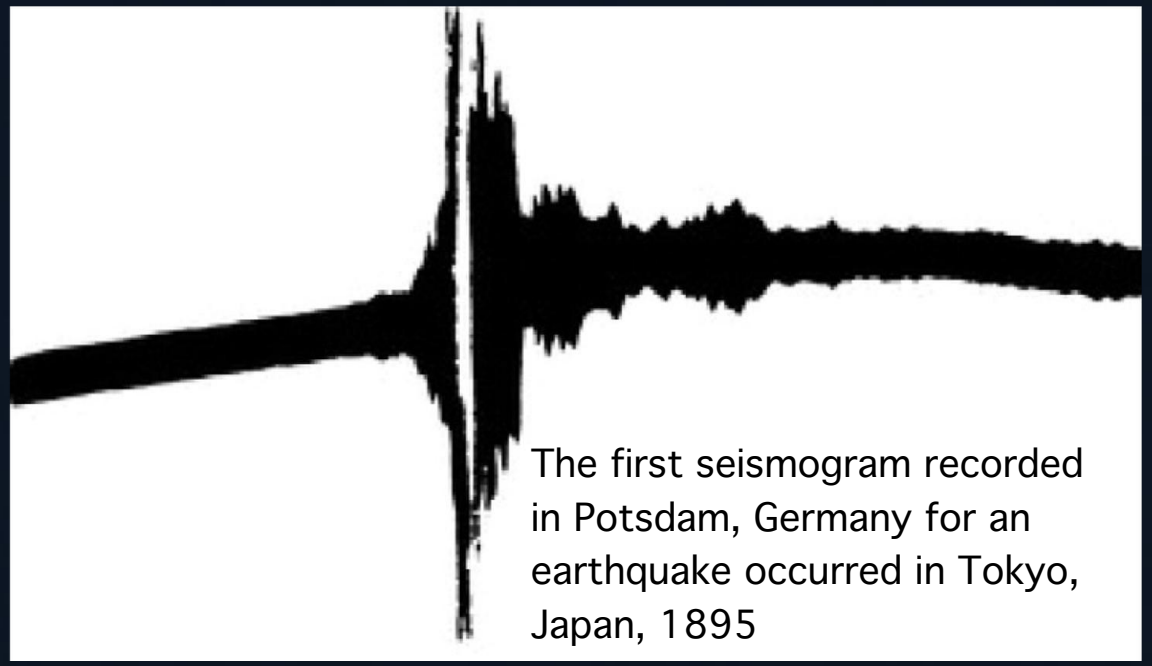
$$\mathbf{T} = \mathbf{c} : \epsilon$$ Hooke's law

www.ornl.gov

SUSTech Southern University of Science and Technology

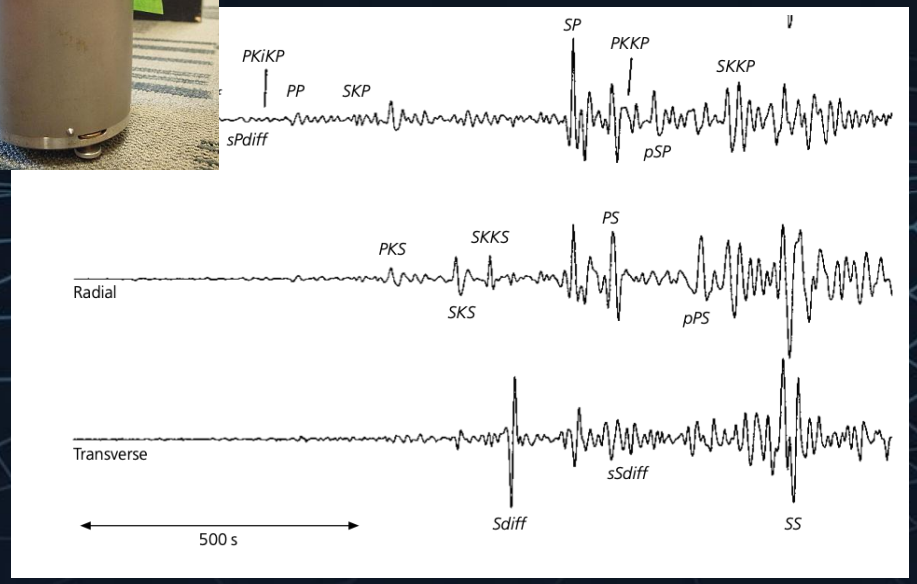
Evolution of seismometers (receivers)

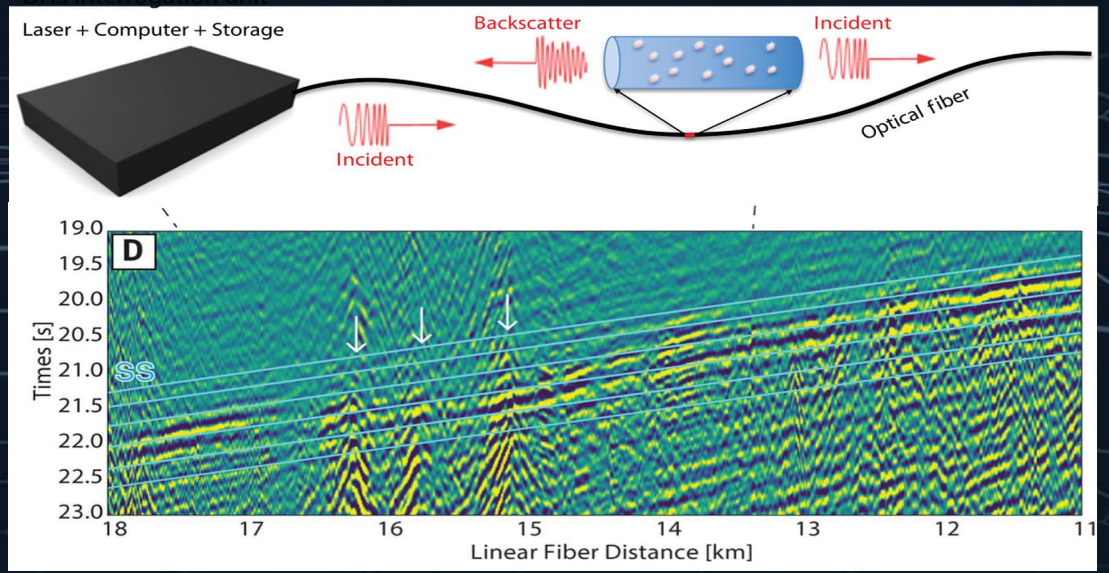




The first seismogram recorded in Potsdam, Germany for an earthquake occurred in Tokyo, Japan, 1895

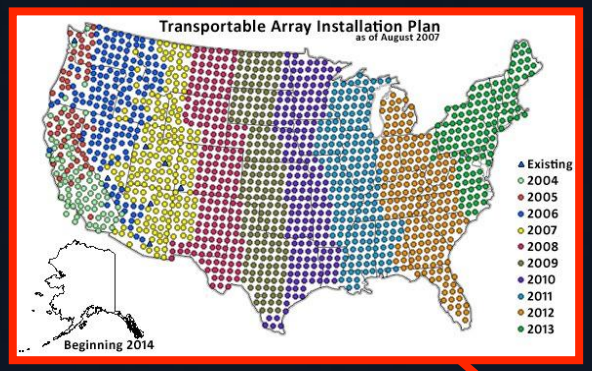


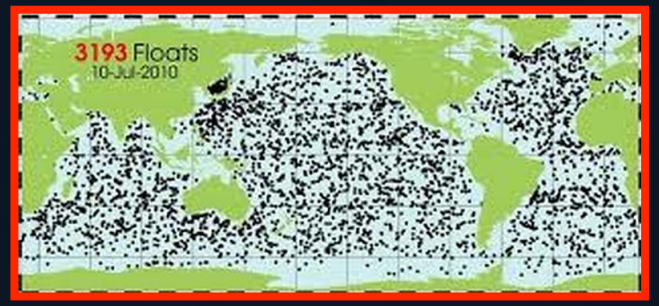


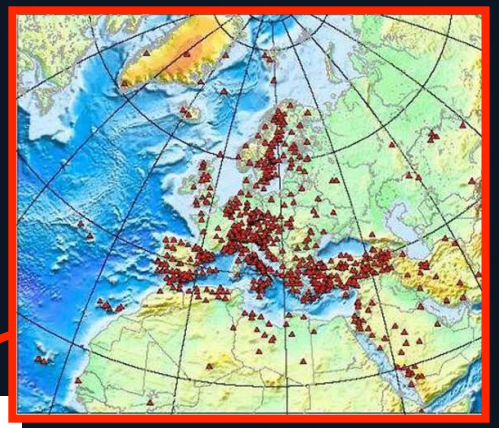


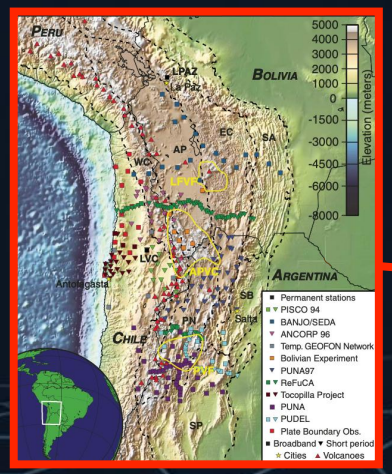
SUSTech Southern University of Science and Technology

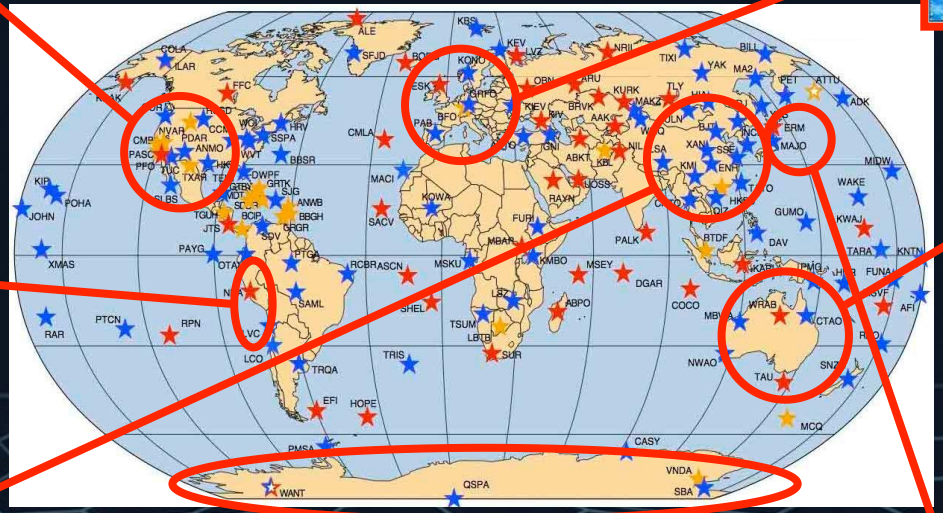
Global and regional seismic networks



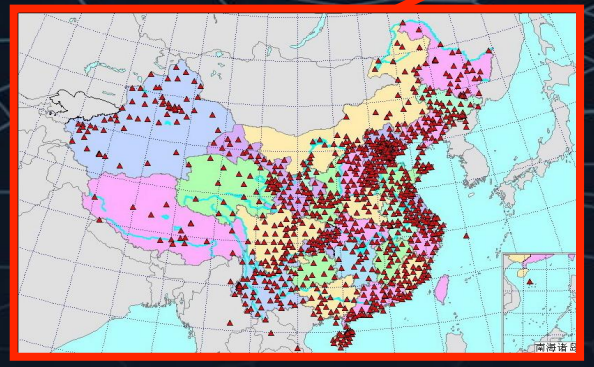


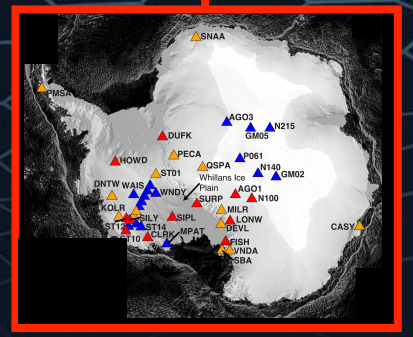


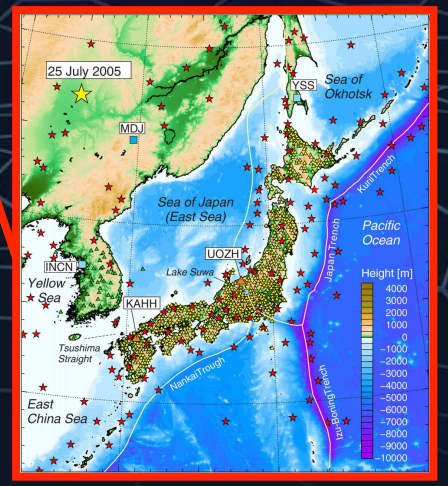






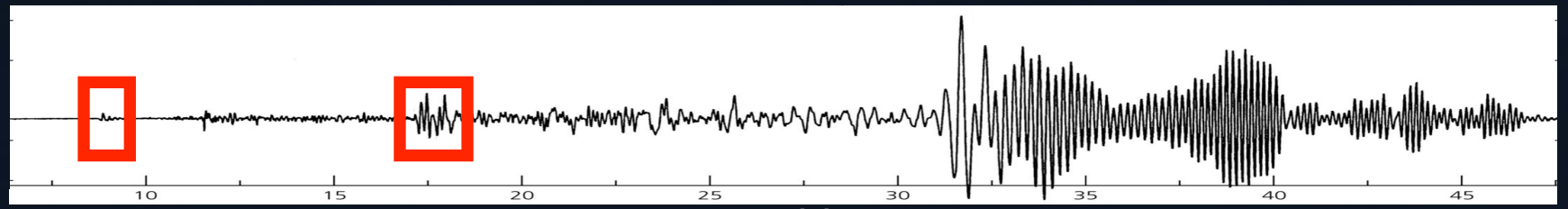


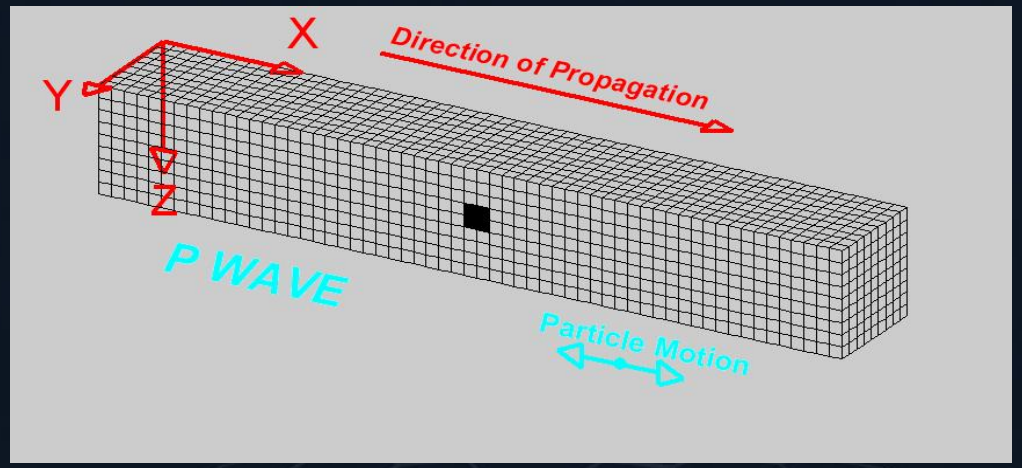


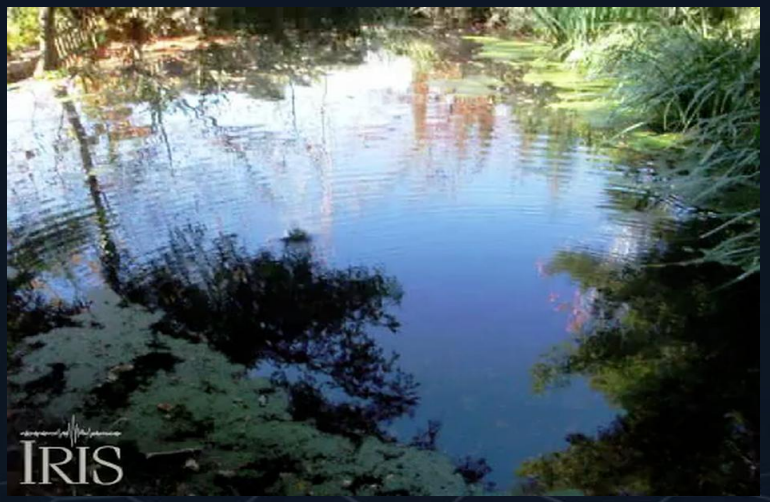


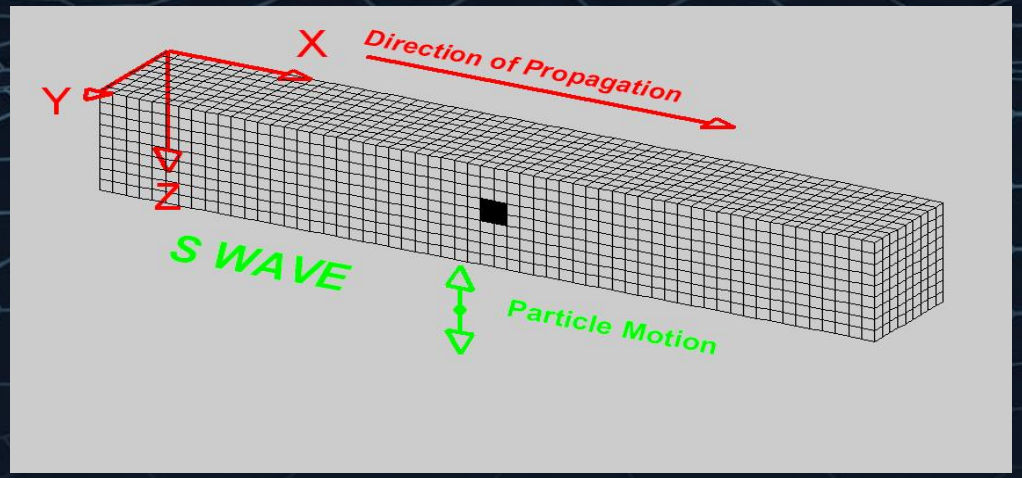
SUSTech Southern University of Science and Technology

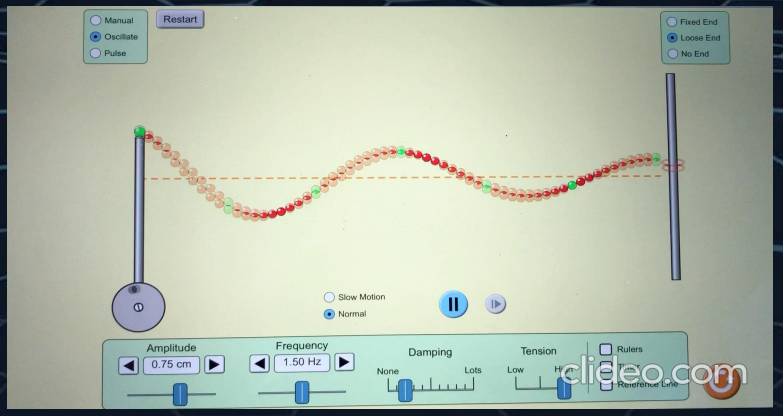
Reading a seismogram 1: body



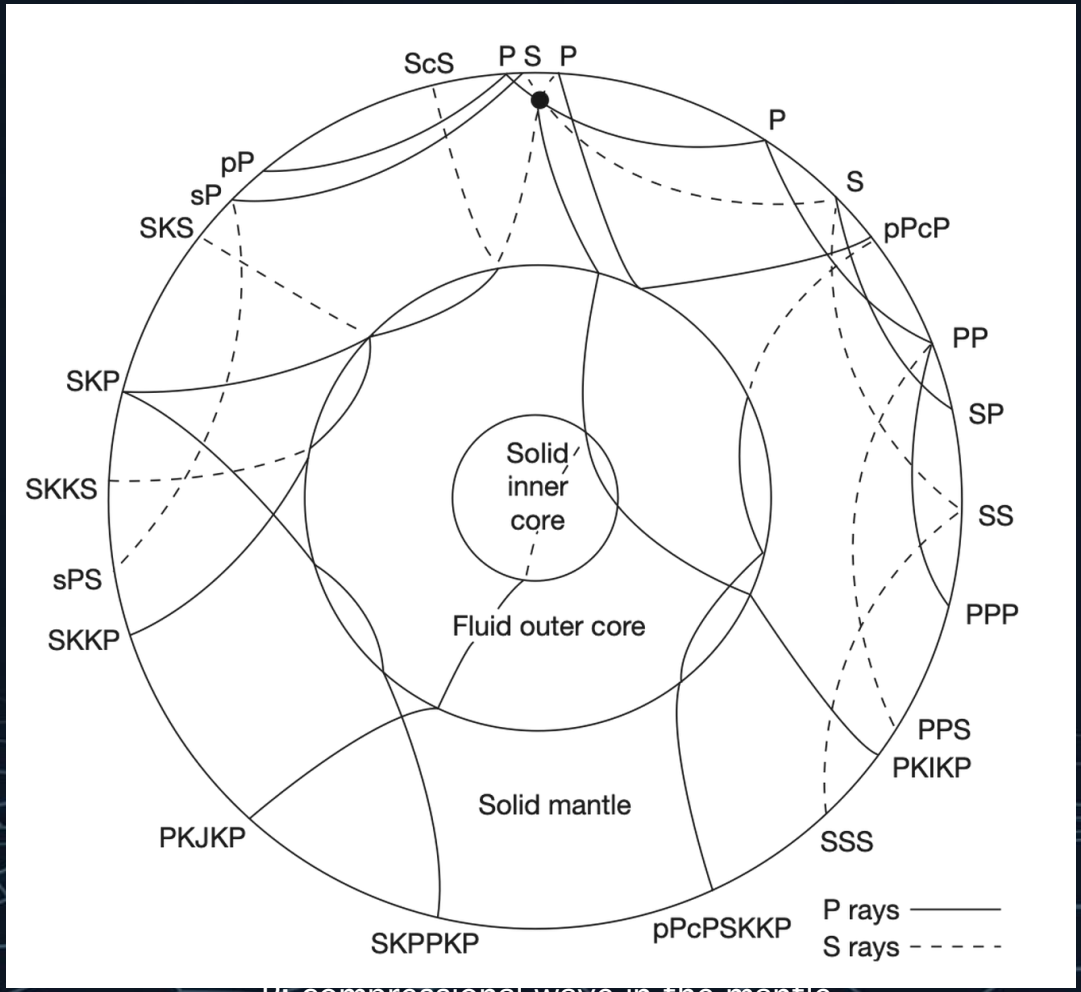


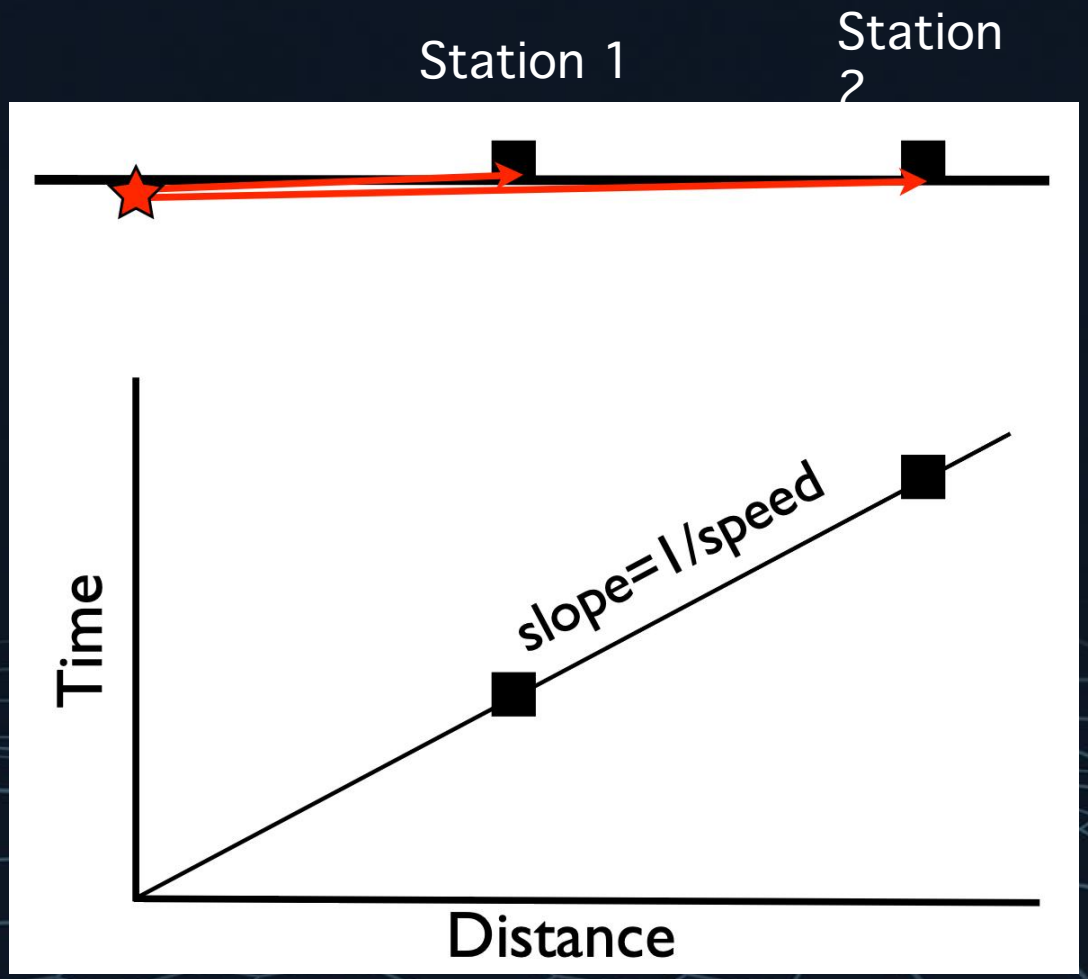






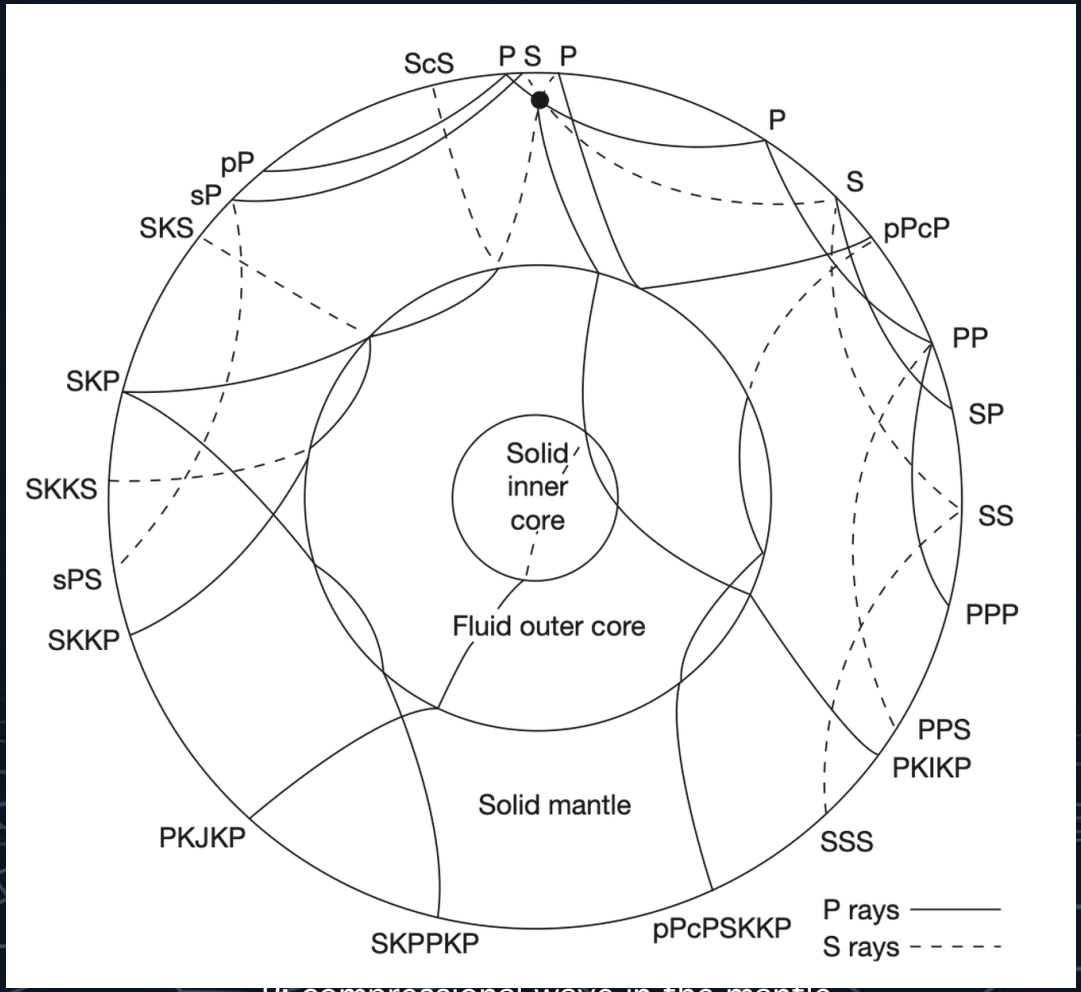
Seismic phases and travel time table



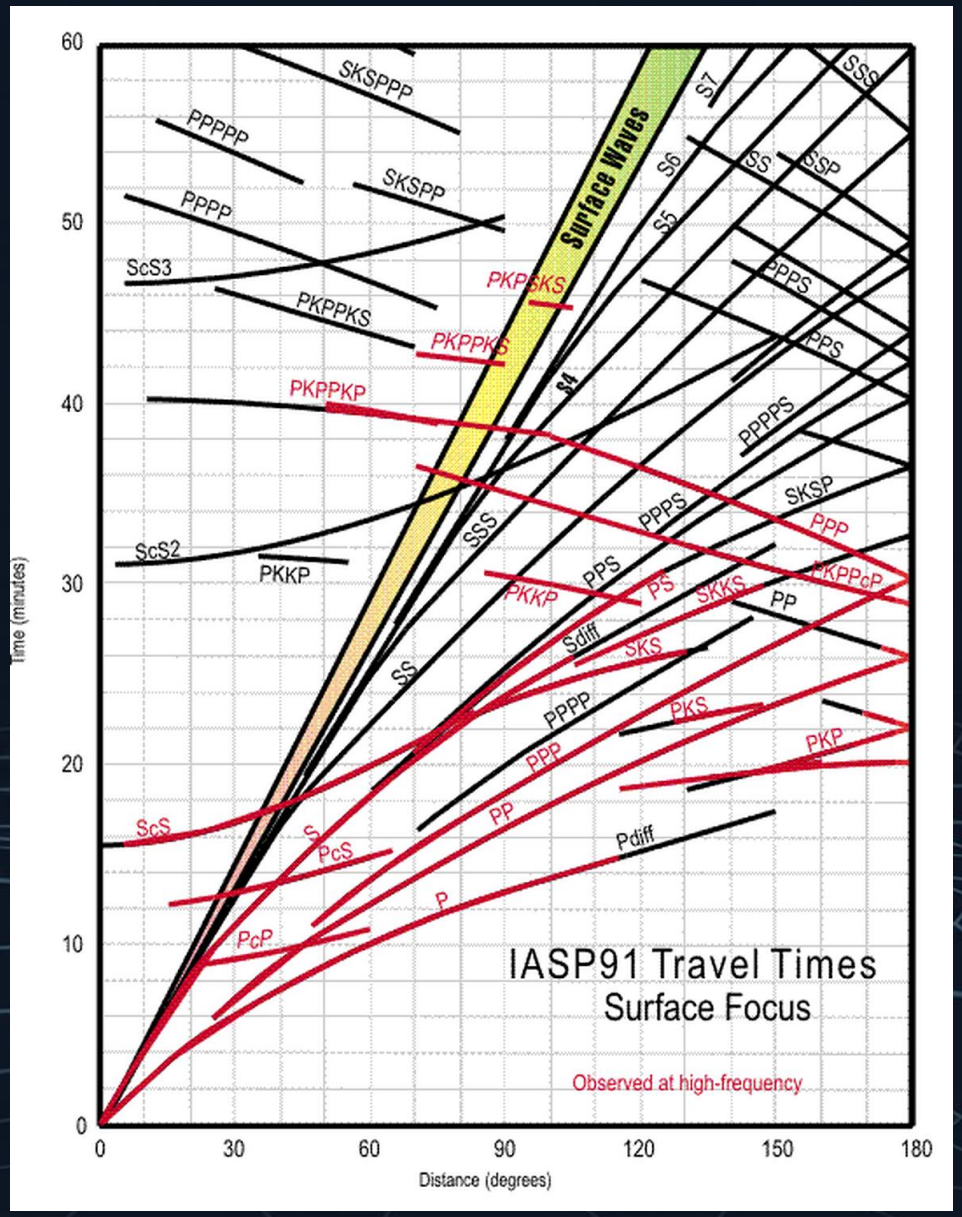


P: compressional wave in the mantle
S: shear wave in the mantle
c: reflection from the CMB
i: reflection from the inner-outer core boundary
K: P wave in the outer core
I: P wave in the inner core

Seismic phases and travel time table

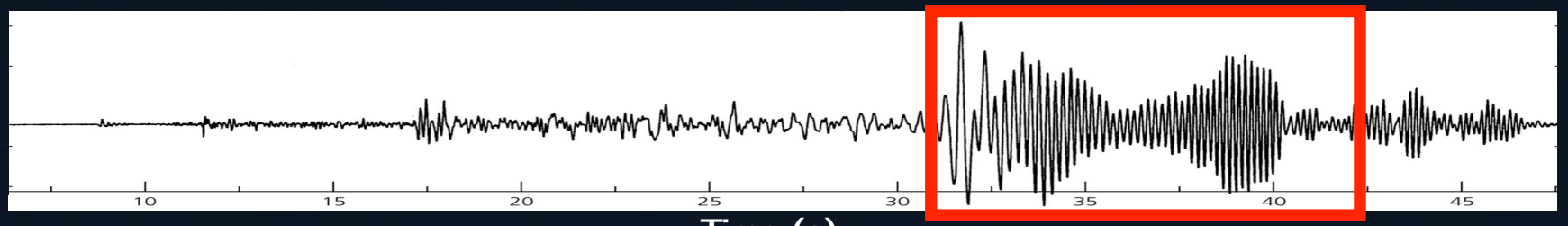


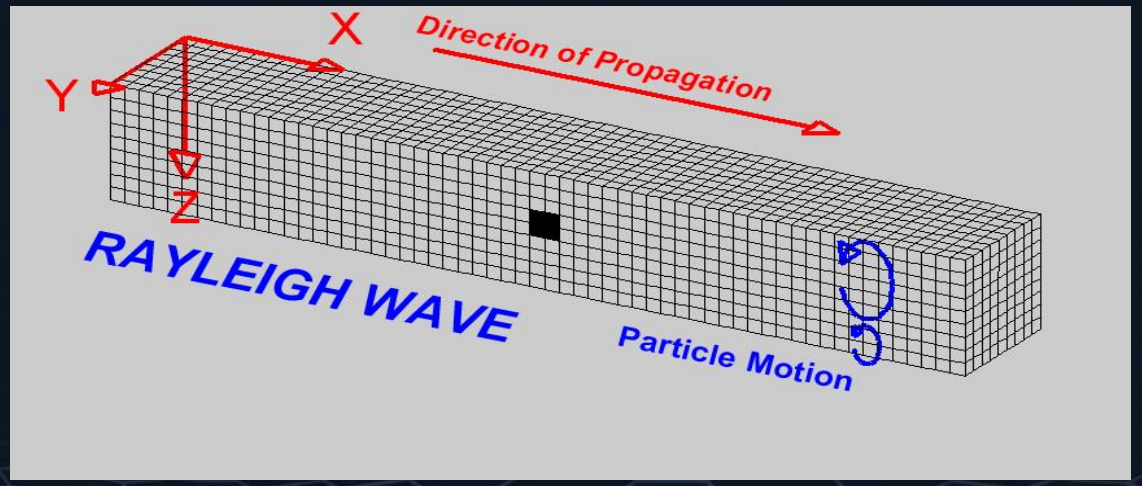
P: compressional wave in the mantle
S: shear wave in the mantle
c: reflection from the CMB
i: reflection from the inner-outer core boundary
K: P wave in the outer core
I: P wave in the inner core

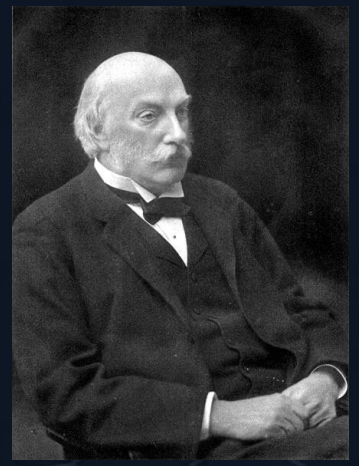


SUSTech Southern University of Science and Technology

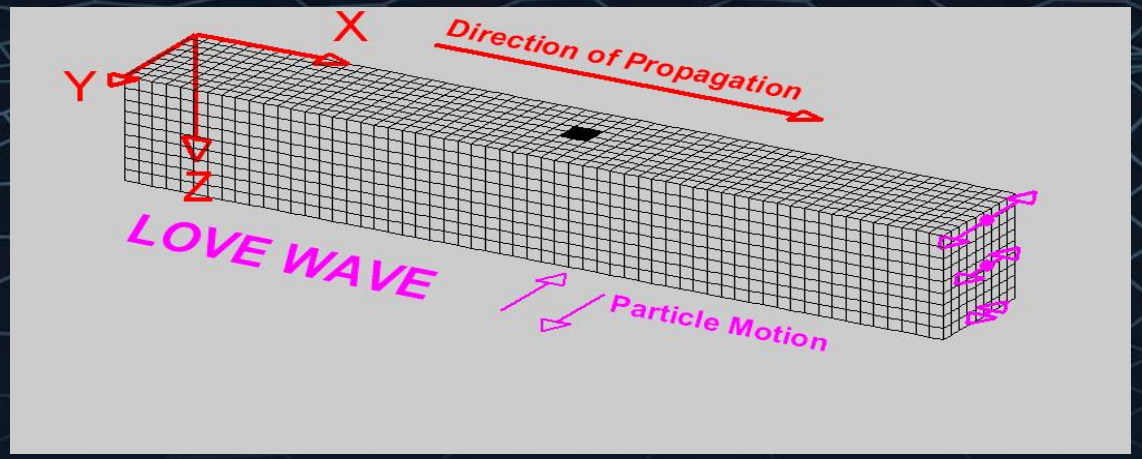
Reading a seismogram 2: surface

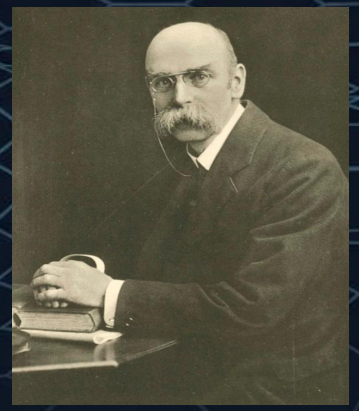






The Lord Rayleigh (1842-1919)
1877 mathematically demonstrated the existence of surface waves

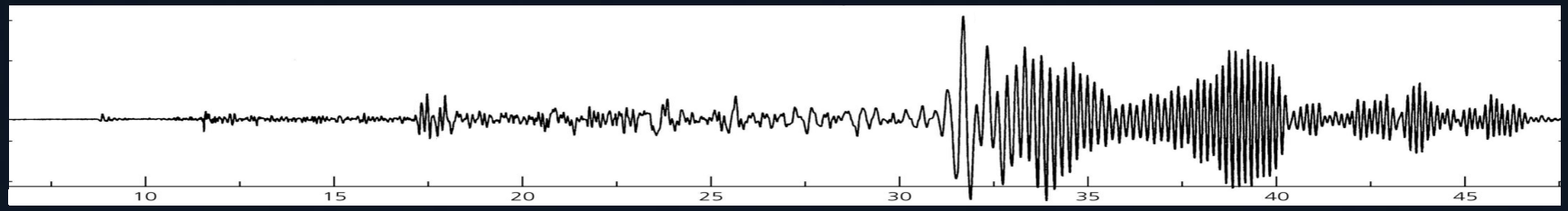




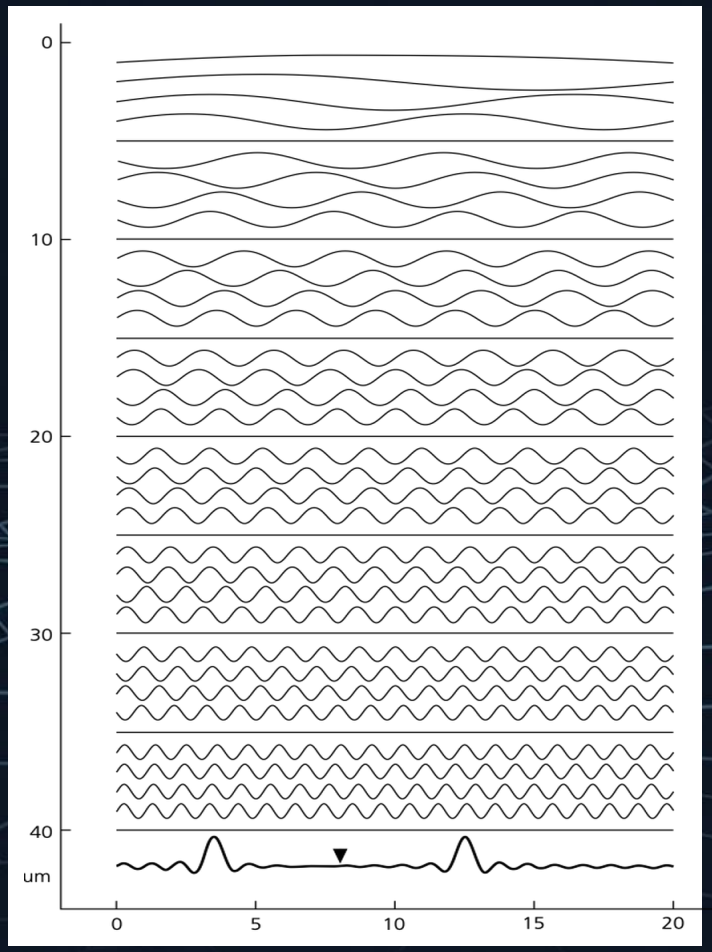
Augustus Love (1863-1940)
1911 mathematically showed the existence of transversely polarized Love waves

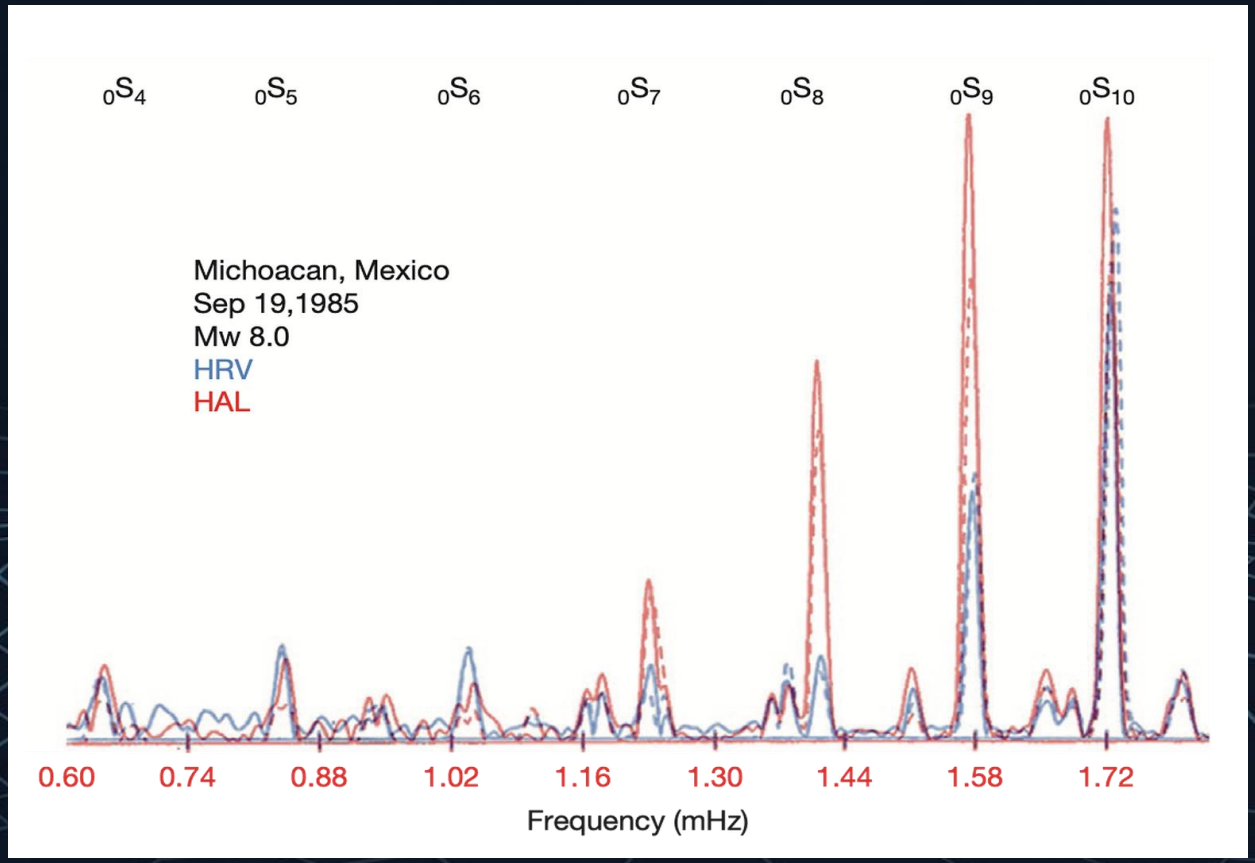
SUSTech Southern University of Science and Technology

Reading a seismogram 3: free oscillation



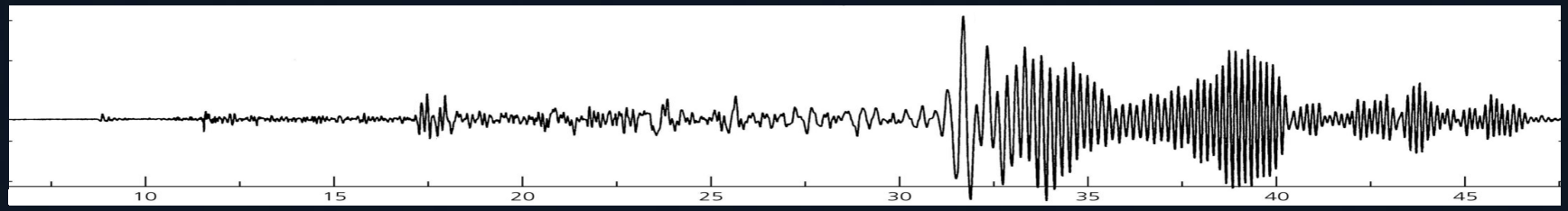
Fourier decomposition

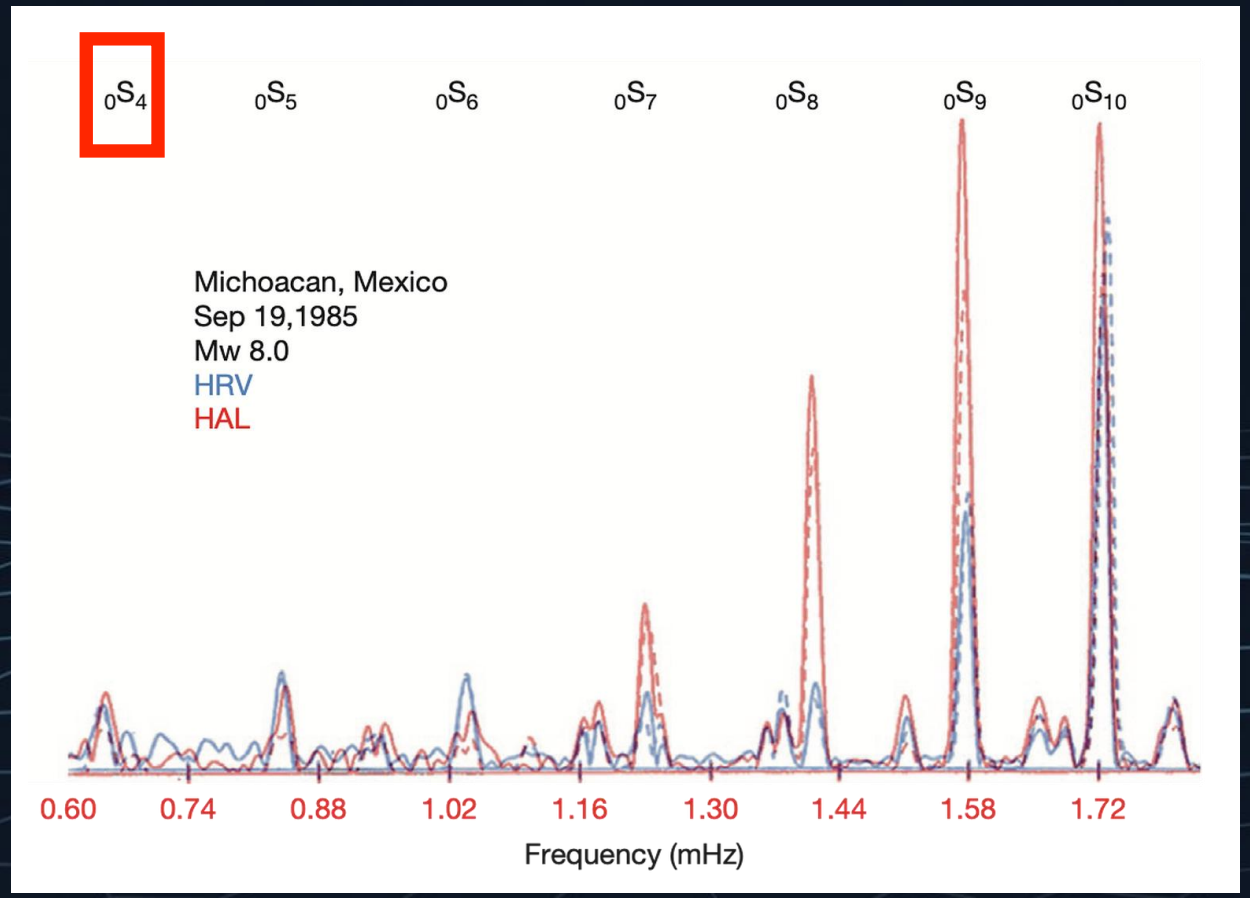


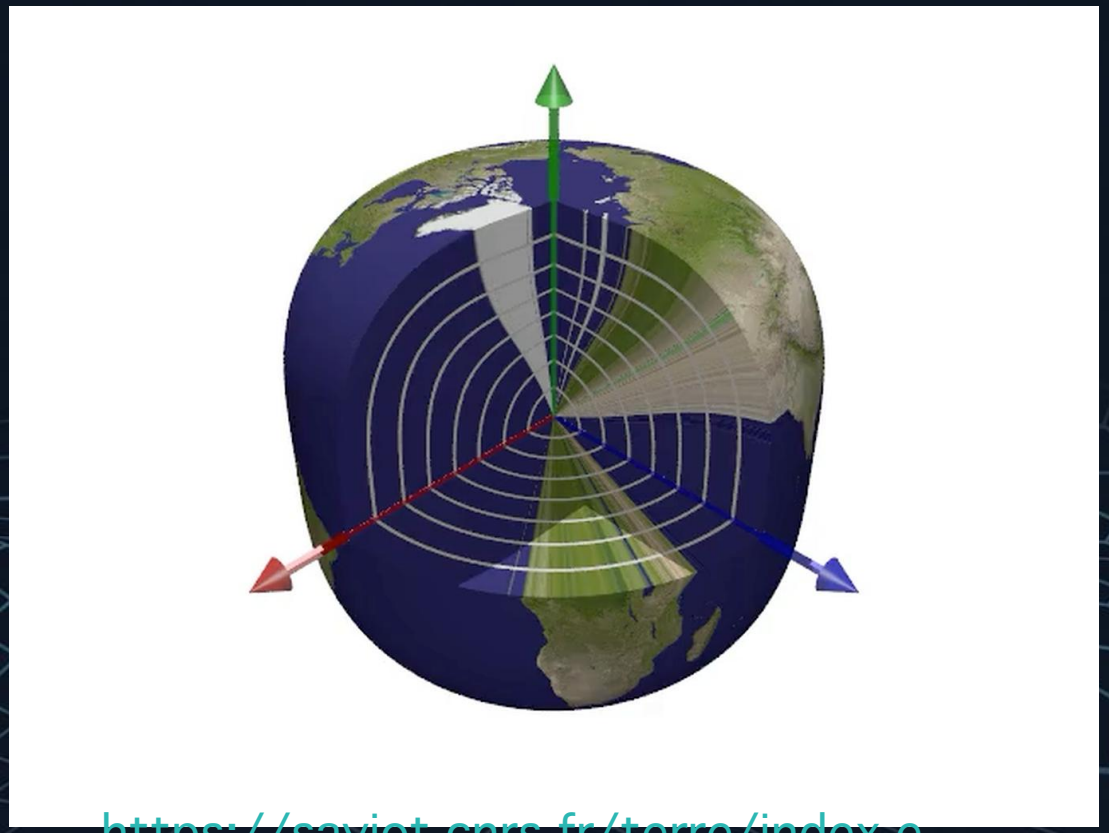


SUSTech Southern University of Science and Technology

Reading a seismogram 3: free oscillation

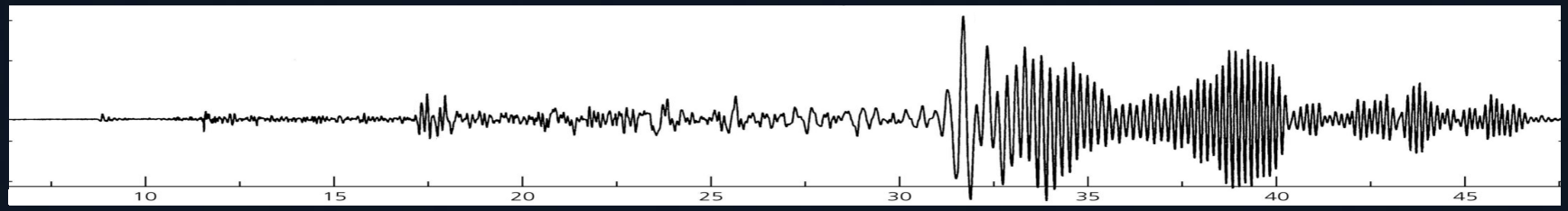


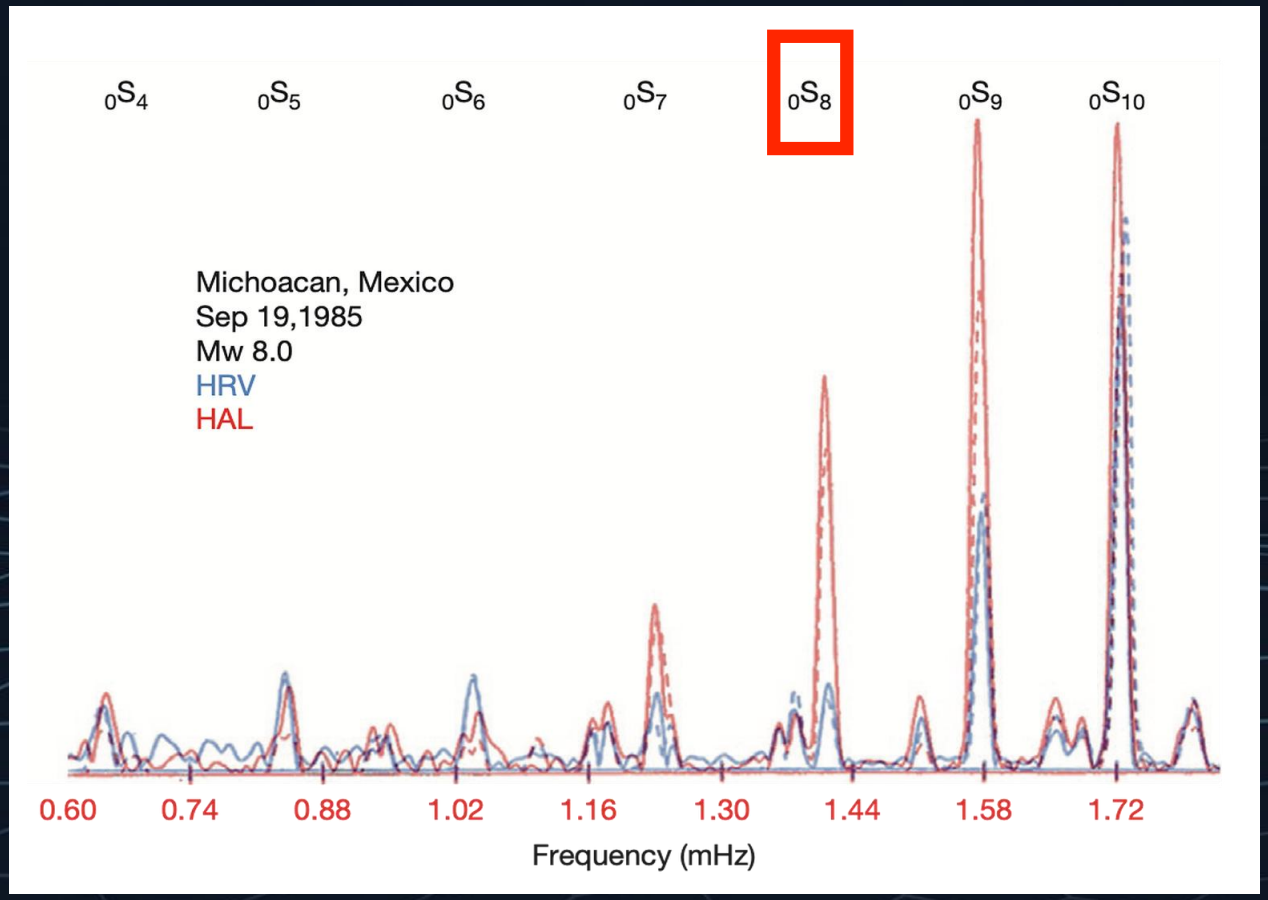


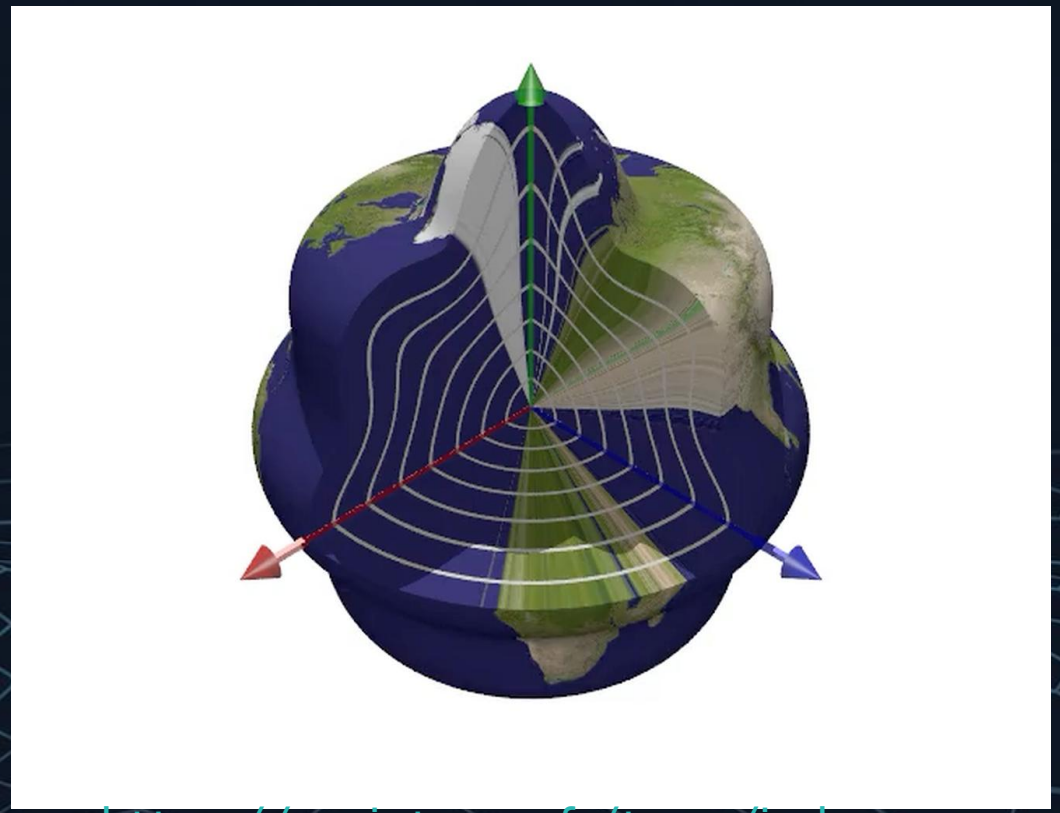


https://saviot.cnrs.fr/terre/index.en.html

Reading a seismogram 3: free oscillation



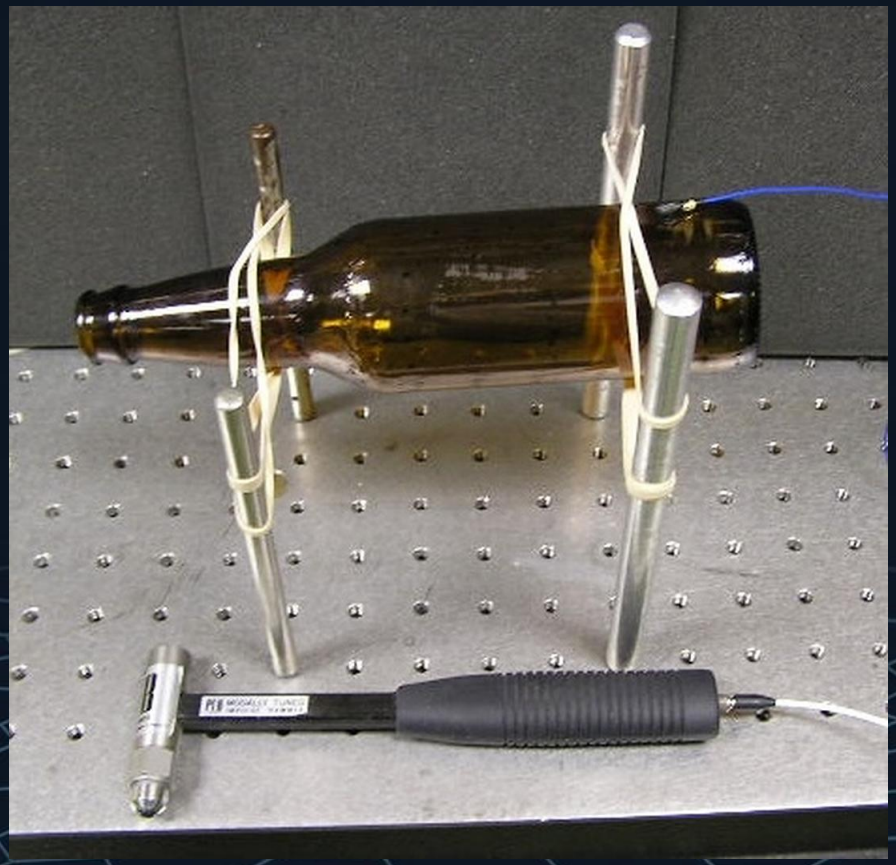


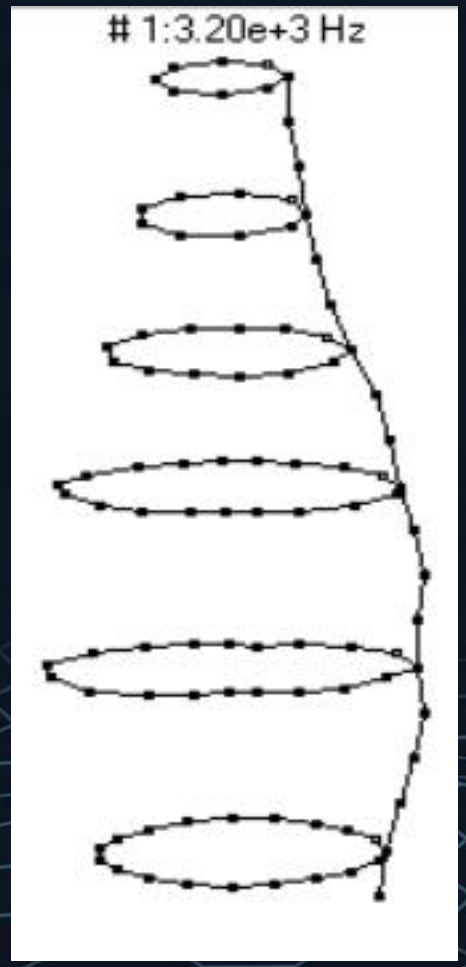


https://saviot.cnrs.fr/terre/index.en.html

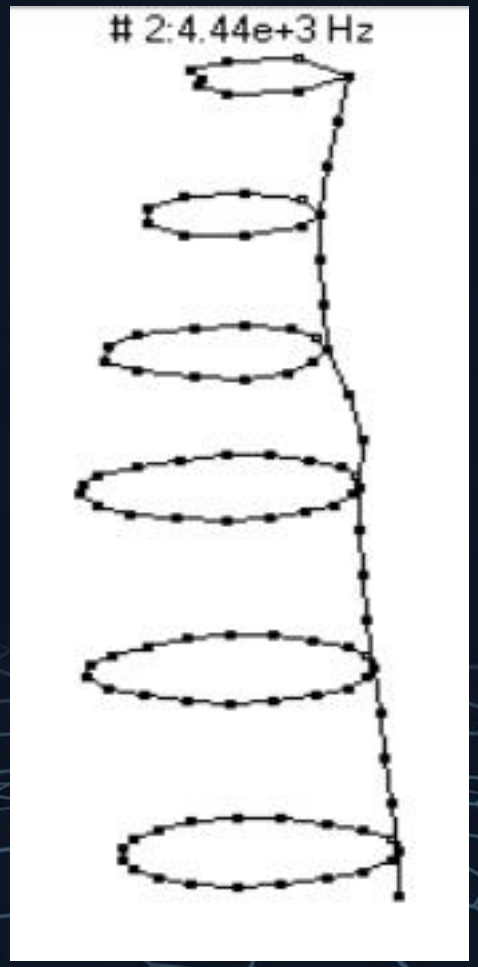
SUSTech Southern University of Science and Technology

Free oscillation of a beer bottle



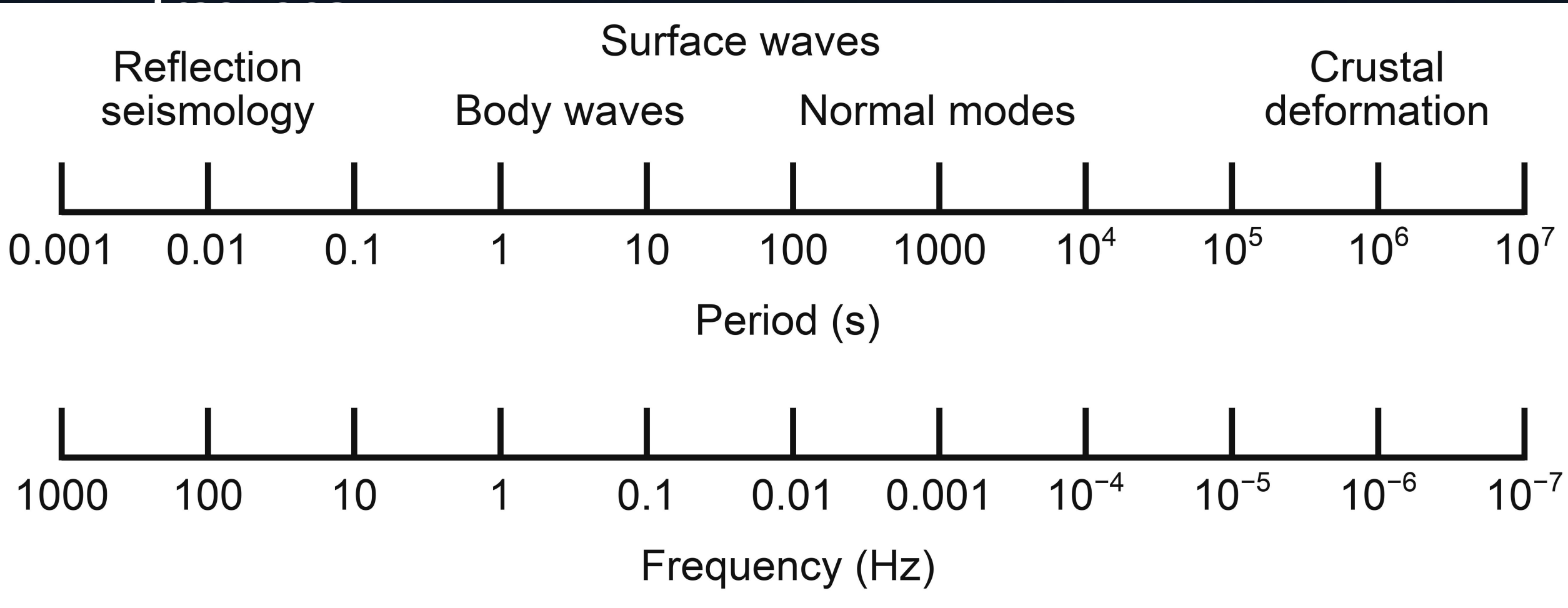






https://www.acs.psu.edu/drussell/demos/beerbottle/beerbottle.h

Seismic data span several orders of magnitude in



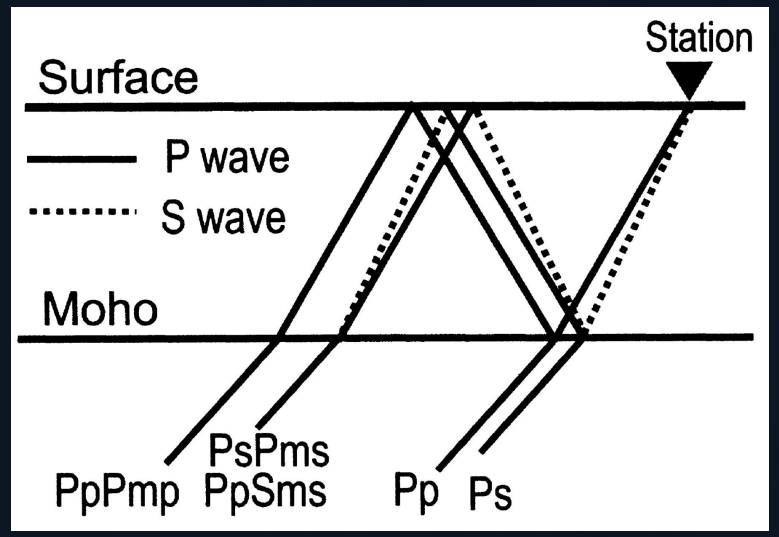


2. Seismic methods for crustal model building

SUSTech Southern University of Science and Technology

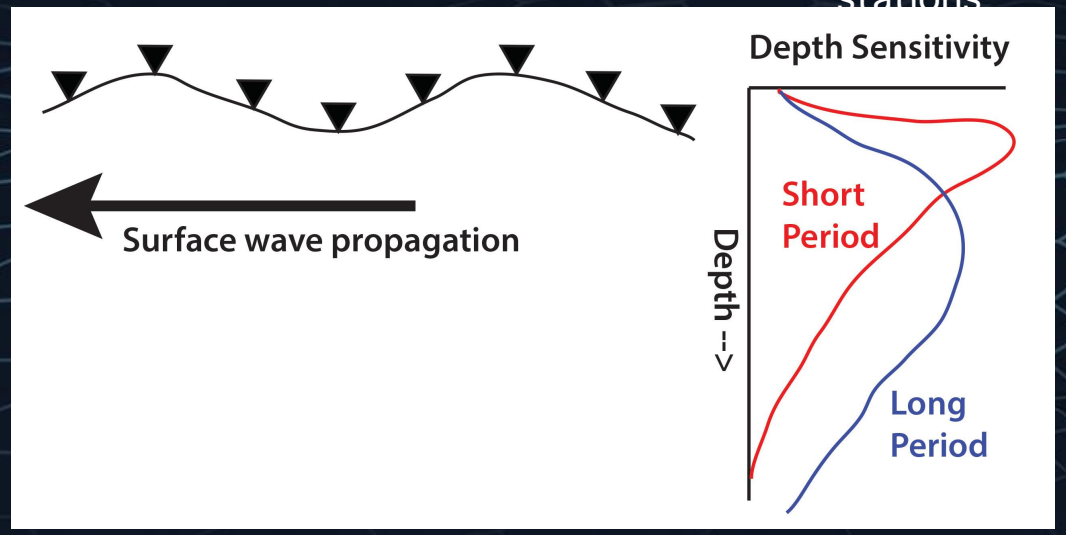
Common Seismic Imaging Methods

Receiver functions:



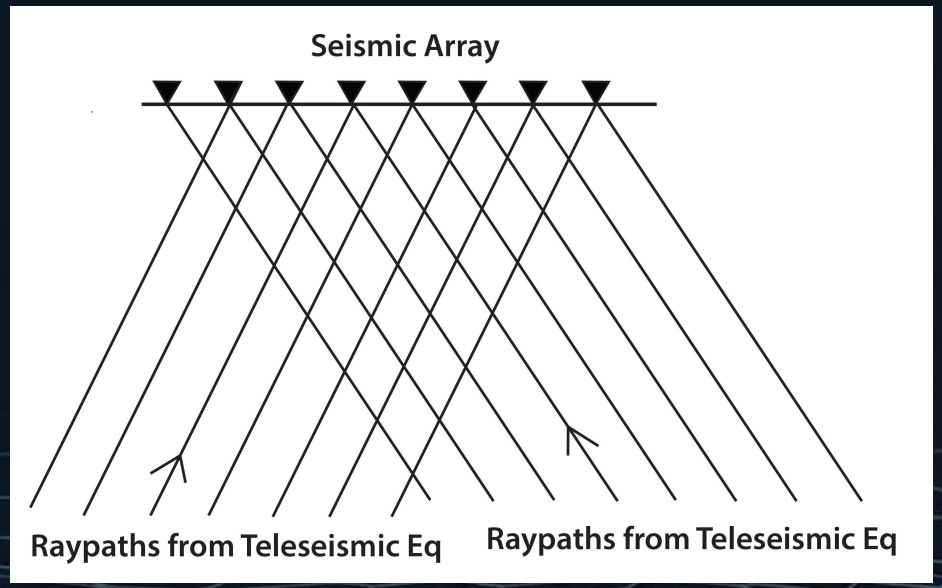
- Strengths: image discontinuities such as the Moho, sediment–basement interface, and 410 and 660 km boundaries
- Limitations: weak constraints on velocity and its gradients; mainly used to image shallow structure beneath stations

Surface-wave imaging:



Body-wave imaging:

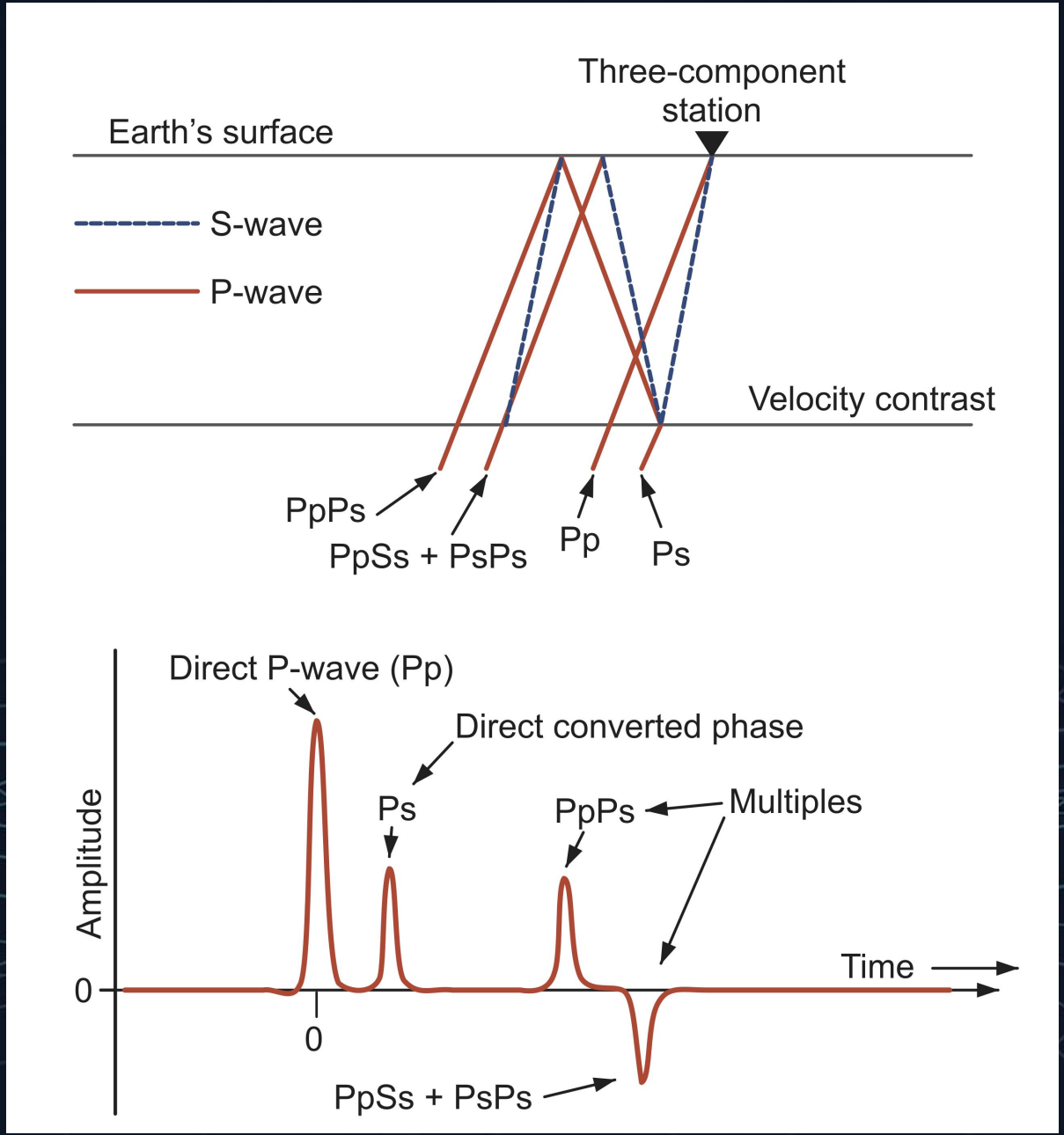
- Strengths: resolves lateral variations at depths of 100–1,000 km
- Limitations: requires dense station coverage and often has poor depth resolution



- Strengths: resolves depth variations and constrains absolute velocities
- Limitations: generally lower lateral resolution; typically limited to the upper 300 km

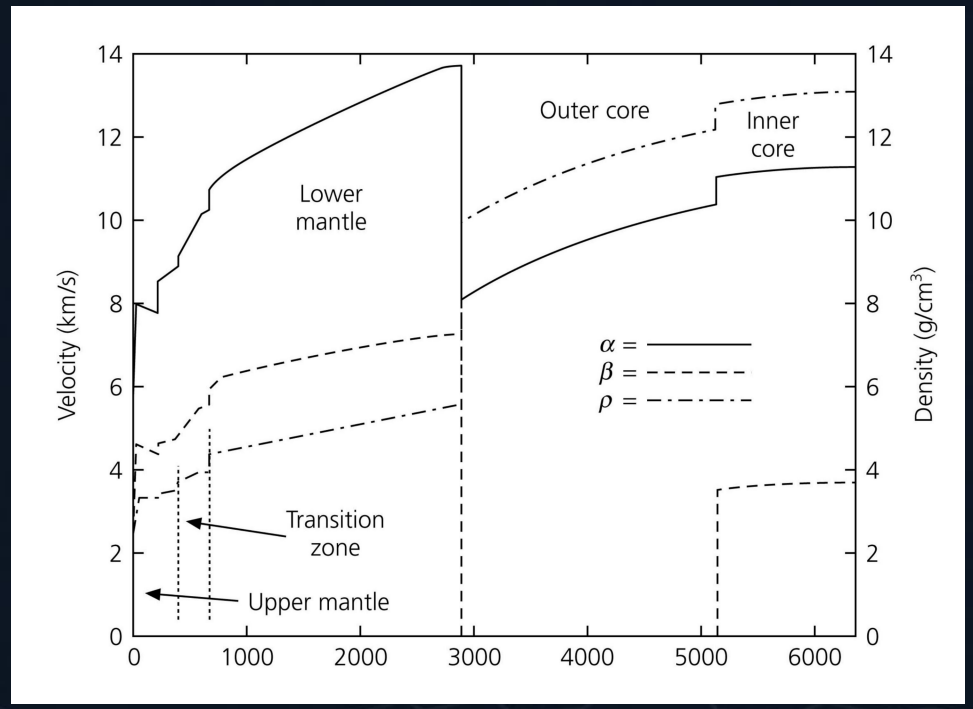
SUSTech Southern University of Science and Technology

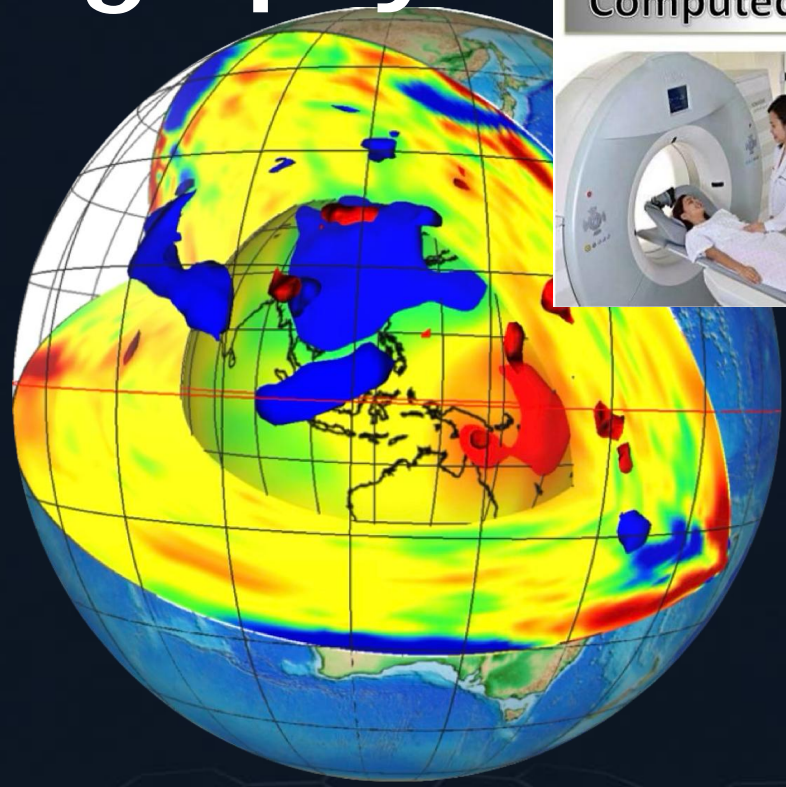
Receiver function analysis

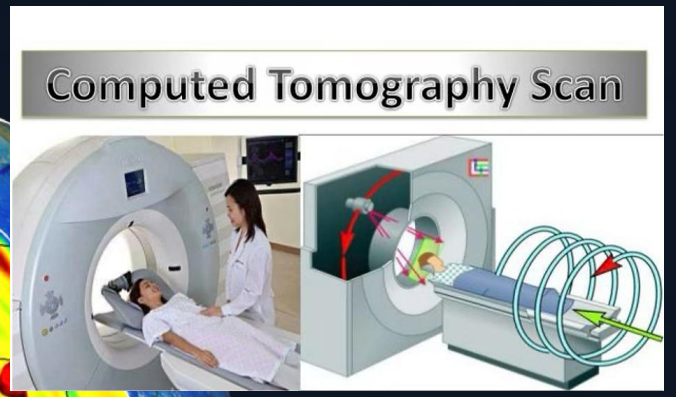


SUSTech Southern University of Science and Technology

Seismic Tomography

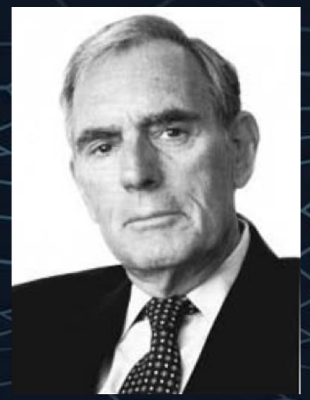








Don Anderson (1933-2014)



Adam Dziewonski (1936-2016)



Keiiti Aki (1930-2005)

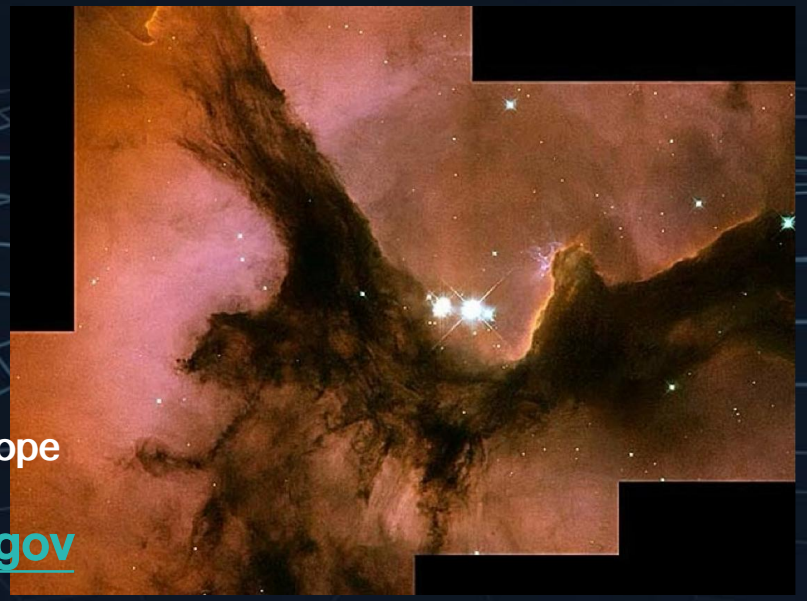


John Woodhouse

High-Resolution Imaging

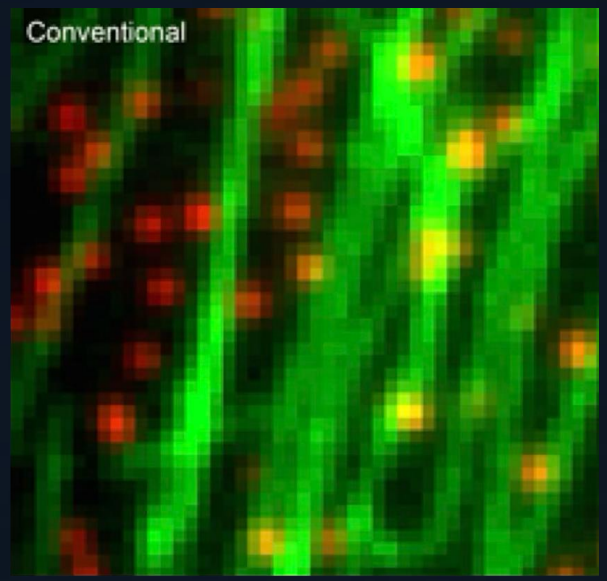
The Trifid Nebula
Messier 20

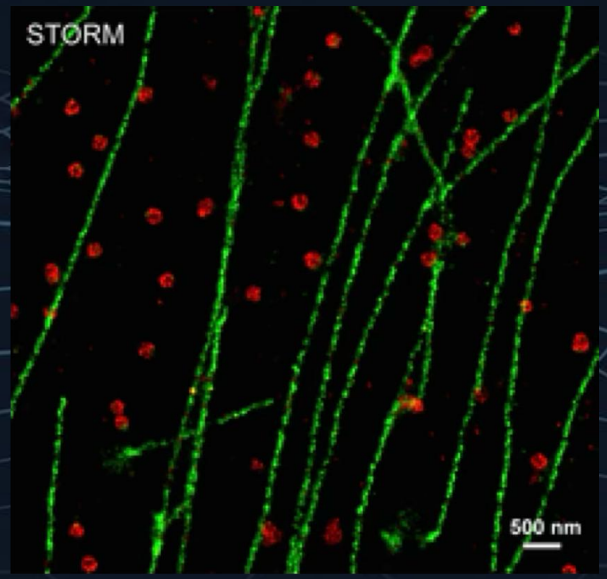




Hubble Space Telescope

www.nasa.gov





Microtubules (green)
Clathrin (red)

STORM: Stochastic Optical Reconstruction Microscopy

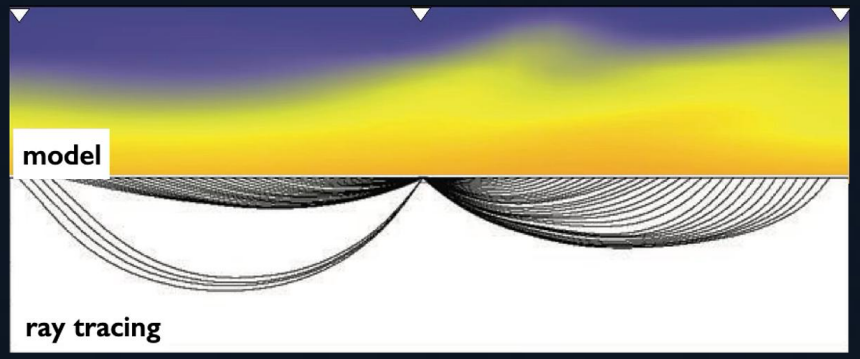
www.zhuang.harvard.edu

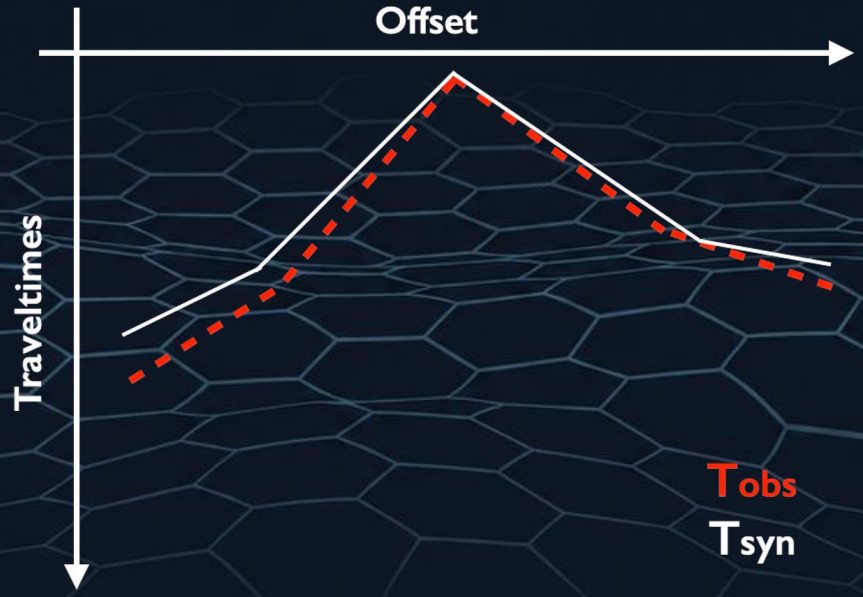
SUSTech Southern University of Science and Technology

Classical Travel-Time Imaging

Misfit: $J = |\mathbf{T}_{\mathbf{syn}} - \mathbf{T}_{\mathbf{obs}}|^2$



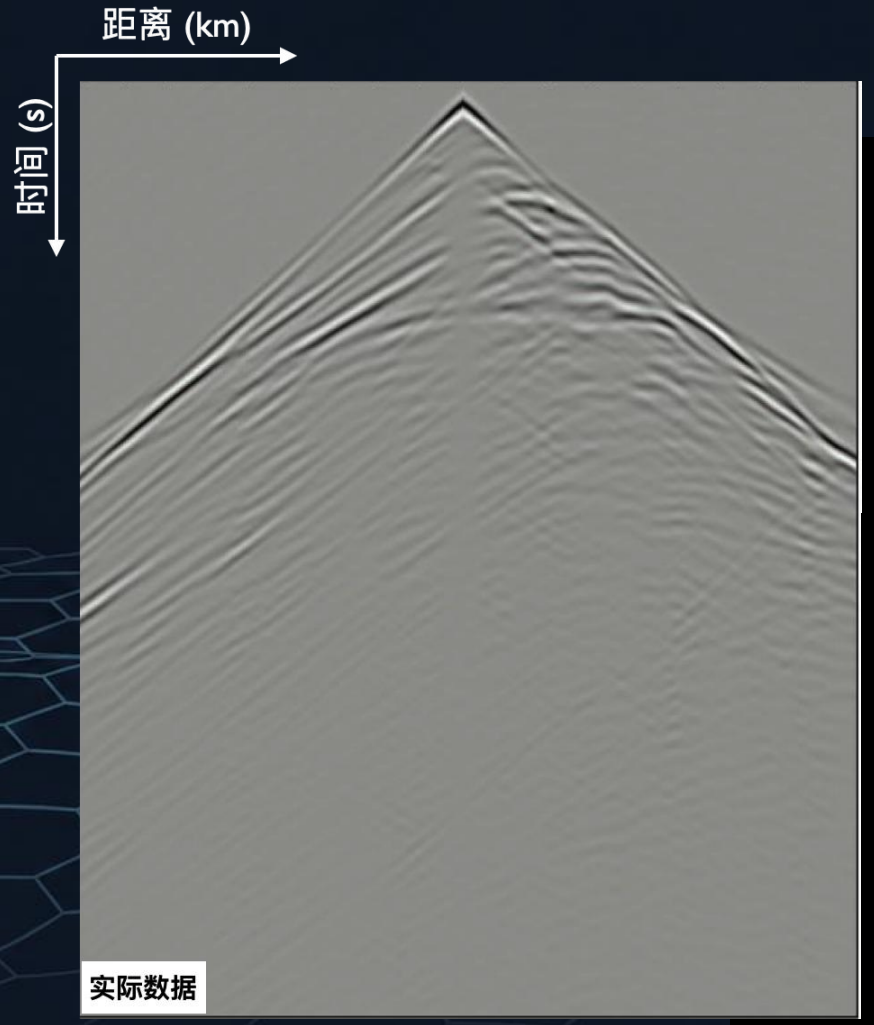


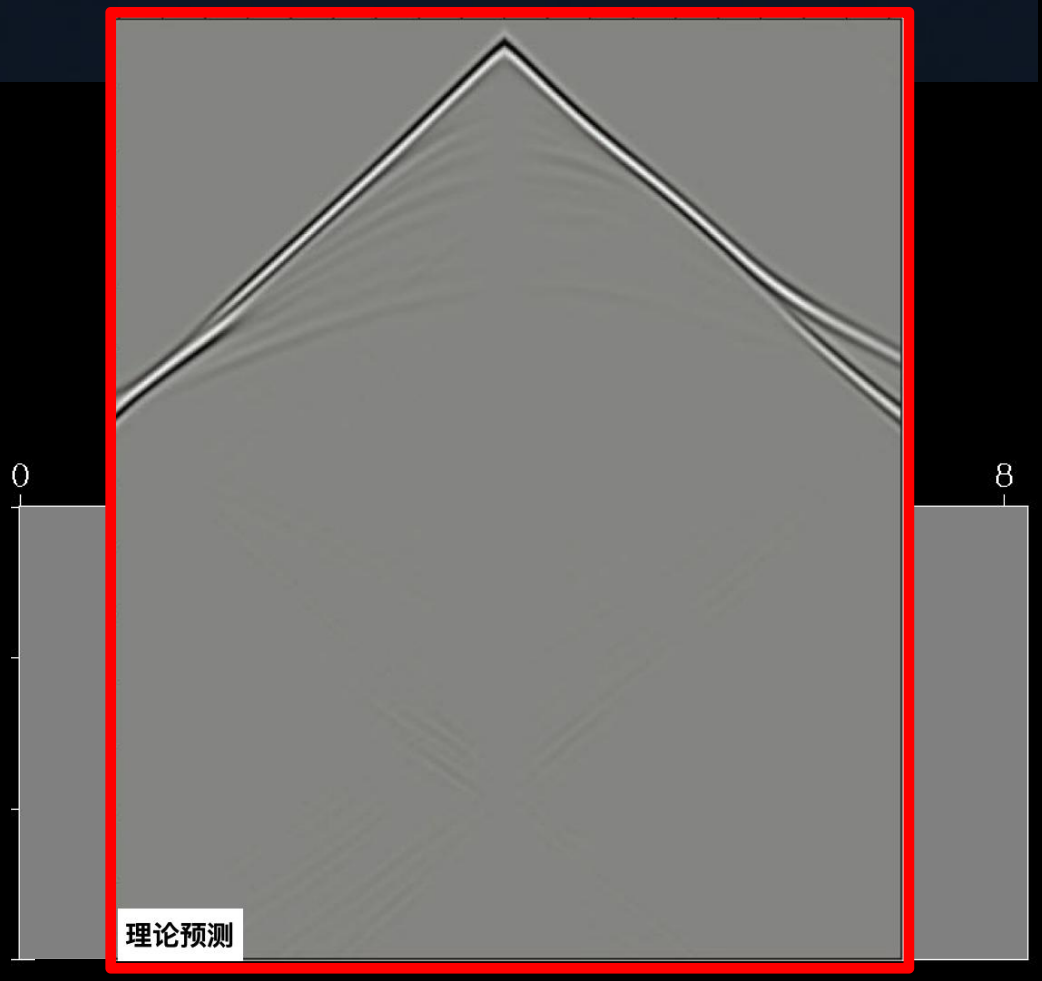


SUSTech Southern University of Science and Technology

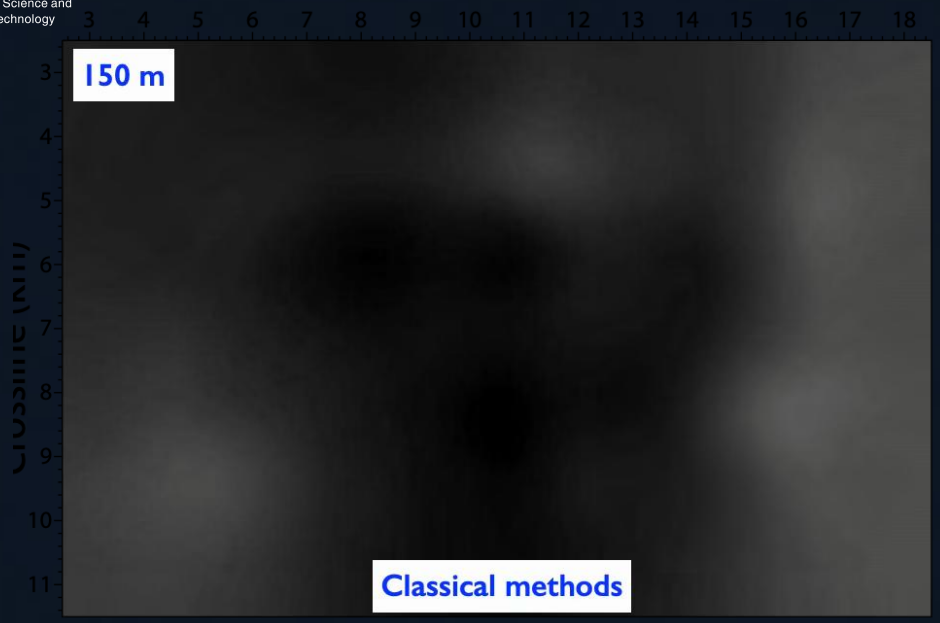
Full-Waveform Inversion

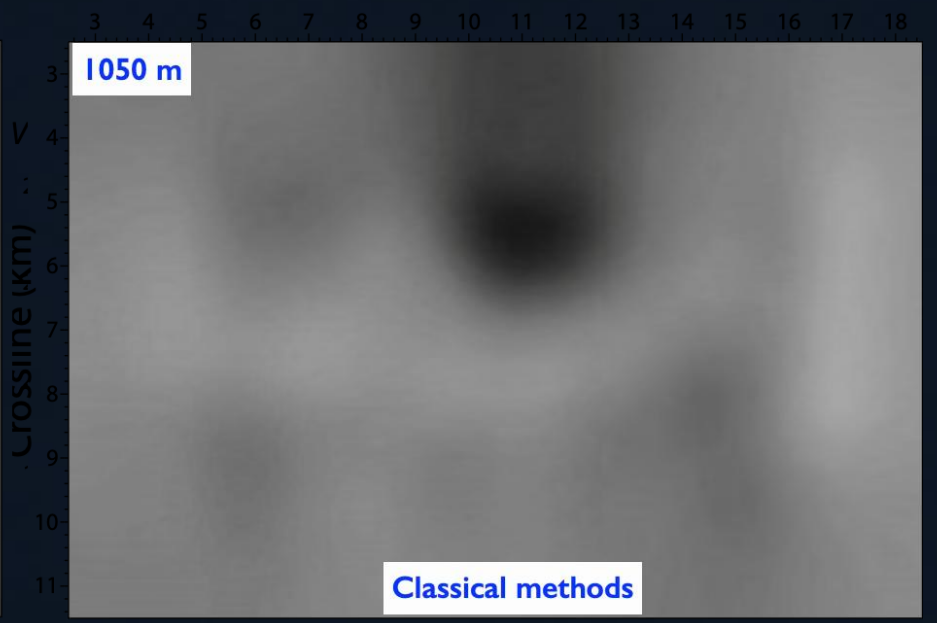
Misfit: $$J = |\mathbf{F}(\mathbf{m}) - \mathbf{d}|^2$$

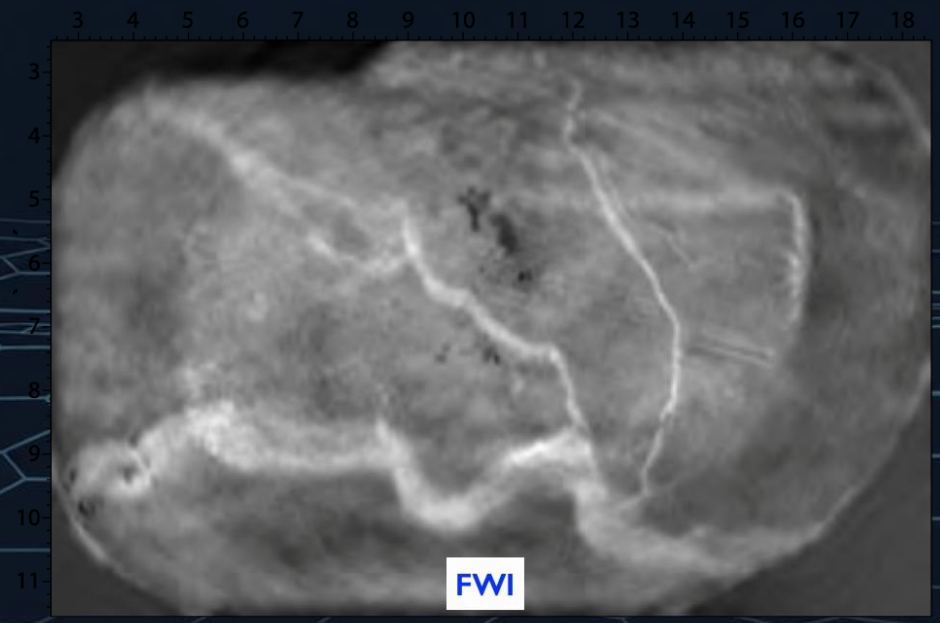


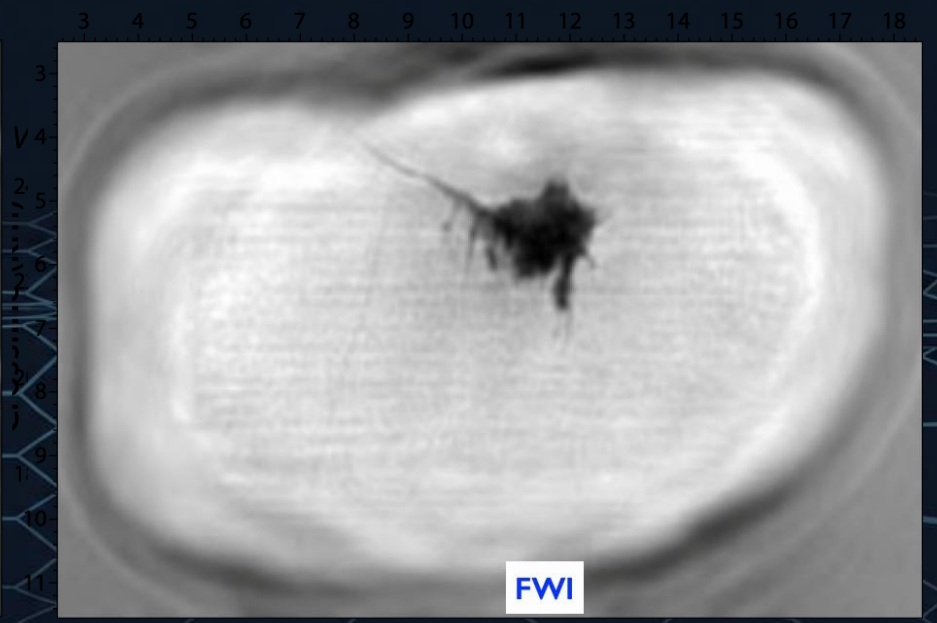


SUSTech Southern University of Science and Technology





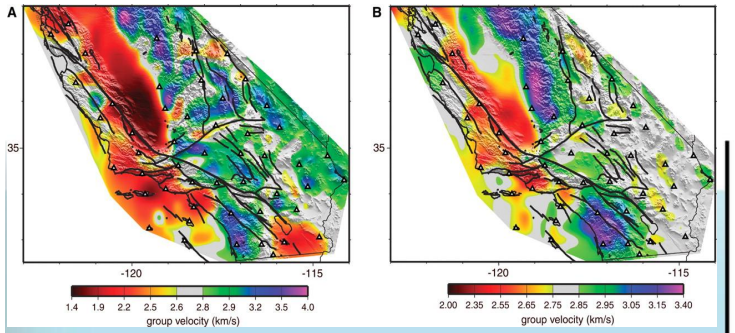




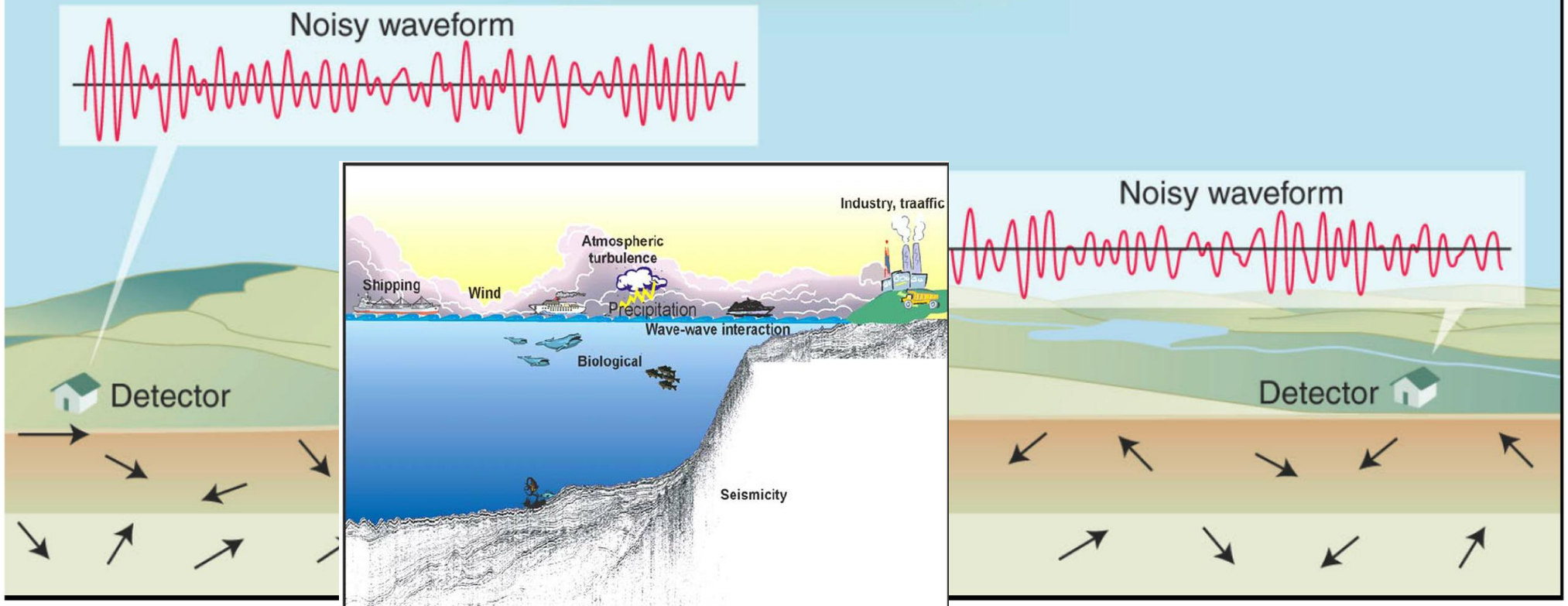
Velocity models of the Valhall field in Norway (L. Sirgue and O. Barkved, BP)

SUSTech Southern University of Science and Technology

Ambient noise tomography

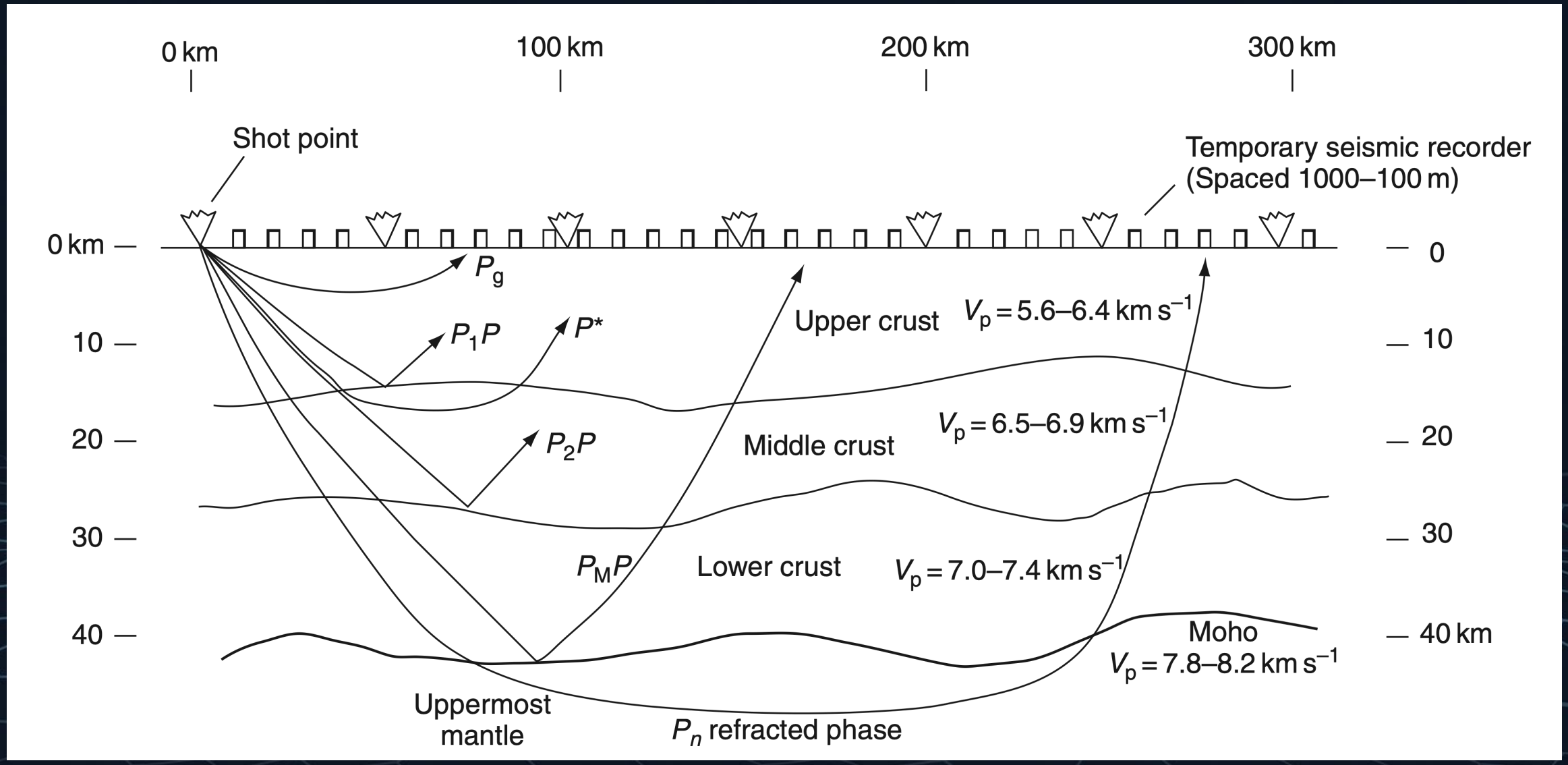


(Shapiro *et al*, Science, 2005)

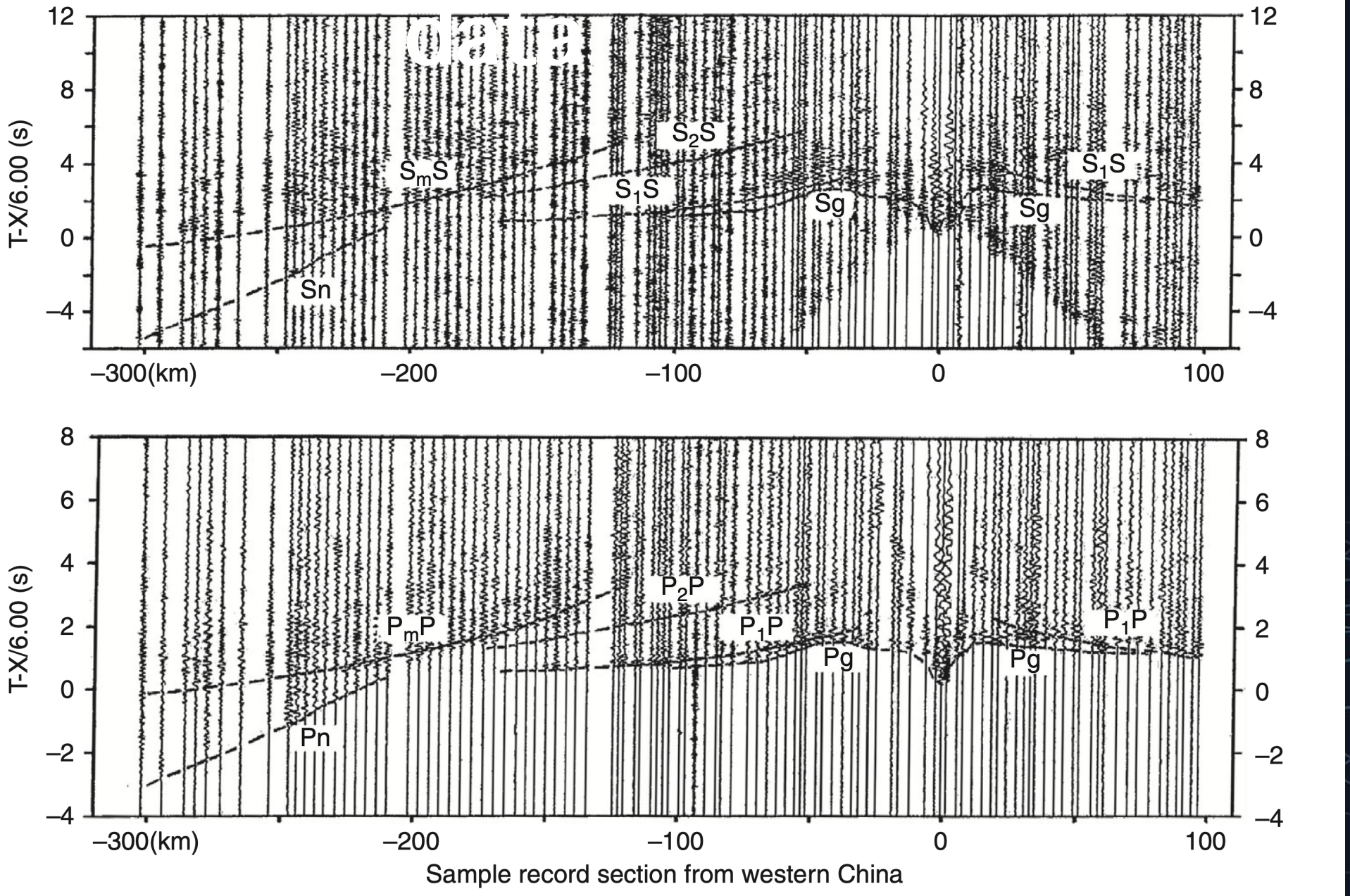


SUSTech Southern University of Science and Technology

Refraction/reflection experiments



Refraction/reflection

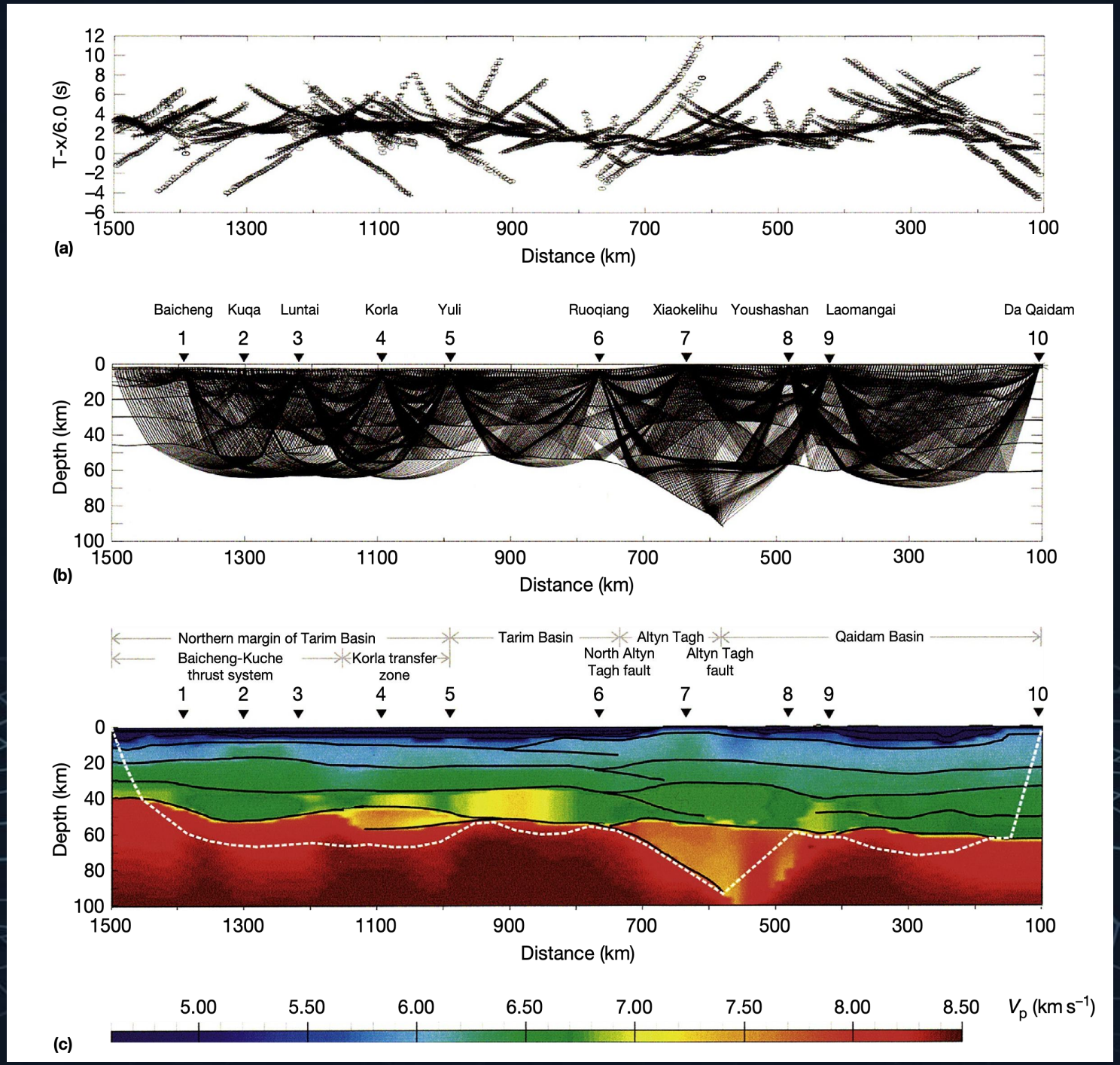


Sample record section from western China

- Pg stays in the crust
- PmP bounces off the Moho
- Pn crosses the Moho

SUSTech Southern University of Science and Technology

An example at northern margin of the Tibetan Plateau

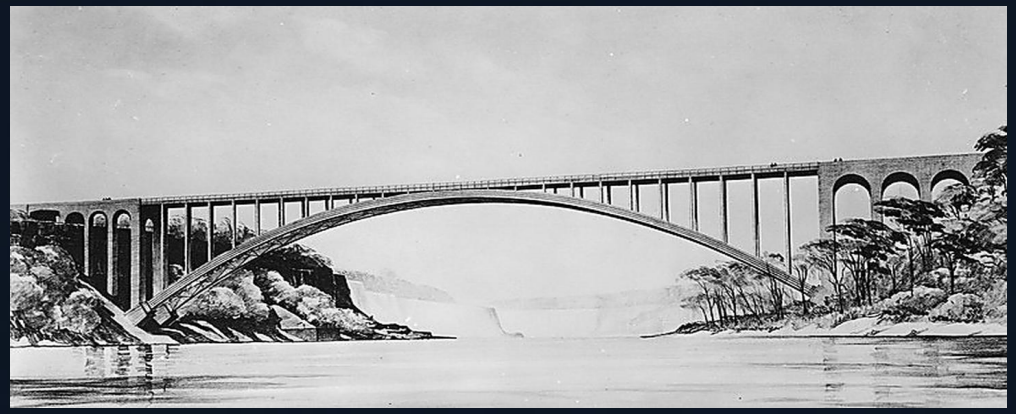


SUSTech Southern University of Science and Technology

Multi-disciplinary investigations

"Models will more faithfully simulate the whole machine, drawing on seismic, mineral physics and subtle geophysical observations such as gravity variations. Another 40 years should do it"
— Science 125 questions, 2005

Wavespeeds
Attenuation
Anisotropy
Density
Reflectivity



Temperature
Water content
Composition
Melting
...

What we have



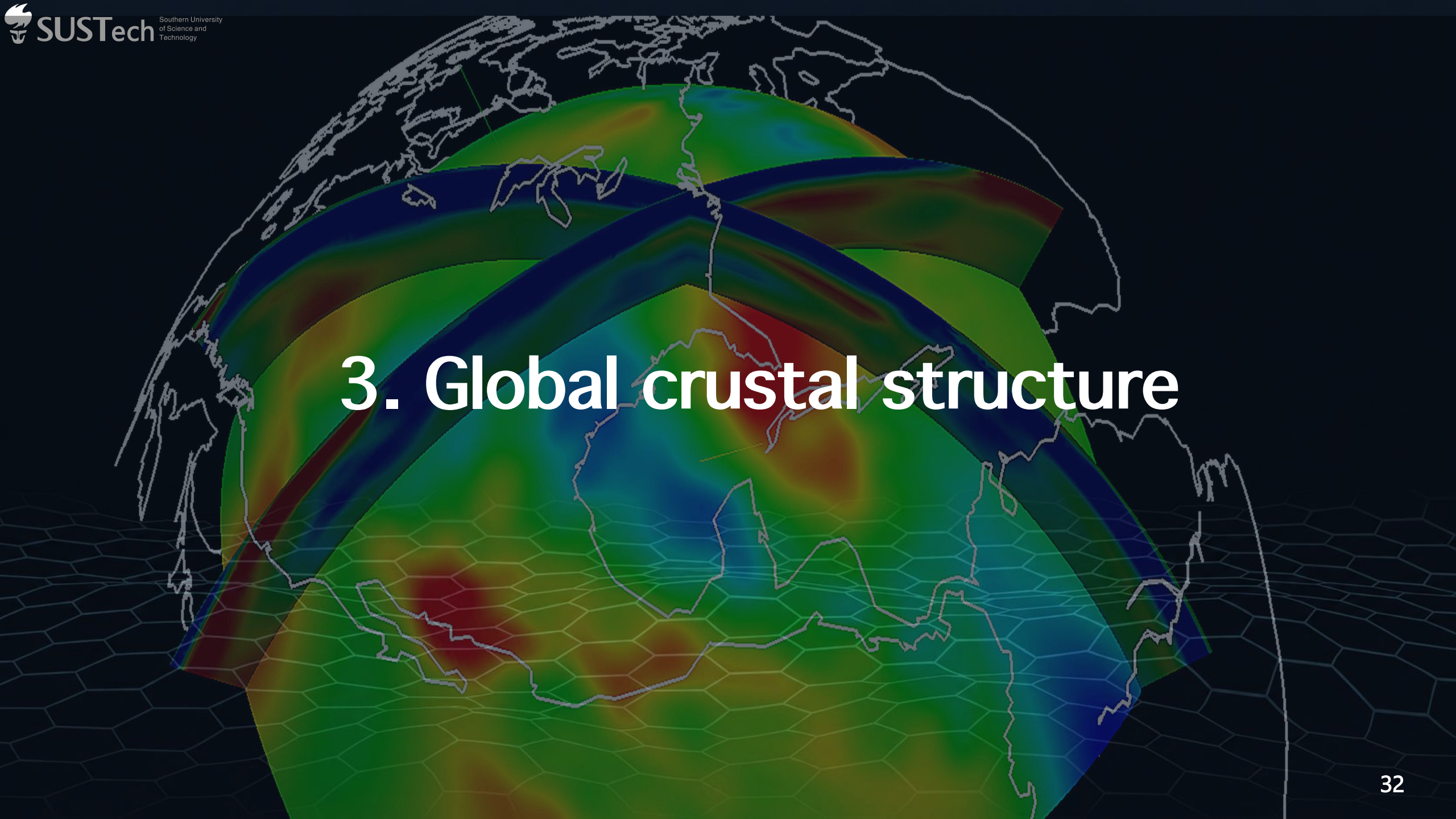
Seismologist

Seismology
Mineral Physics
Geodynamics
Earth Sciences
Tectonics
Petrology
Geochemistry

What we want



Earth Scientist



3. Global crustal structure

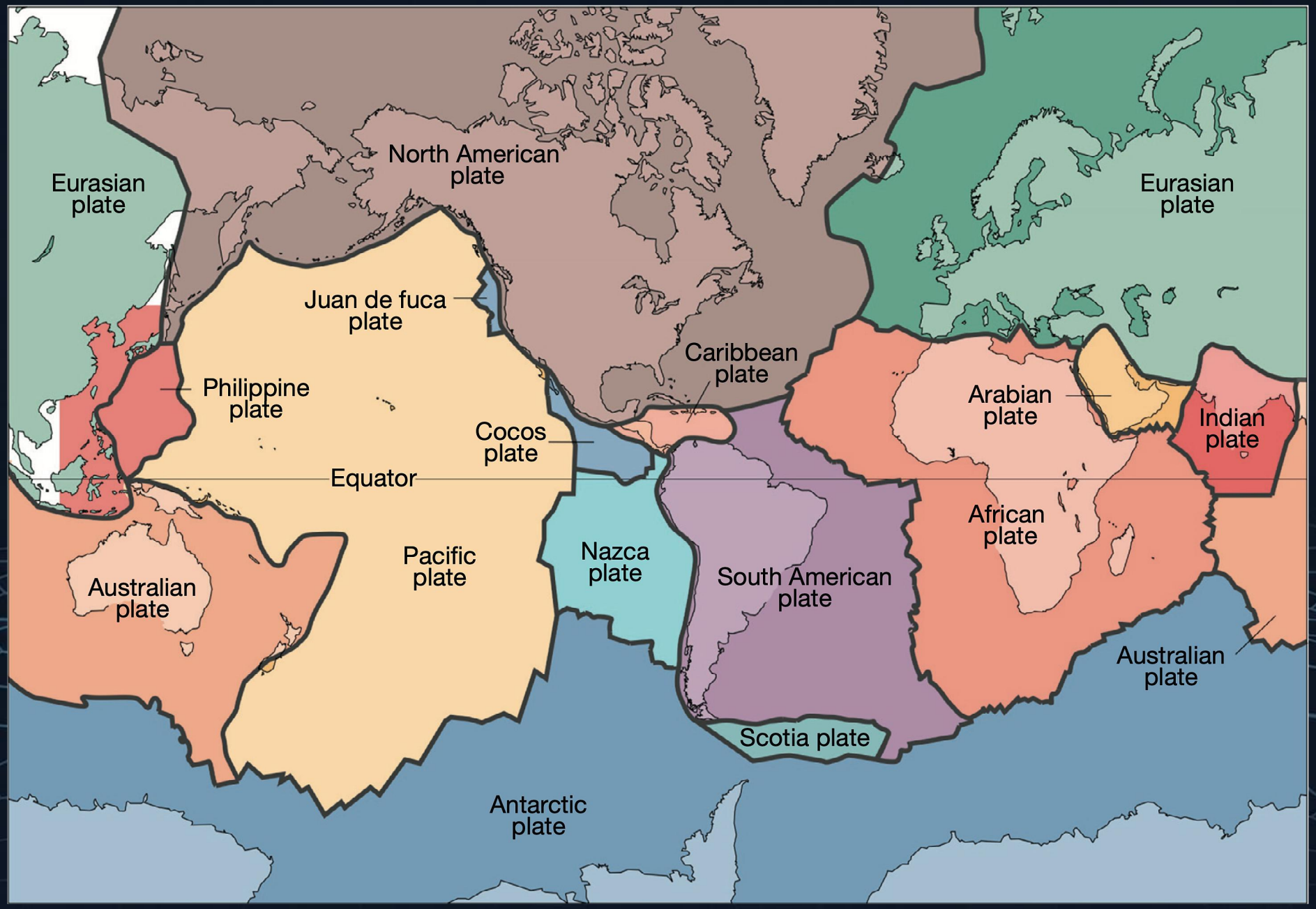
SUSTech Southern University of Science and Technology

Importance of studying the crust

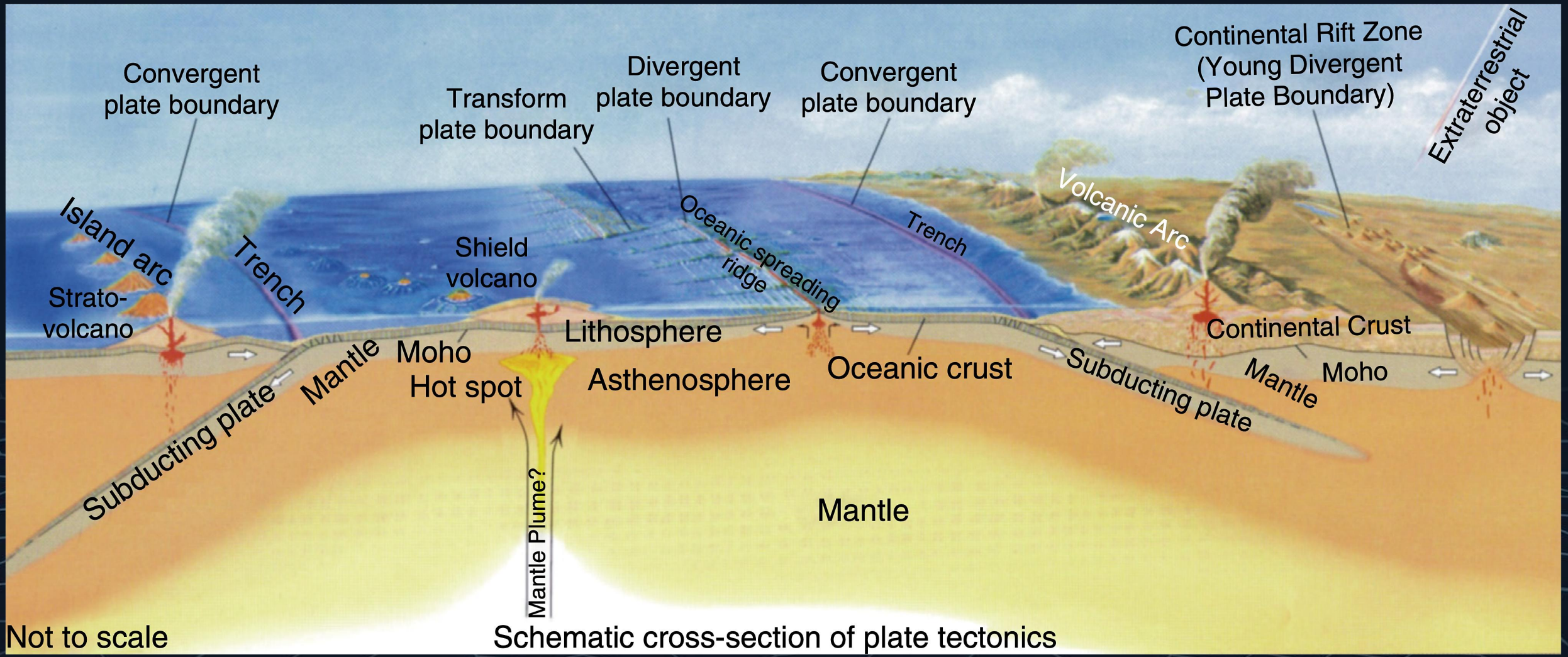
- Record of the evolution of our planet
- Nature resources (oil, gas, minerals …)
- Social challenges for nature hazards, earthquakes, volcanoes
- Melt extracted from the mantle forms the crust (ocean+continent)
- Old picture of crust (top granitic layer Vp=6-6.2 km/s and lower basaltic layer Vp=6.5-7 km/s)
- Recent advances on properties of Moho, mid-crustal discontinuities, deep crustal fluids, geometry of crustal fault, lateral crustal flow, crustal anisotropy

SUSTech Southern University of Science and Technology

Tectonic plates

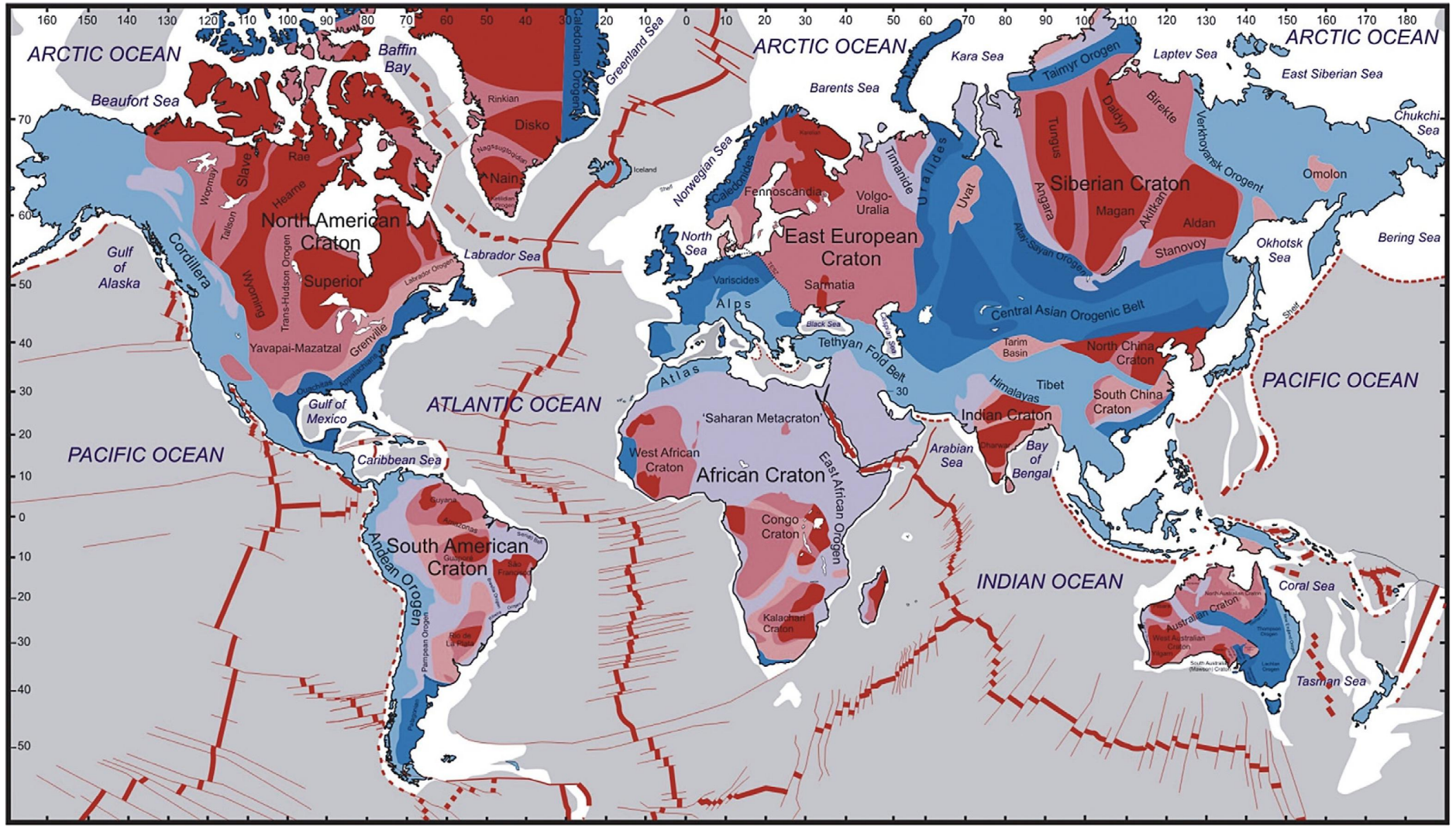


Divergent v.s. convergent plate boundaries



SUSTech Southern University of Science and Technology

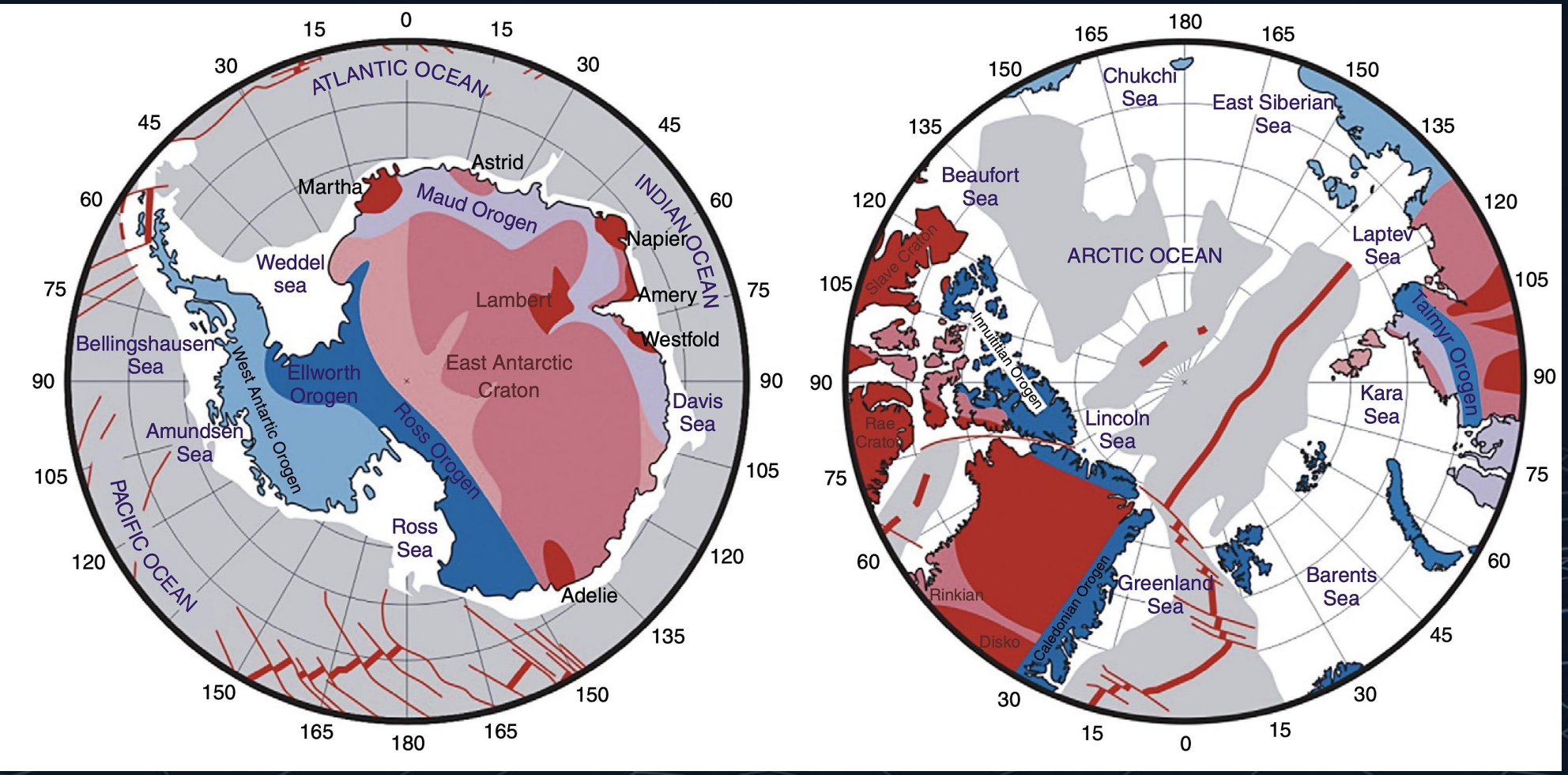
Age of continental basement



Subduction zone
Mid-oceanic ridges and transform faults
Oceanic crust
Continental crust
Shelf
Mesozoic–cenozoic (250–0 Ma)
Late Paleozoic-(400–250 Ma)
Early Paleozoic (543–400 Ma)
Neoproterozoic (1.0–0.54 Ga)
Mesoproterozoic (1.6–1.0 Ga)
Paleoproterozoic (2.5–1.6 Ga)
Archaean (3.8–2.5 Ga)

SUSTech Southern University of Science and Technology

North and South Poles

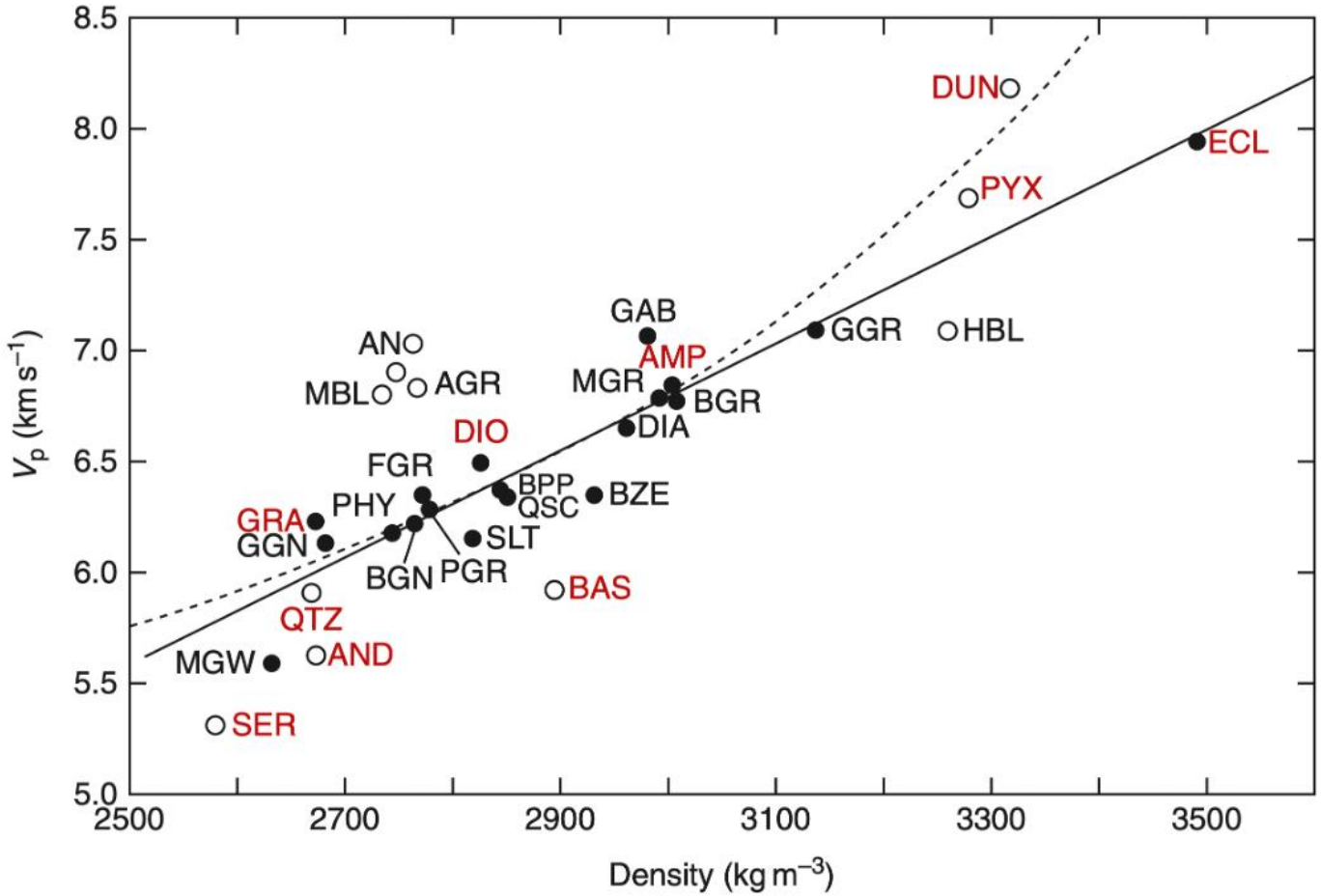


SUSTech Southern University of Science and Technology

Continental versus oceanic crust

Property	Continental crust	Oceanic crust
P-wave velocity (Vp)	~6.45 km/s on average generally increases with depth	~3–6.5 km/s in the upper crust ~6.5–7.3 km/s in the lower crust
Bulk density	~2.8 g/cm³	~3.0 g/cm³
Age	Newly formed to ~4 billion years old	Newly formed at mid-ocean ridges most is younger than ~200 million years
Thickness	Typically 30–50 km can exceed 70 km beneath major mountain belts	Typically 6–8 km, excluding sediment
Common rock types	Granite/granodiorite（花岗闪长岩）common in the upper crust, gneiss（片麻岩） and mafic granulite（麻粒岩） at depth	Basalt flows and diabase（辉绿岩）dikes above gabbro often with a sediment cover

Velocity and density relation (Birch's law) for different rocks



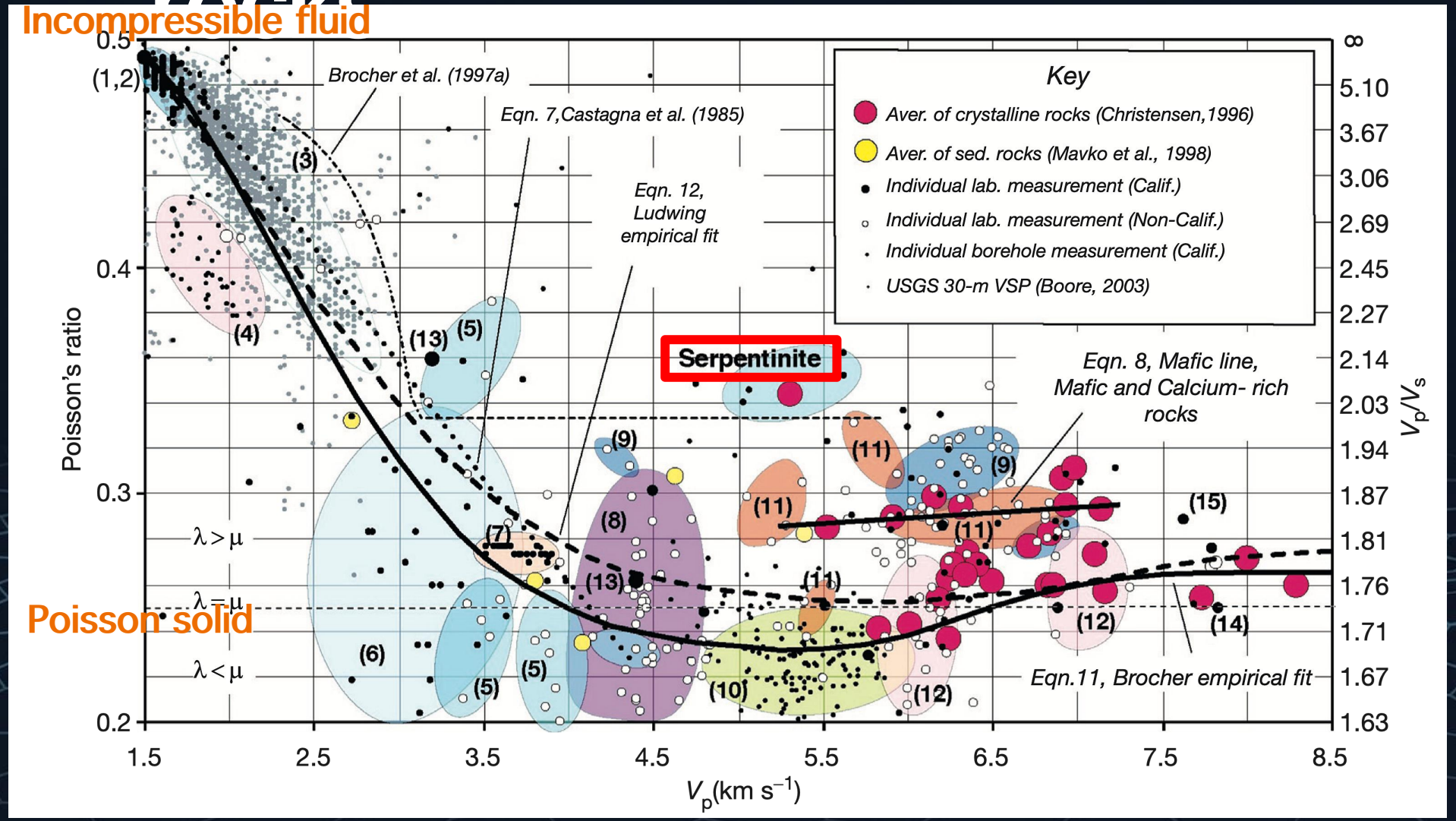
20 km depth and 309 deg

Abbreviation	Rock type
AGR	Anorthositic granulite
AMP	Amphibolite
AND	Andesite
ANO	Anorthosite
BAS	Basalt
BGN	Biotite (Tonalite) gneiss
BGR	Greenschist facies basalt
BPP	Prehnite-pumpellyite facies basalt
BZE	Zeolite facies basalt
DIA	Diabase
DIO	Diorite
DUN	Dunite
ECL	Mafic eclogite
FGR	Felsic granulite
GAB	Gabbro-norite-troctolite

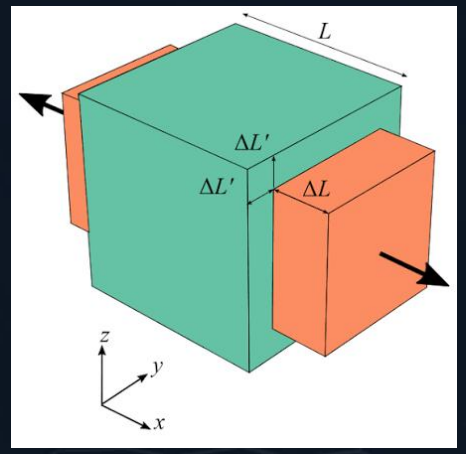
Abbreviation	Rock type
GGN	Granite gneiss
GGR	Mafic garnet granulite
GRA	Granite-Granodiorite
HBL	Hornblendite
MBL	Calcite marble
MGR	Mafic granulite
MGW	Metagraywacke
PGR	Paragranulite
PHY	Phyllite
PYX	Pyroxenite
QSC	Mica quartz schist
QTZ	Quartize
SER	Serpentinite
SLT	Slate

Vp and Poisson's ratio for different rocks

Incompressible fluid



Poisson solid



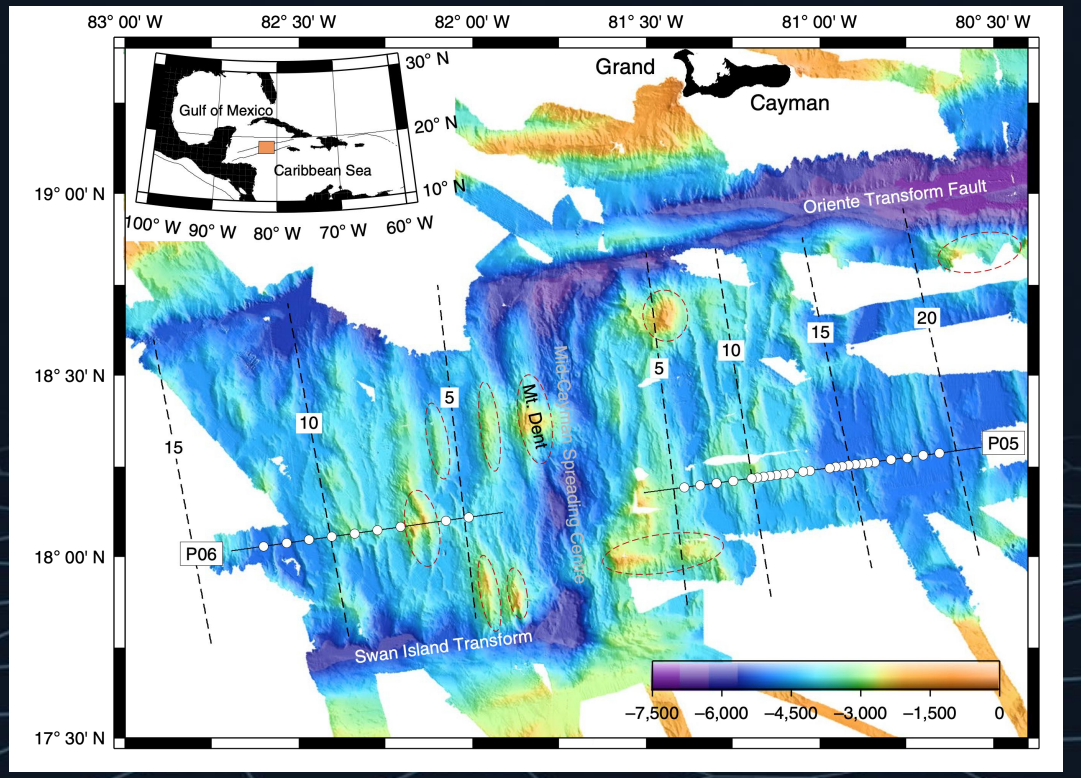
Poisson's effect

(Brocher, BSSA, 2005)

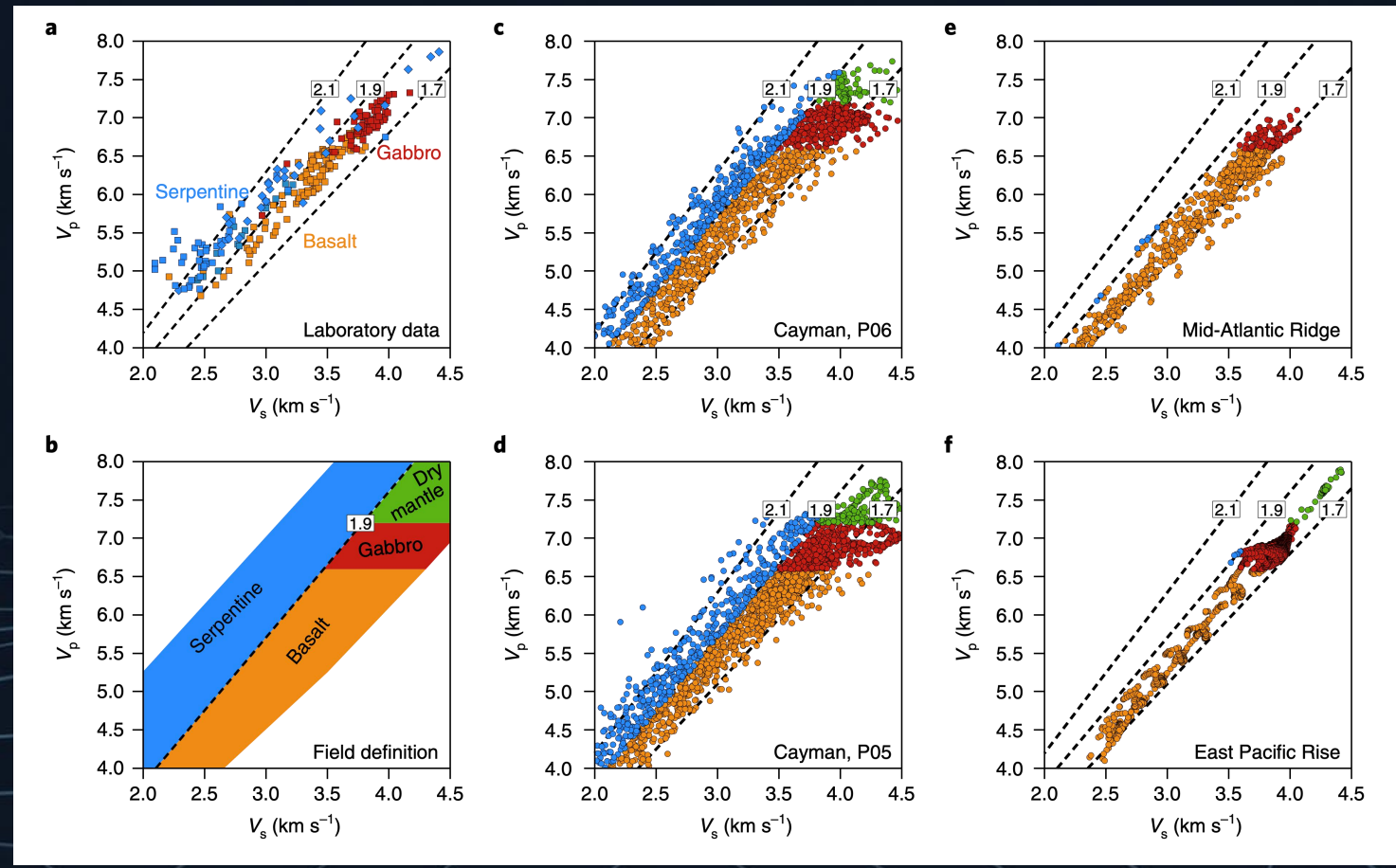
SUSTech Southern University of Science and Technology

Measurements from mid-ocean ridges

Cayman trough

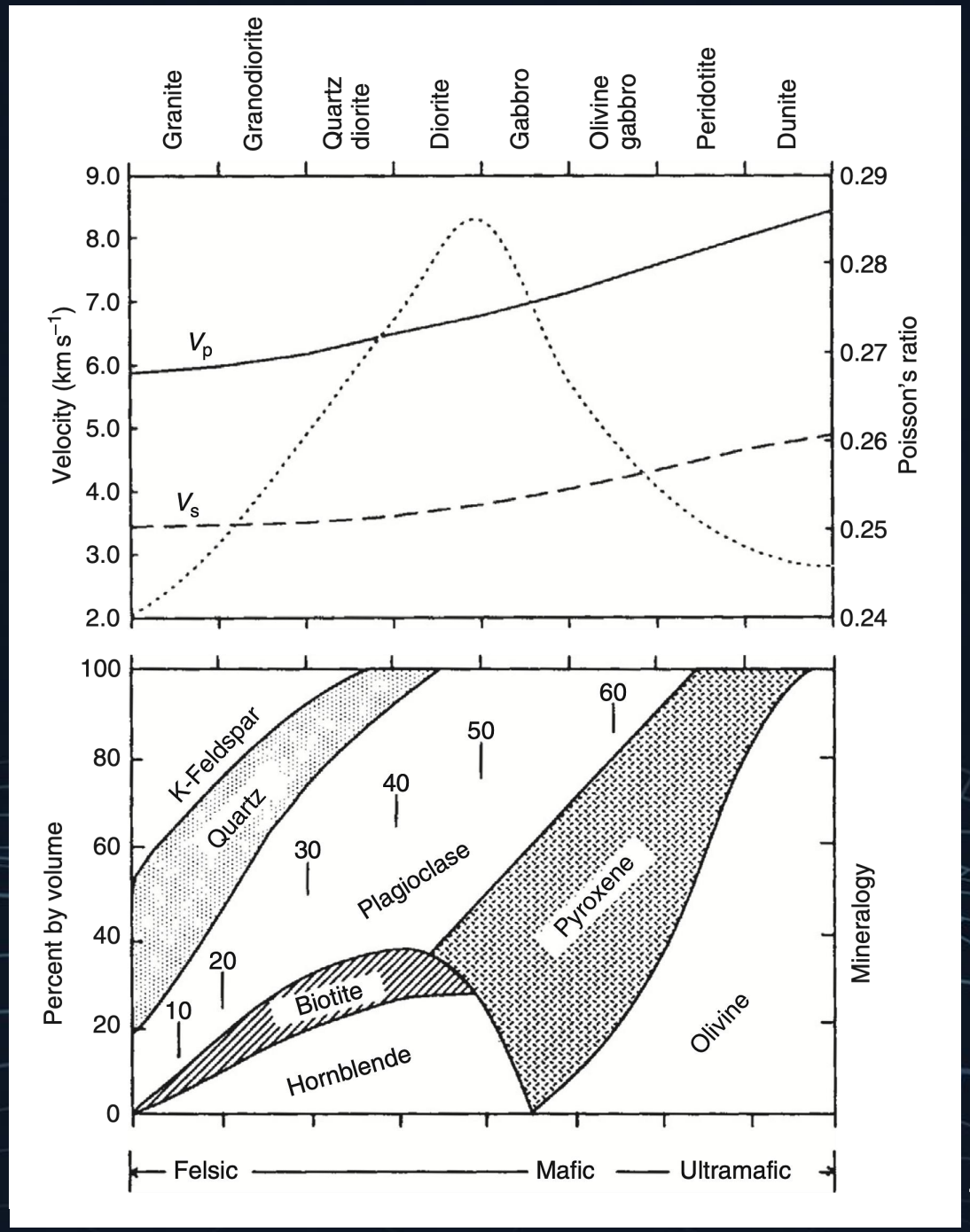


(Grevemeyer et al, NG, 2018)

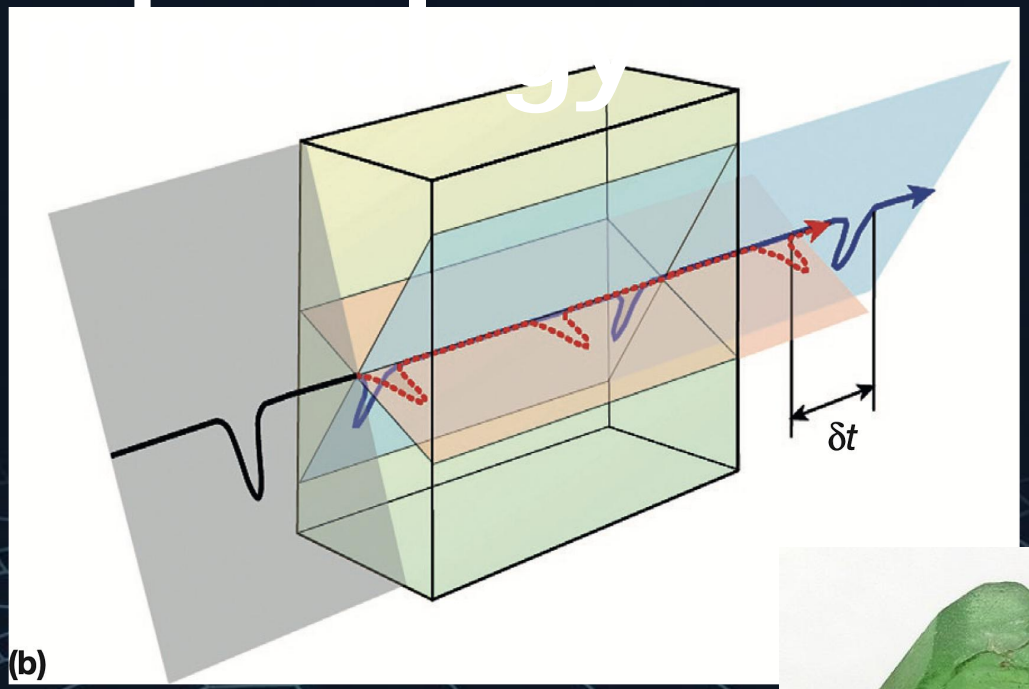


SUSTech Southern University of Science and Technology

Vp, Vs and Poisson's ratio for different mineralogy



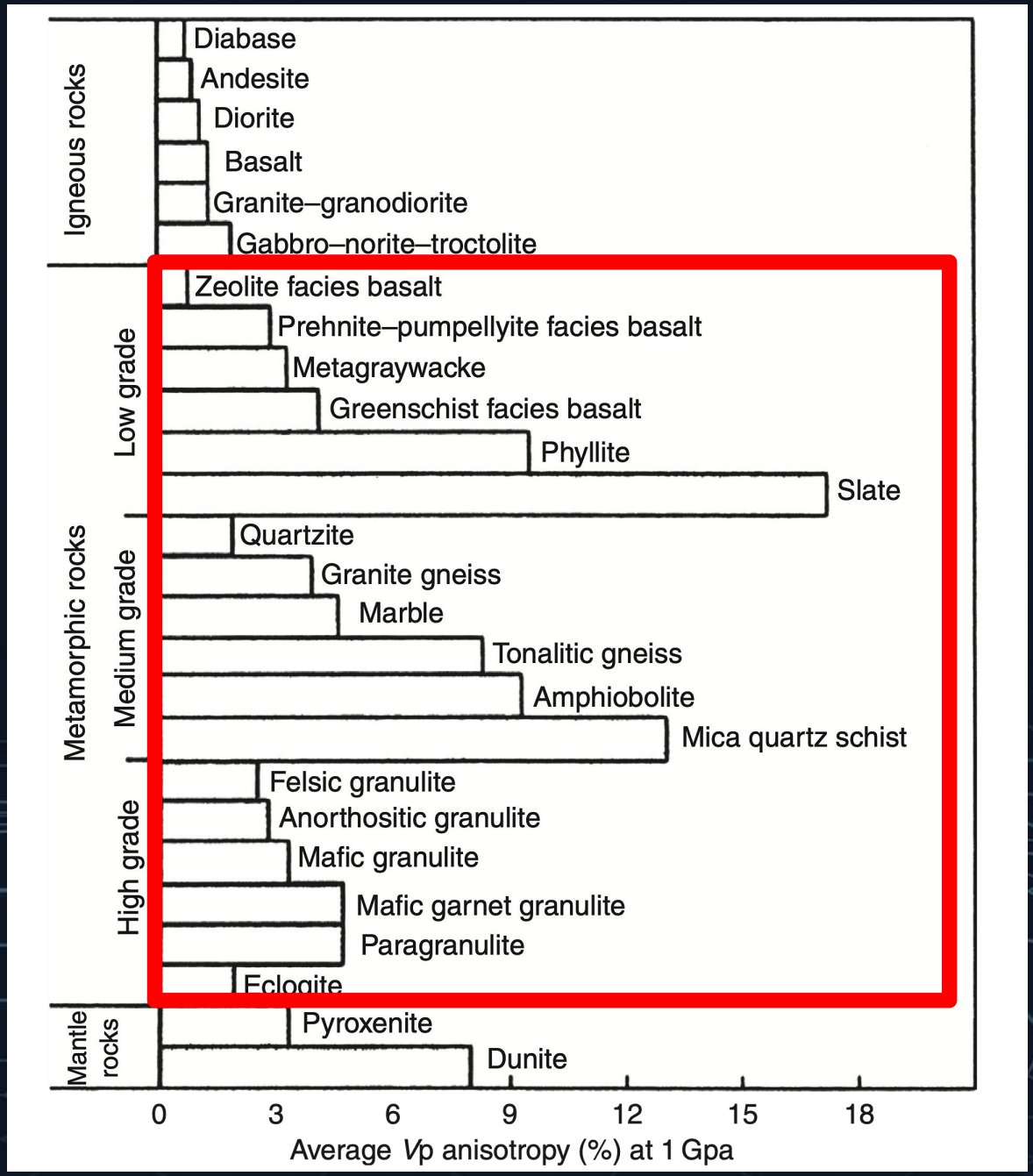
Seismic anisotropy and



Shear wave splitting

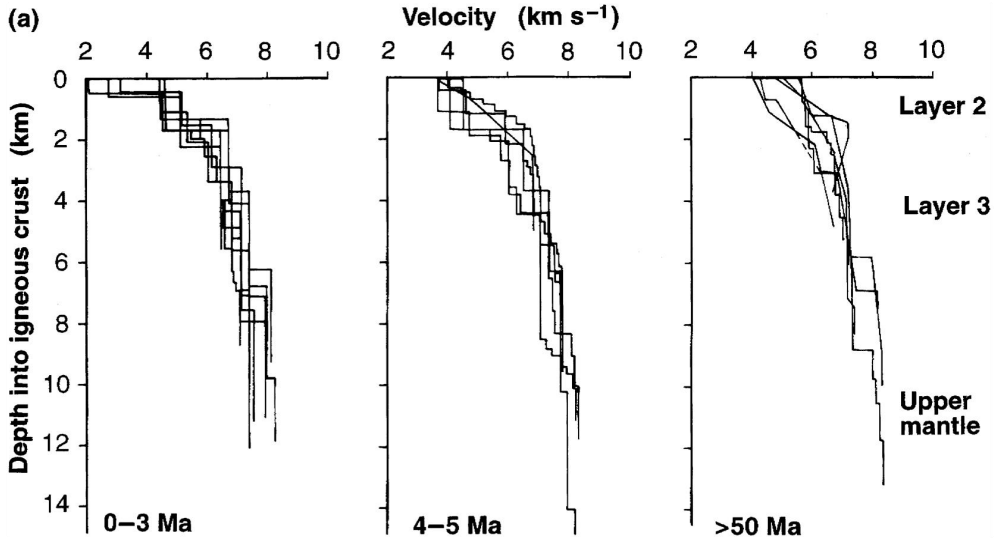


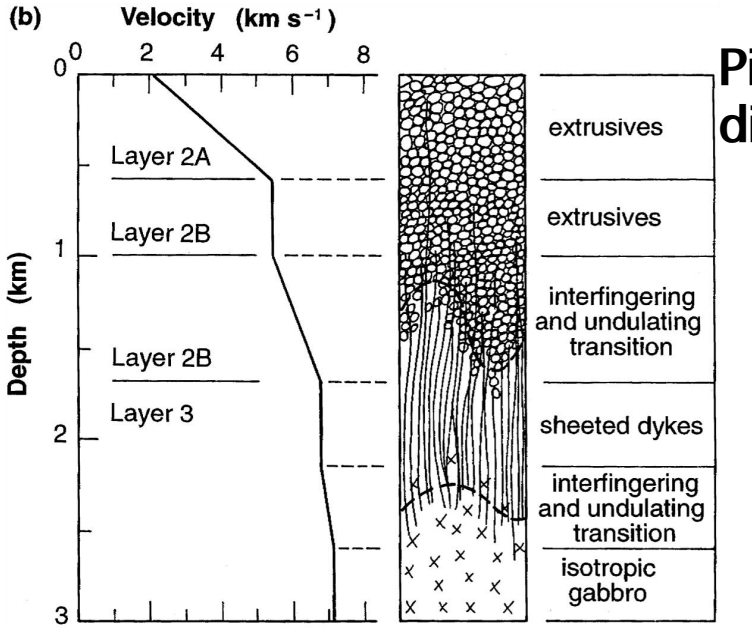
Olivine crystal



SUSTech Southern University of Science and Technology

Typical Oceanic crust





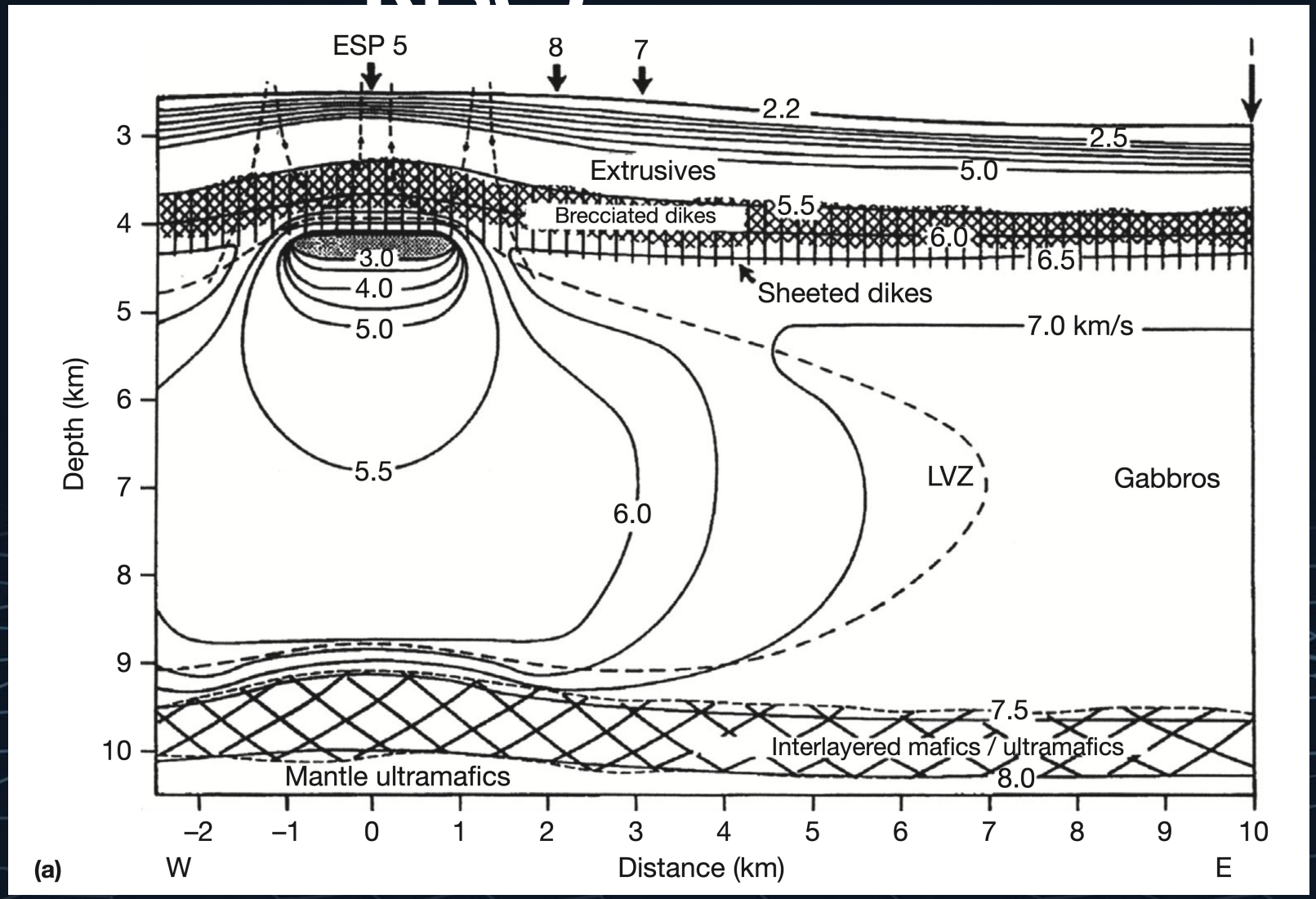
Pillow basalt

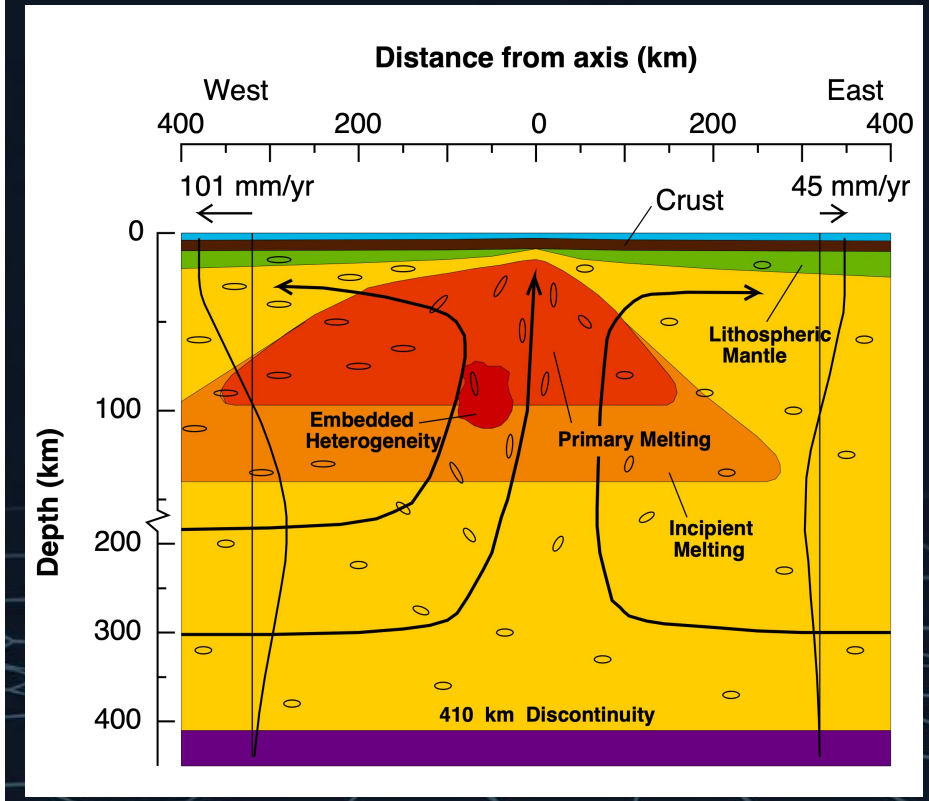
dikes

- Layer 1 underneath 4.5 km seawater, composed of sediment, typically 0.5 km thickness
- Layer 1 to 2 is often transitional
- Layer 2 to 3 is relatively sharp
- Layer 2A pillow basalt (lower velocity)
- Layer 2B diabase dikes (higher velocity)

SUSTech Southern University of Science and Technology

Mid-ocean ridge (East Pacific Rise)

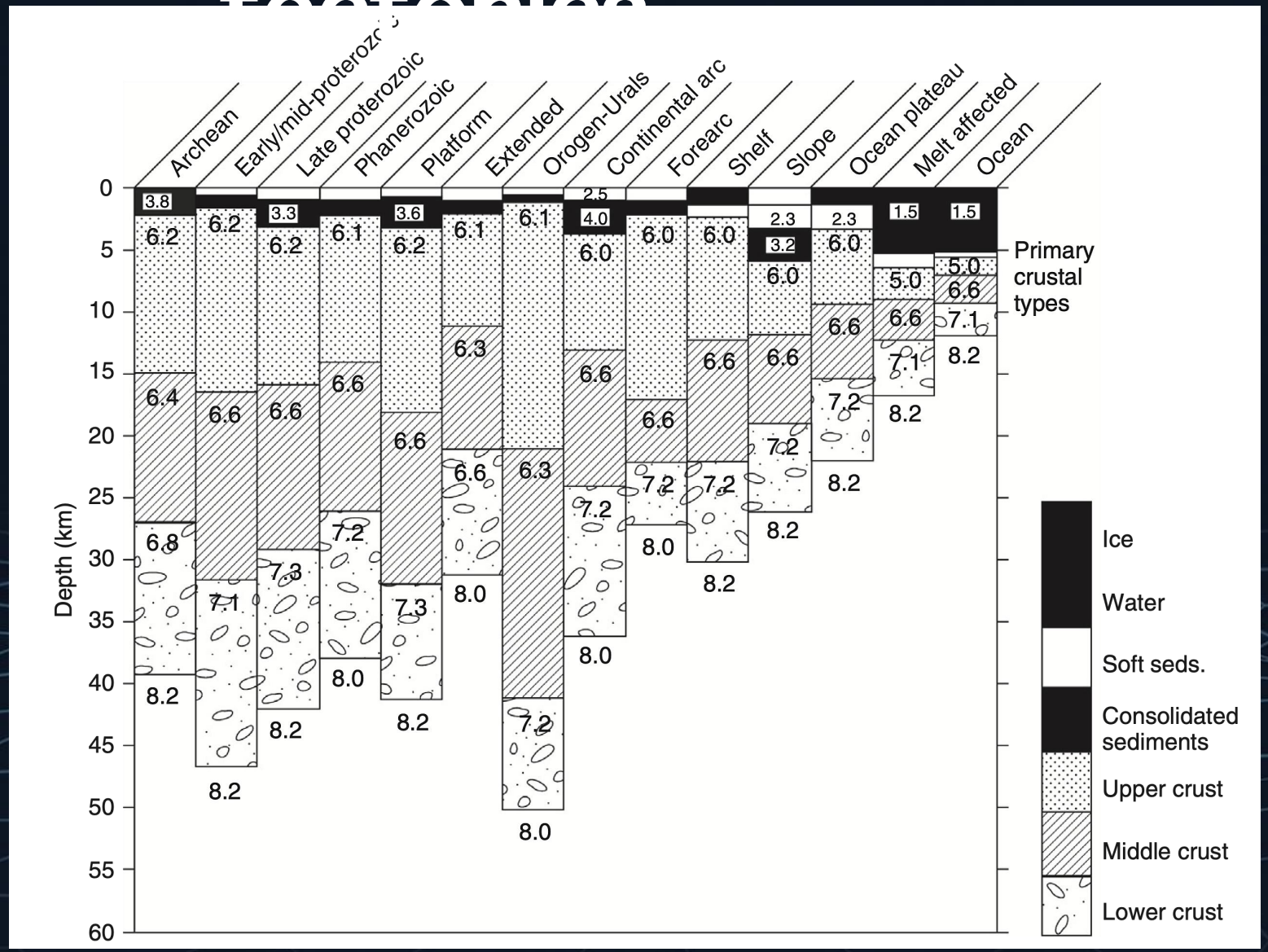




The Melt Seismic Team, Science, 19

SUSTech Southern University of Science and Technology

Velocity profiles for different tectonics



Igneous differentiation of the crust

Silicic melts rise into the upper and middle crust, leaving a mafic lower crust

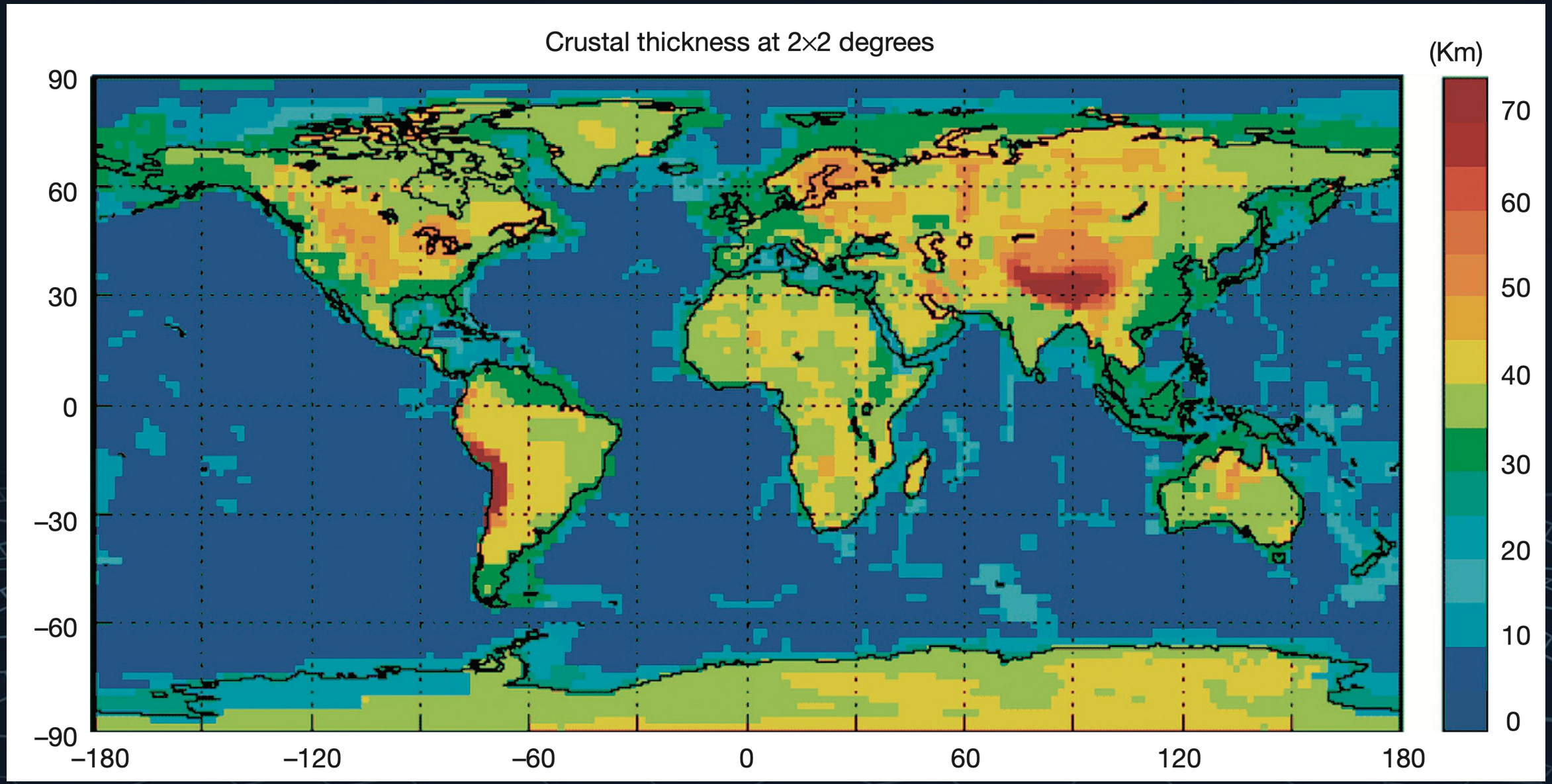
SUSTech Southern University of Science and Technology

History of global crustal models

Model	Year and citation	Grid spacing	How it was built and what changed
3SMAC	1996 Nataf & Ricard	2° × 2°	An a priori crust and upper-mantle model Combined compilations of crustal layer thickness with thermal plate models, mineralogy, and laboratory measurements to predict seismic velocities, density, and attenuation.
CRUST5.1	1998 Mooney et al.	5° × 5°	Compiled seismic refraction profiles and grouped them by tectonic setting. Assigned a representative seven-layer profile to each grid cell, including two sediment layers and three crystalline crustal layers.
CRUST2.0	2000 Bassin et al.	2° × 2°	Refined CRUST5.1 with updated sediment, ice, and crustal thickness compilations. Retained the seven-layer structure and better represented coastlines, continental shelves, and mountain belts.
CRUST1.0	2013 Laske et al.	1° × 1°	Used updated sediment and elevation data to build a distinct eight-layer profile for each cell, with three sediment layers. Crustal types assign properties to crystalline layers; layer thicknesses can vary within each

SUSTech Southern University of Science and Technology

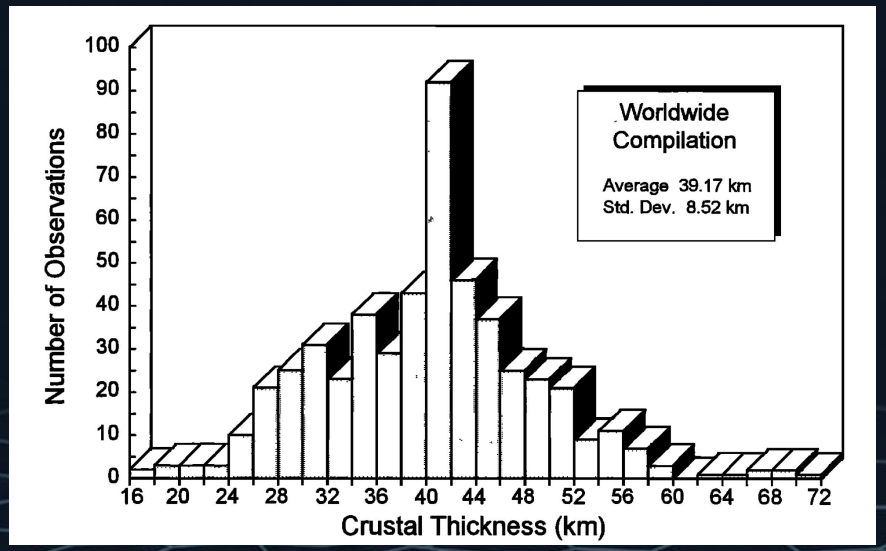
Crustal thickness from CRUST 2.0

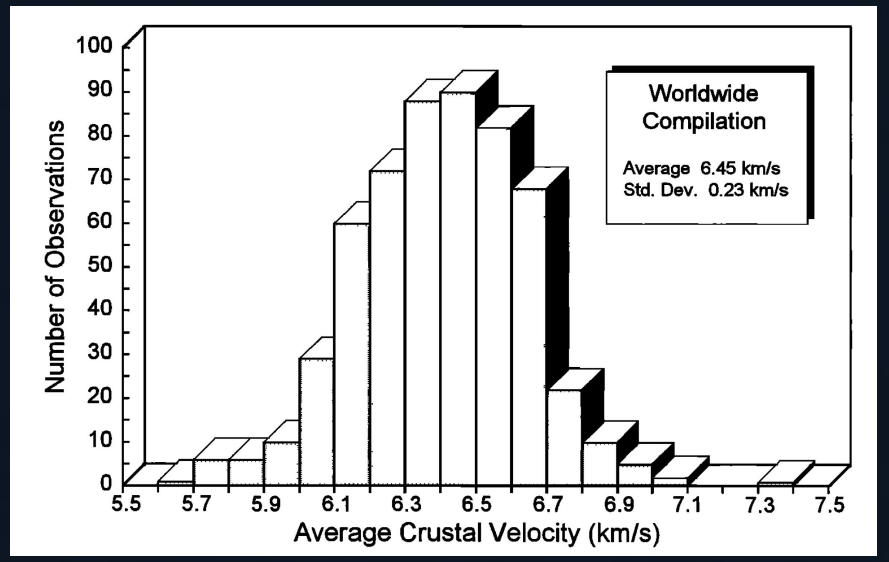


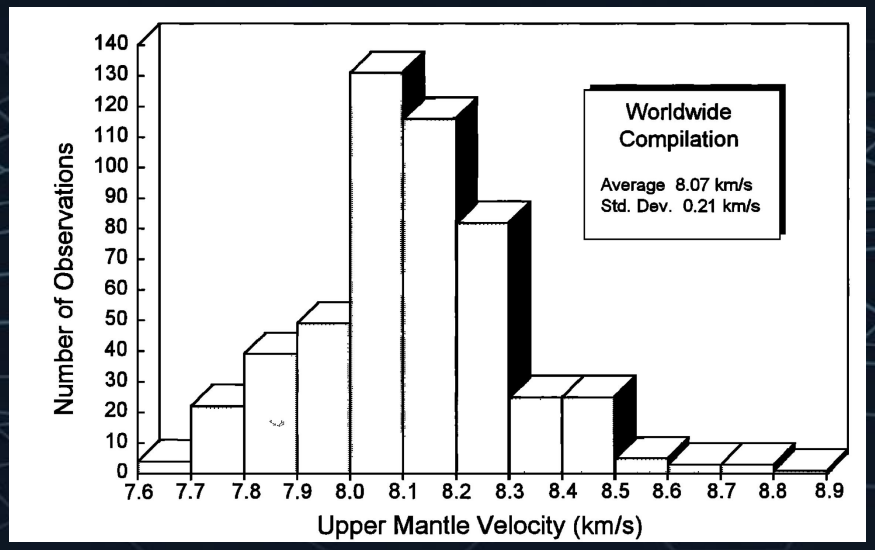
SUSTech Southern University of Science and Technology

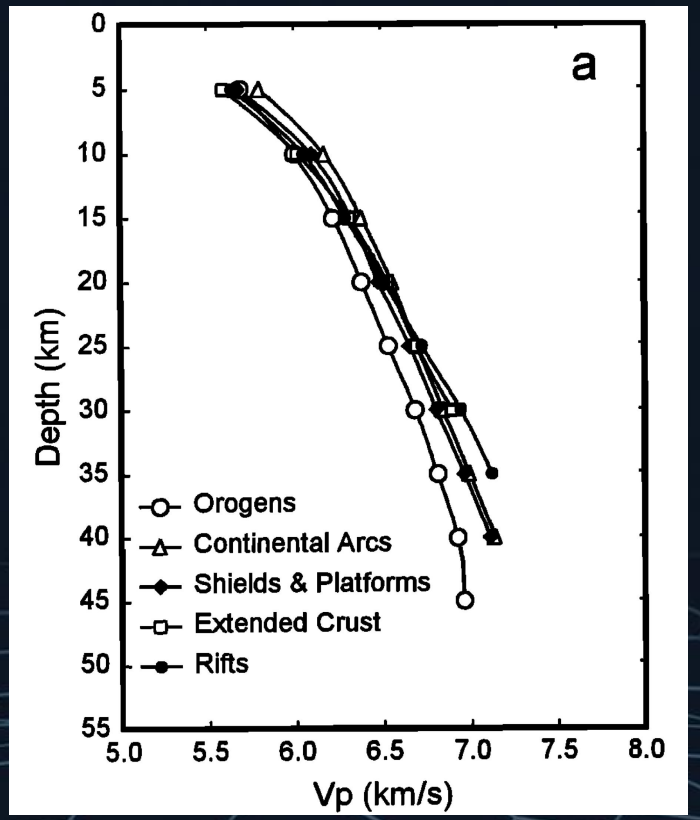
Distribution of seismic parameters

Continental crust





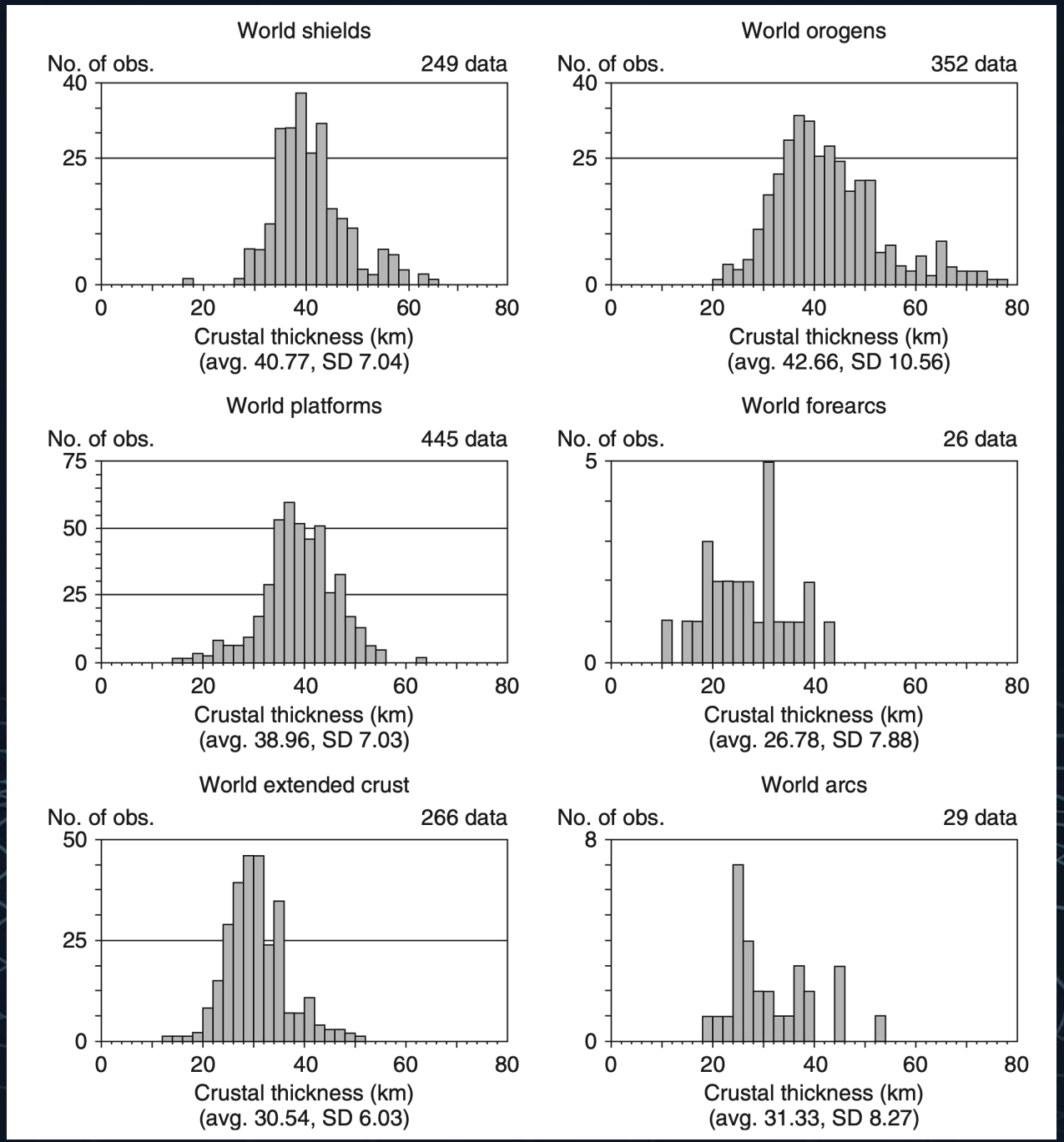




(Christensen and Mooney, JGR, 1995)

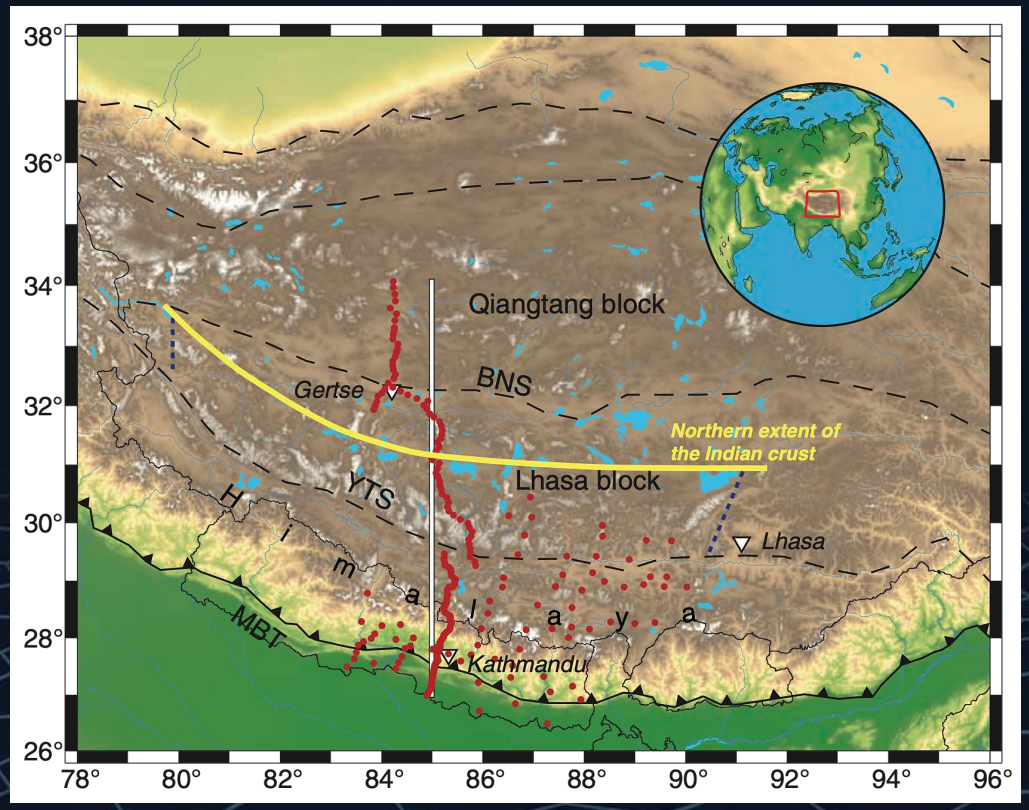
SUSTech Southern University of Science and Technology

Distribution of crustal thickness for different tectonics

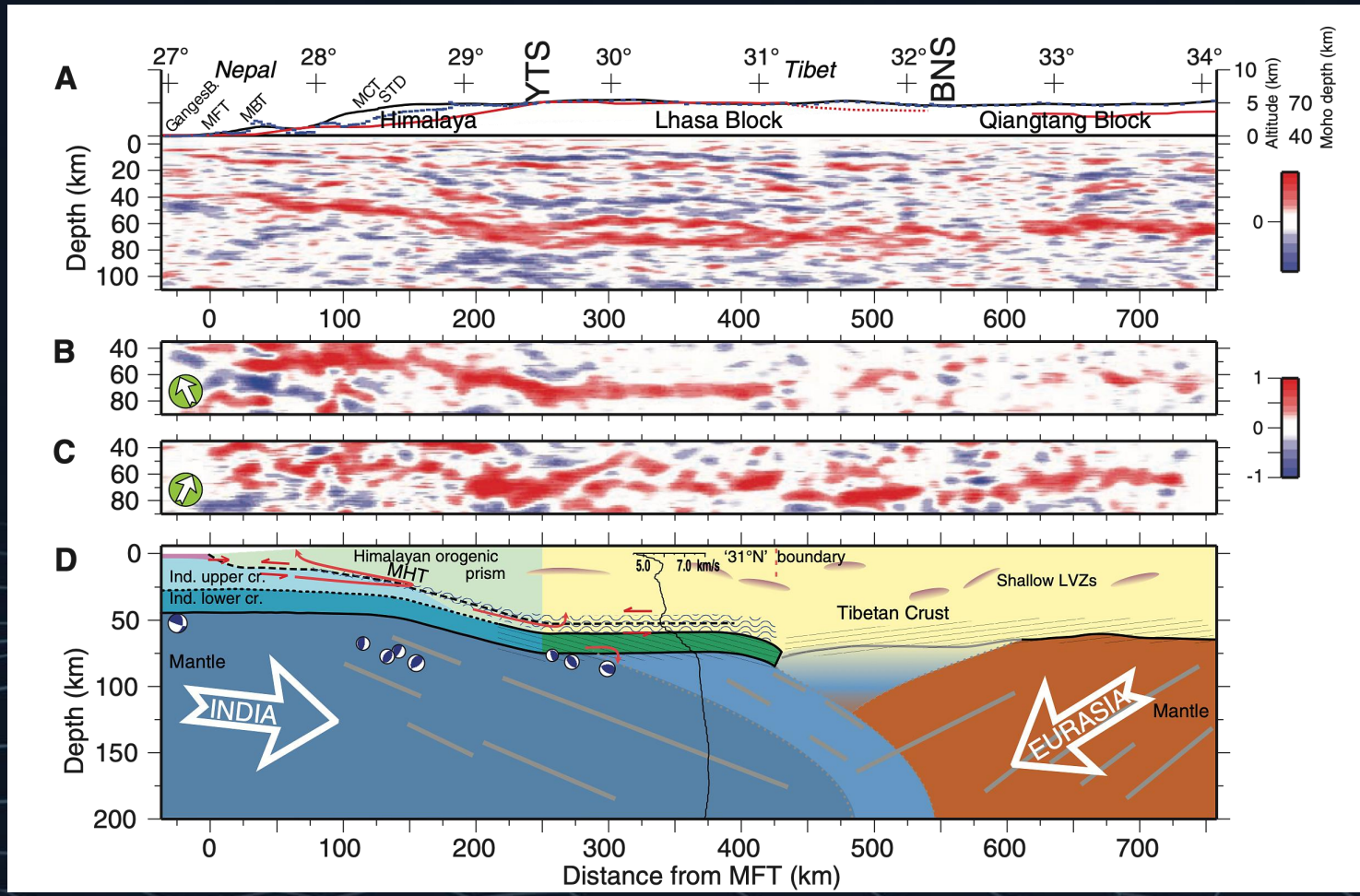


SUSTech Southern University of Science and Technology

Moho underneath Tibet plateau

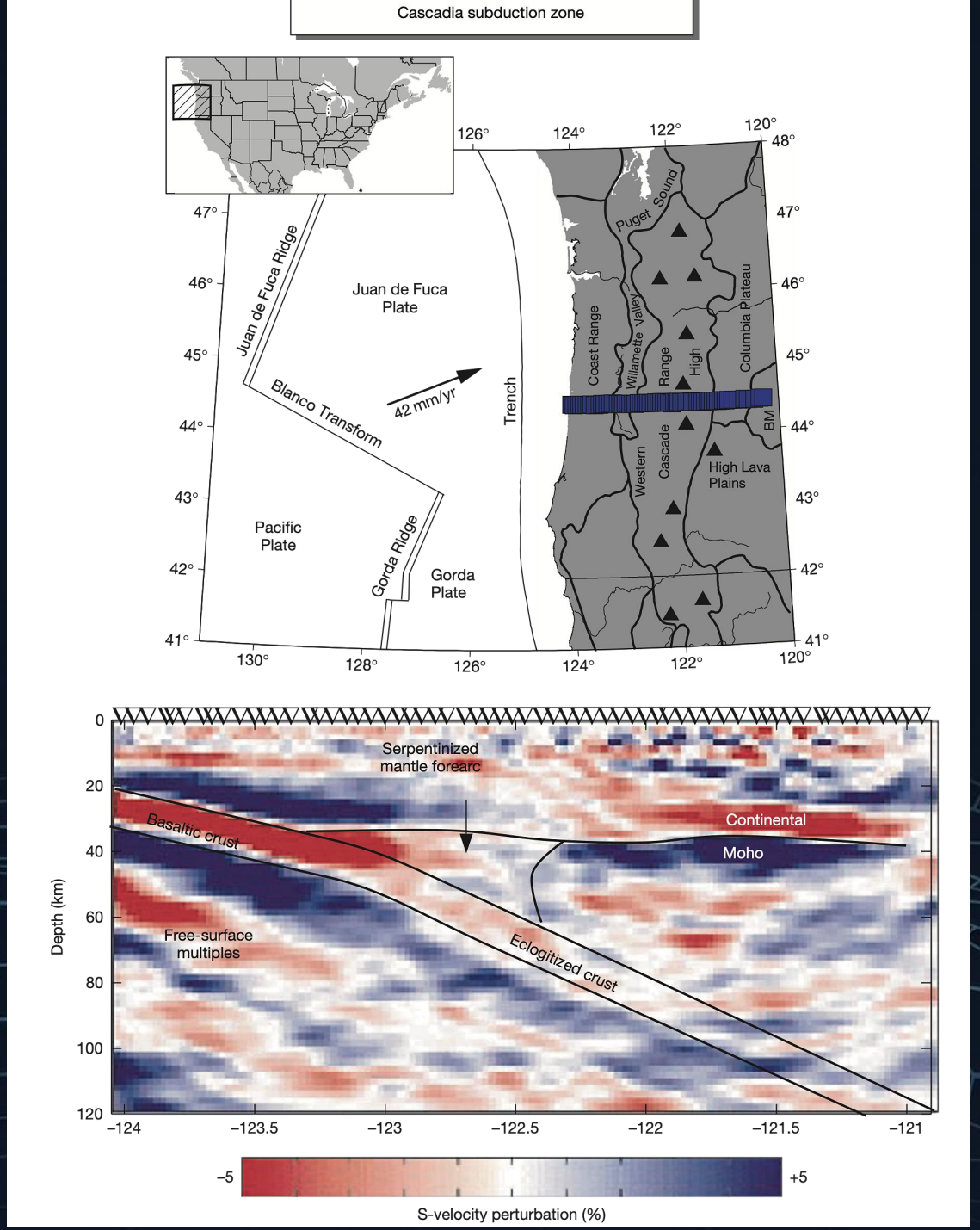


(Nabelek, et al, Science, 2009)

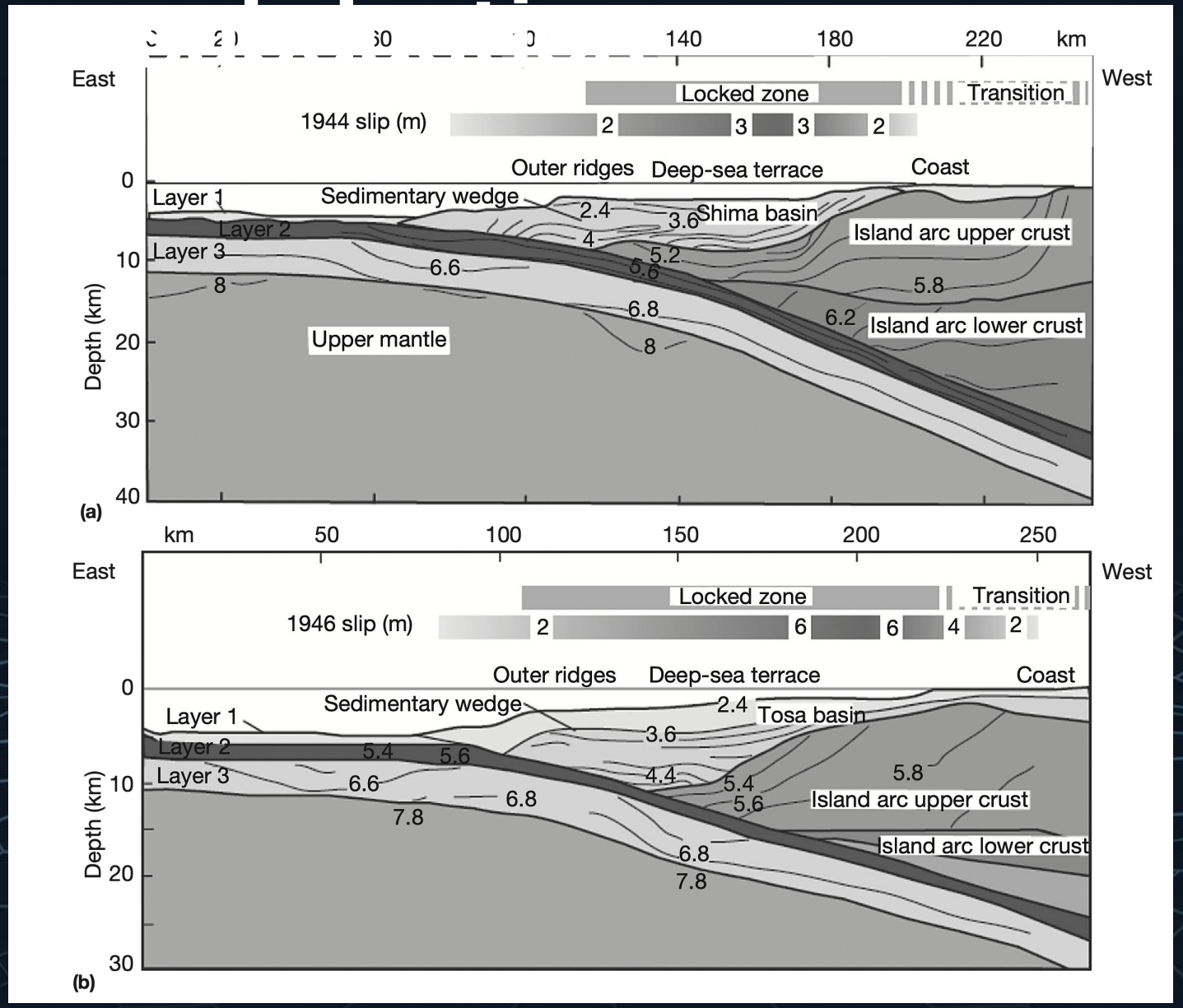


SUSTech Southern University of Science and Technology

Crustal structure underneath the Cascadia subduction zone



Crustal structure for Japan

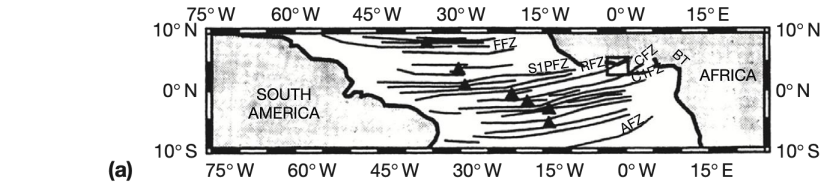


Tonanki subduction zone

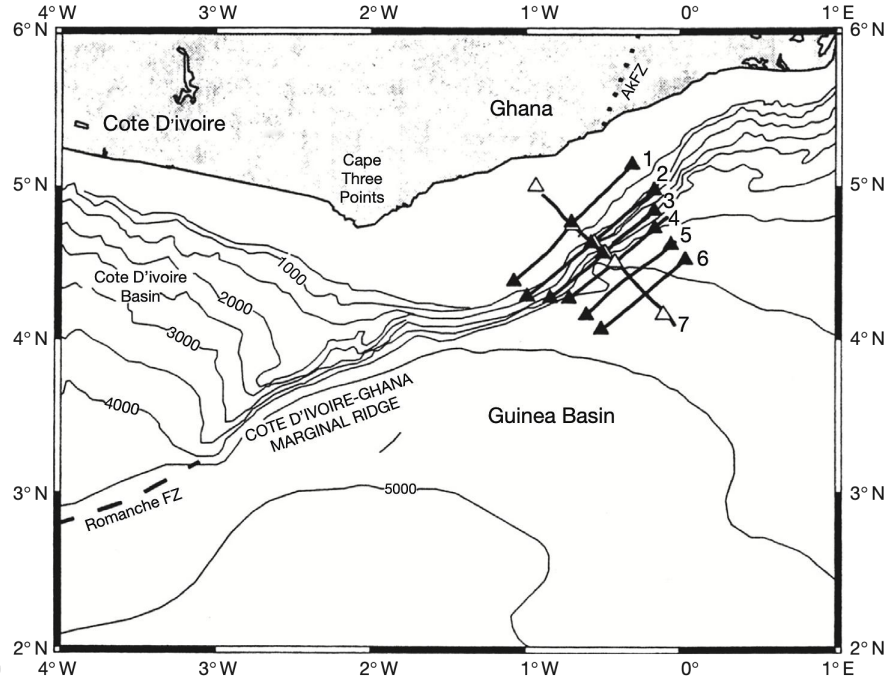
Nankai Trough

SUSTech Southern University of Science and Technology

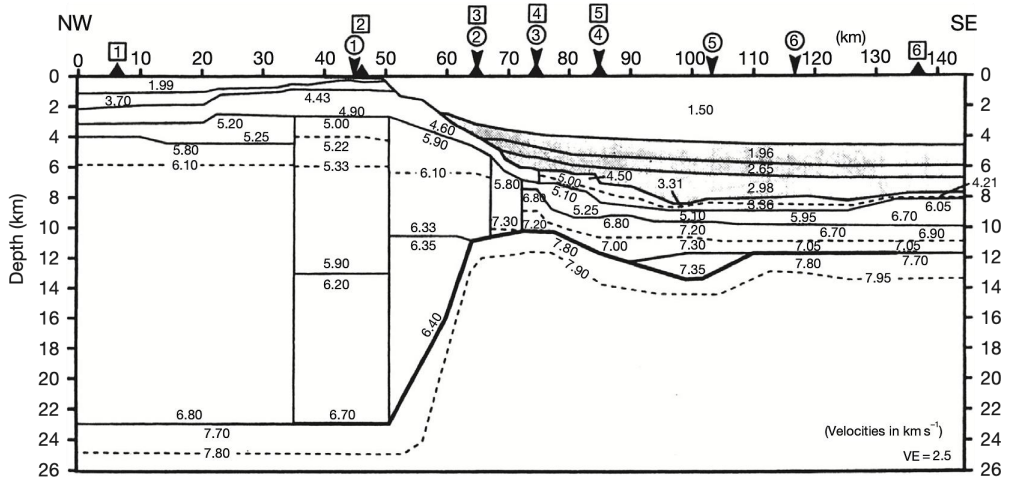
Crustal structure of Passive continental margin



(a)



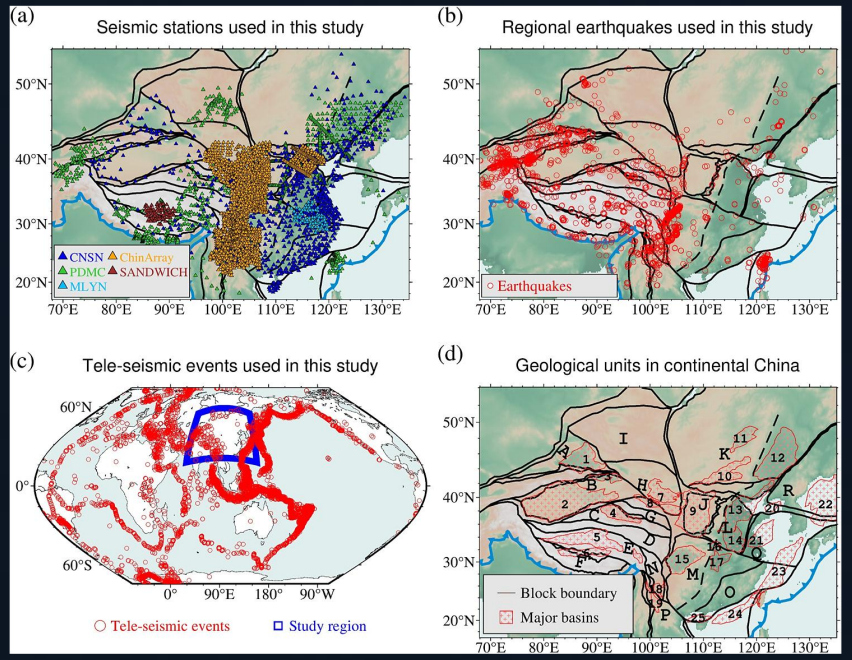
(b)

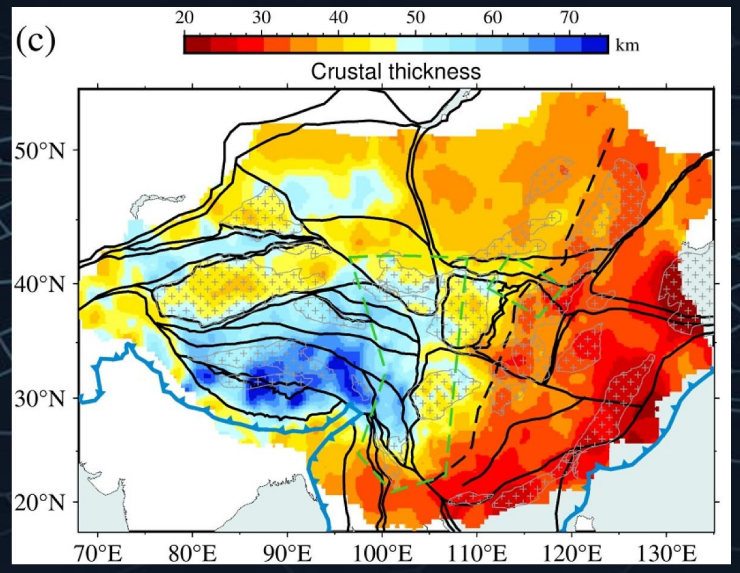


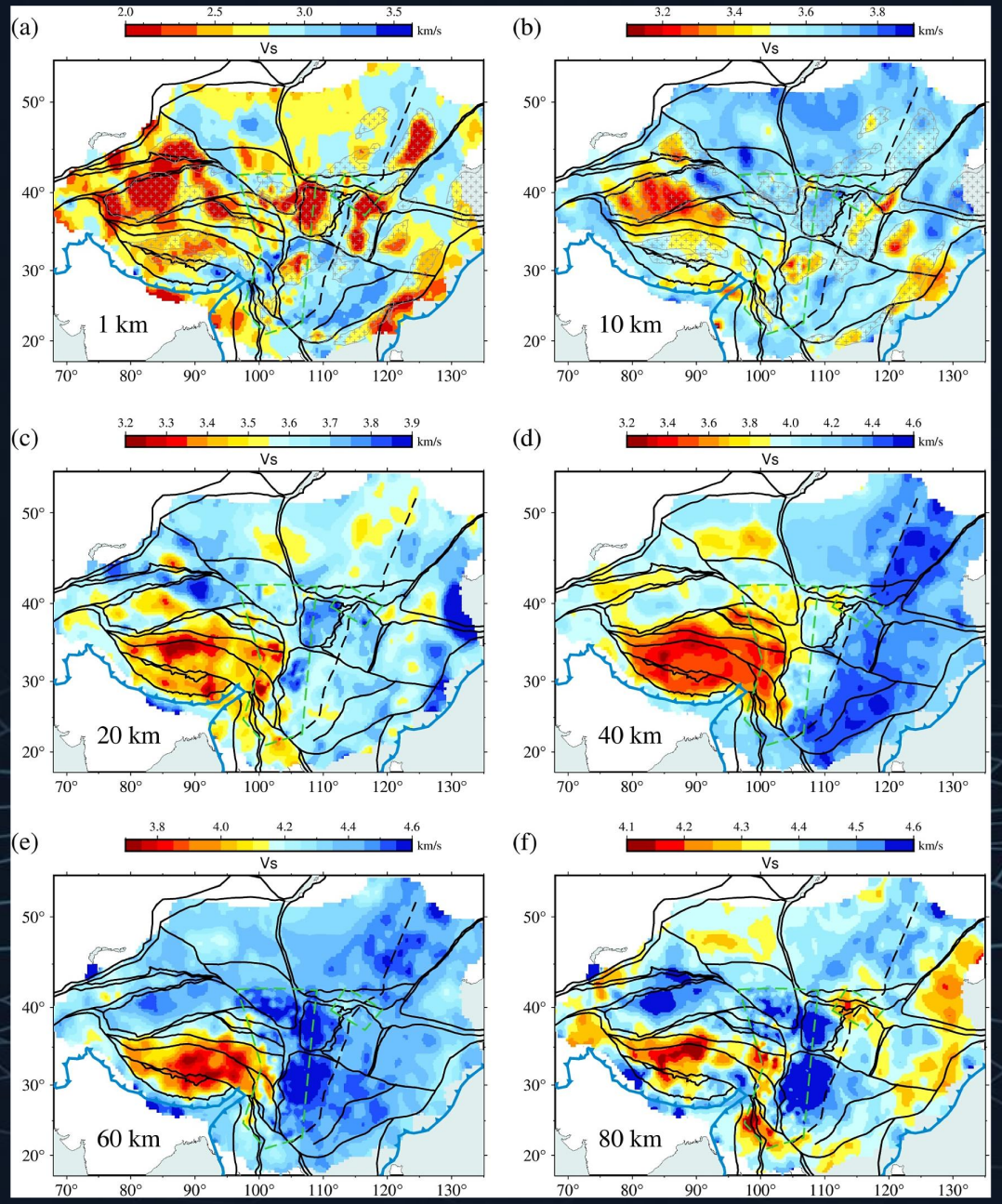
(c)

SUSTech Southern University of Science and Technology

Crustal model for China



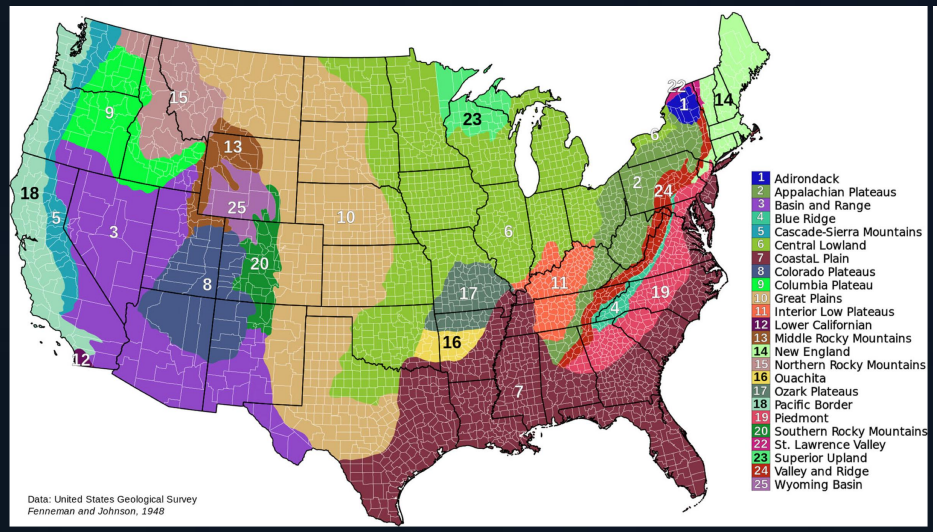


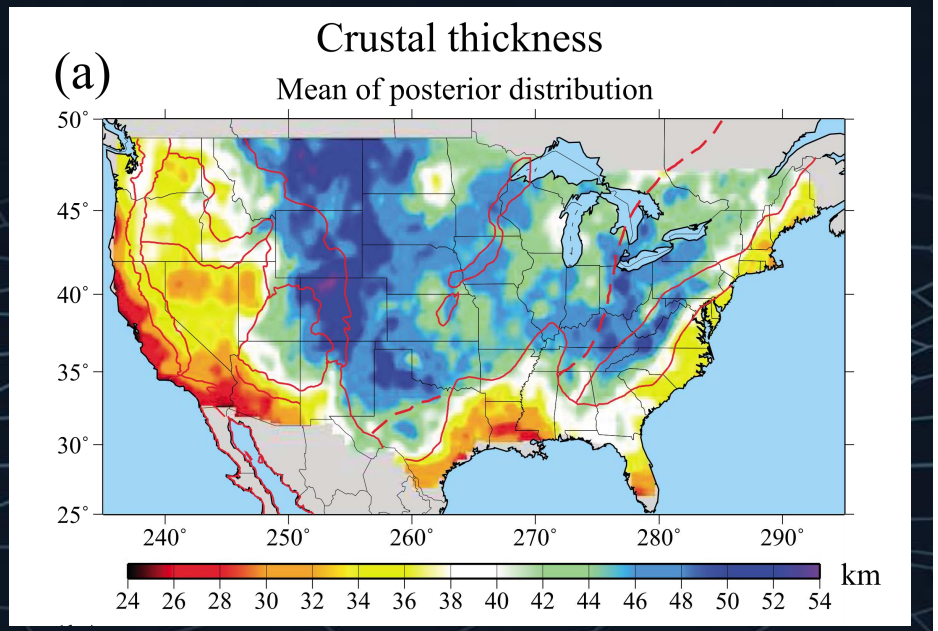


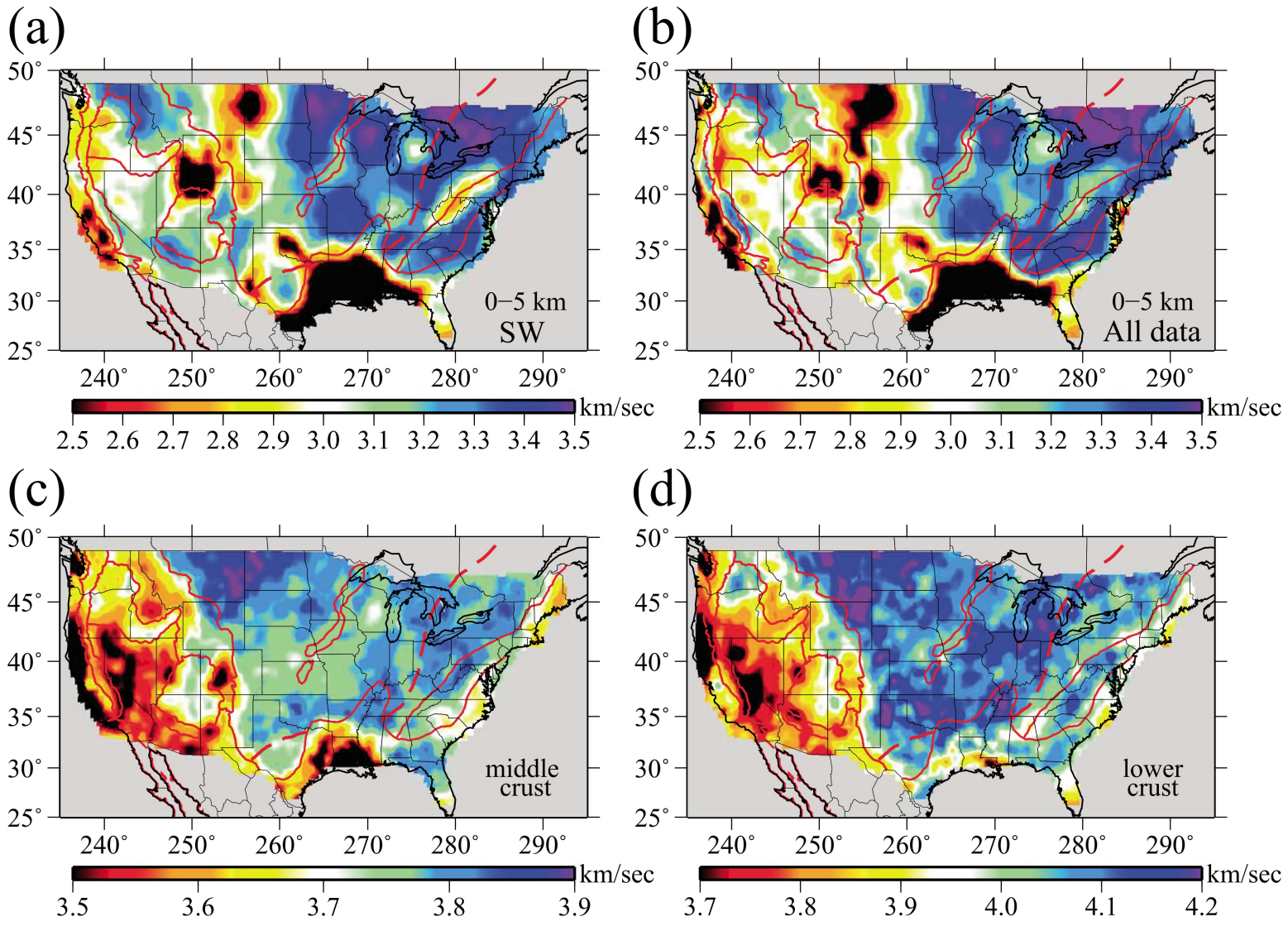
(Xiao et al, JGR, 2024

SUSTech Southern University of Science and Technology

Crustal model for US



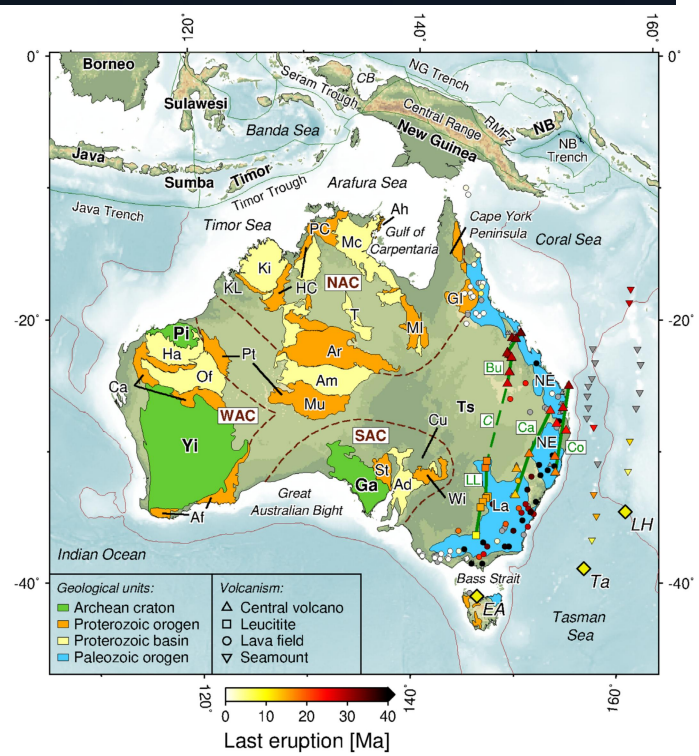




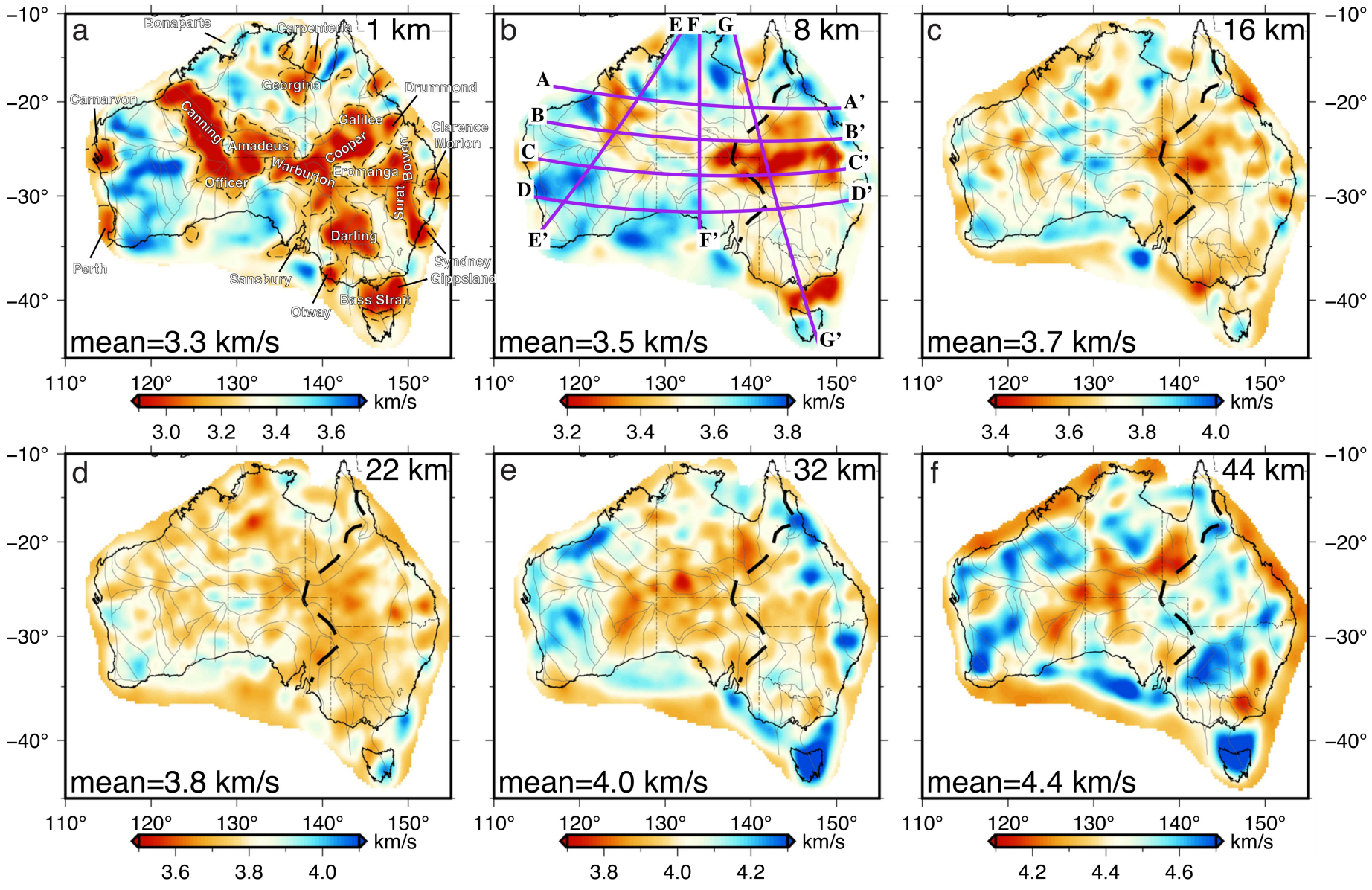
(Shen et al, JGR, 2016)

SUSTech Southern University of Science and Technology

Crustal model for Australia

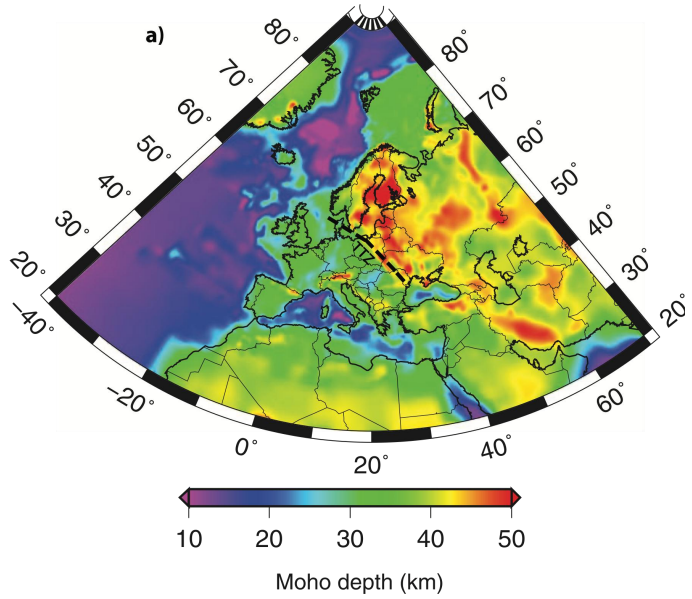


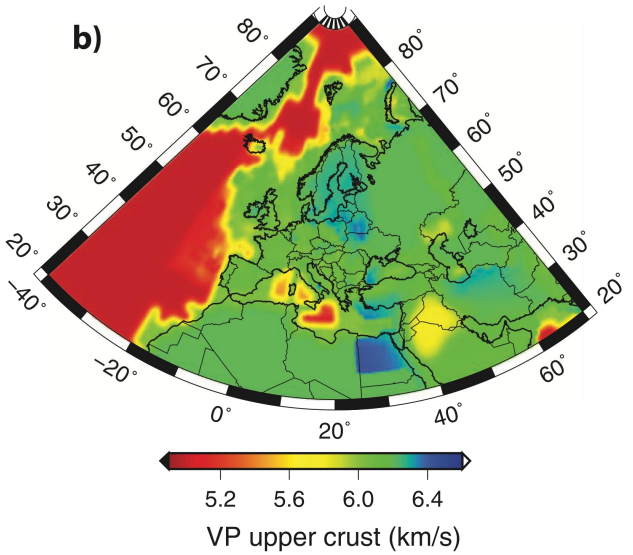
(Chen et al, NC, 2023)

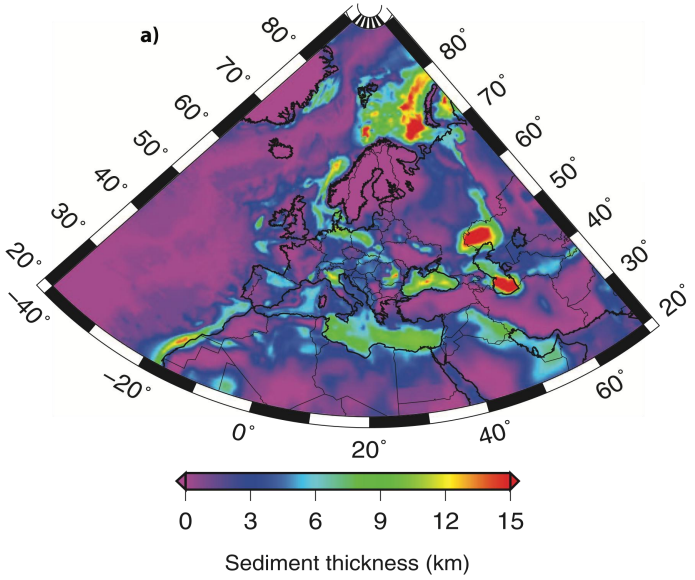


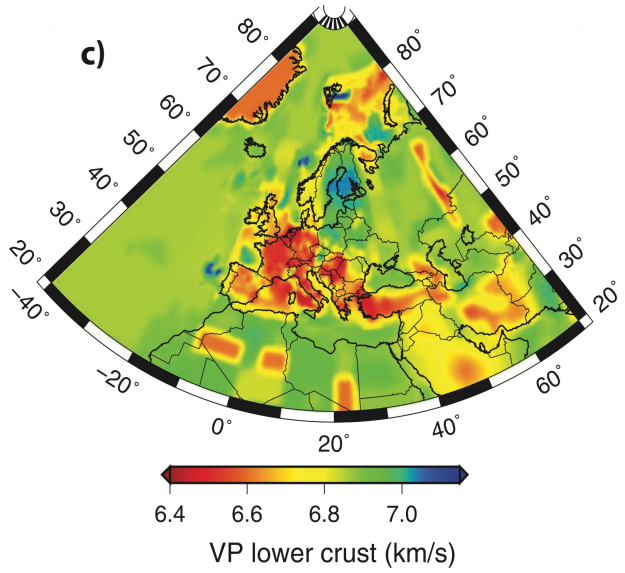
SUSTech Southern University of Science and Technology

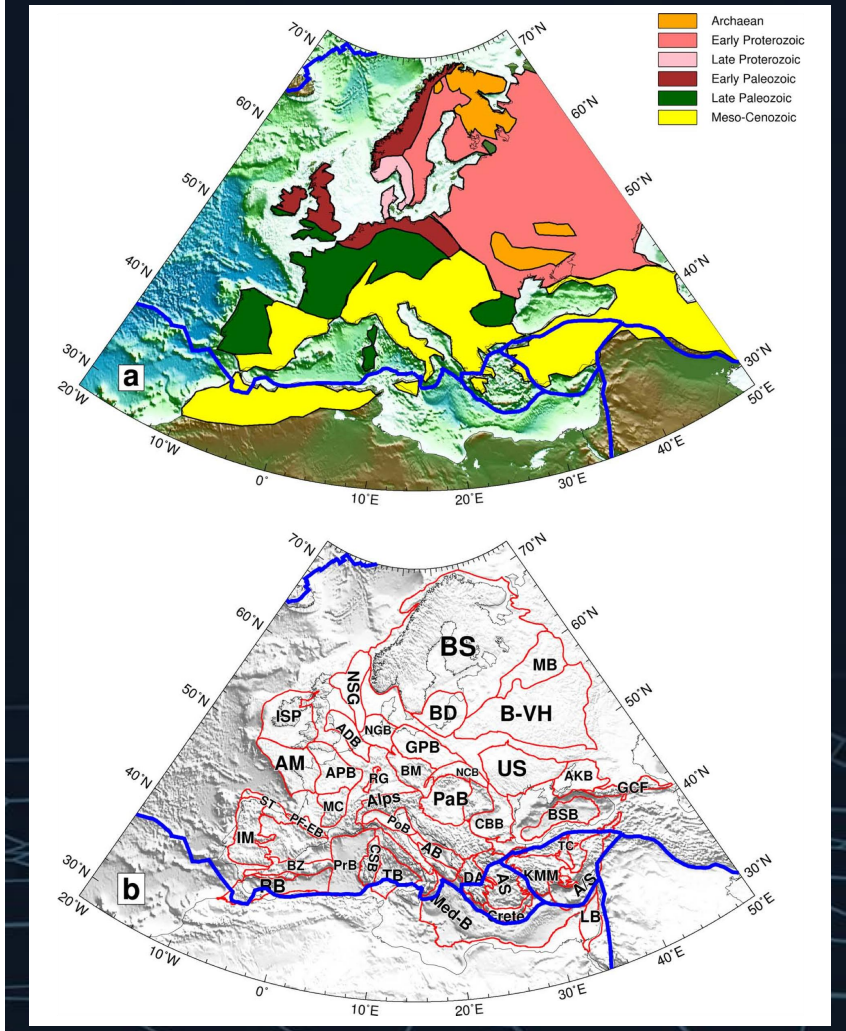
Crustal model for Europe



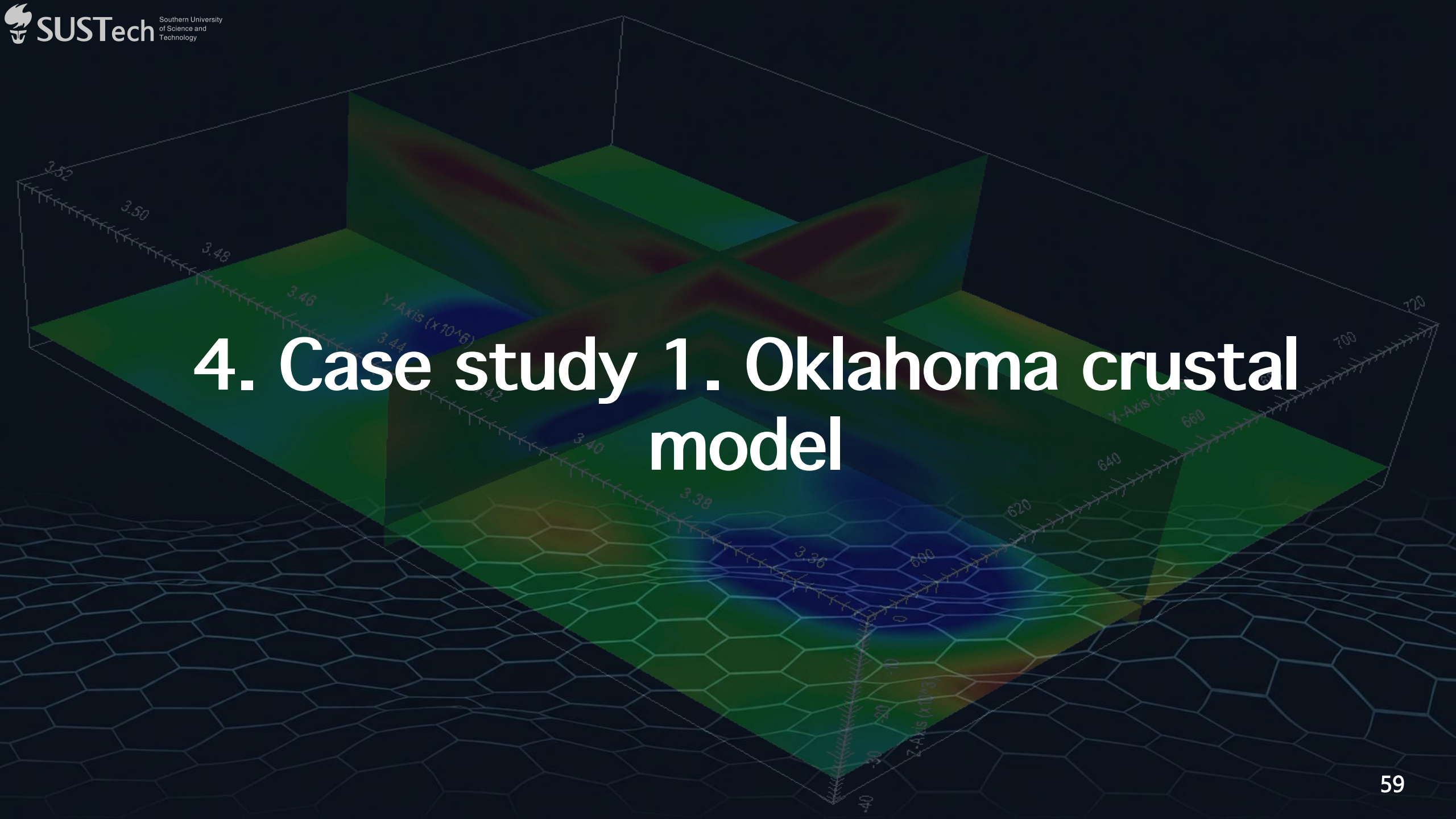








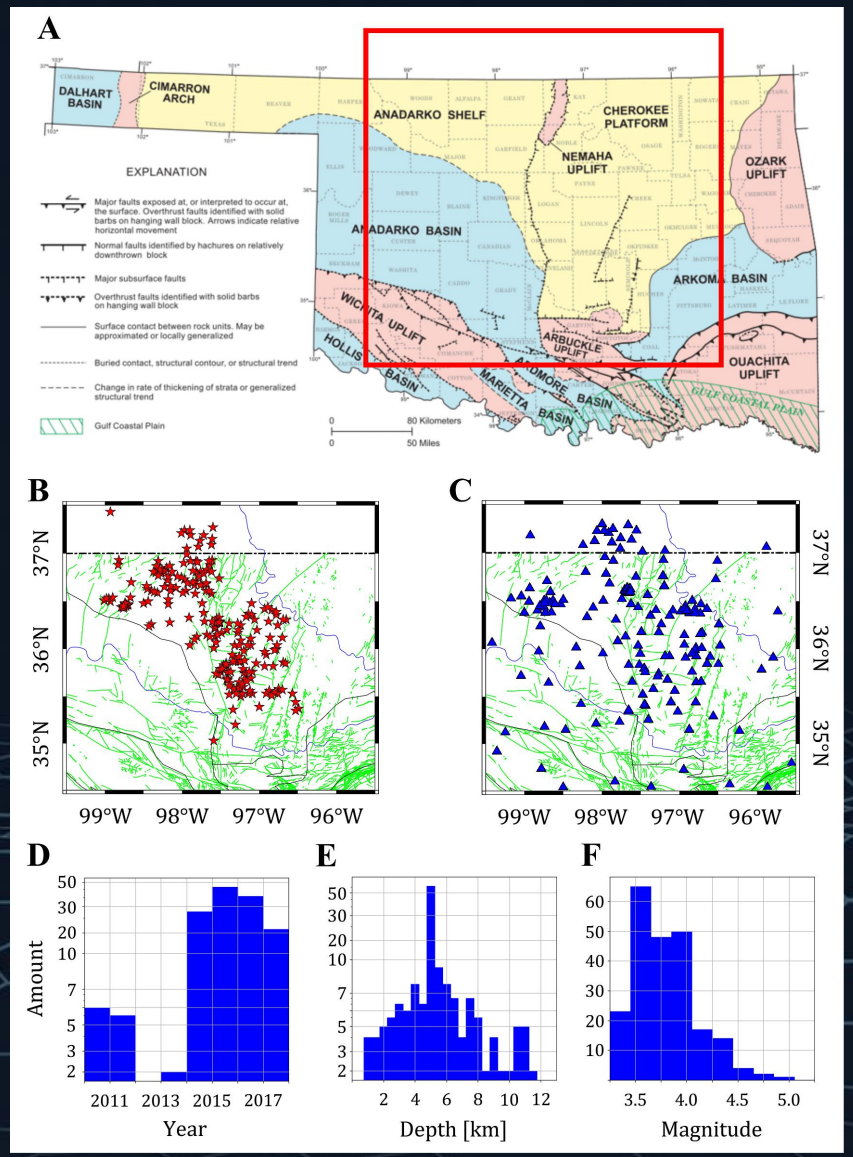
(Molinari and Morelli, GJI, 2011

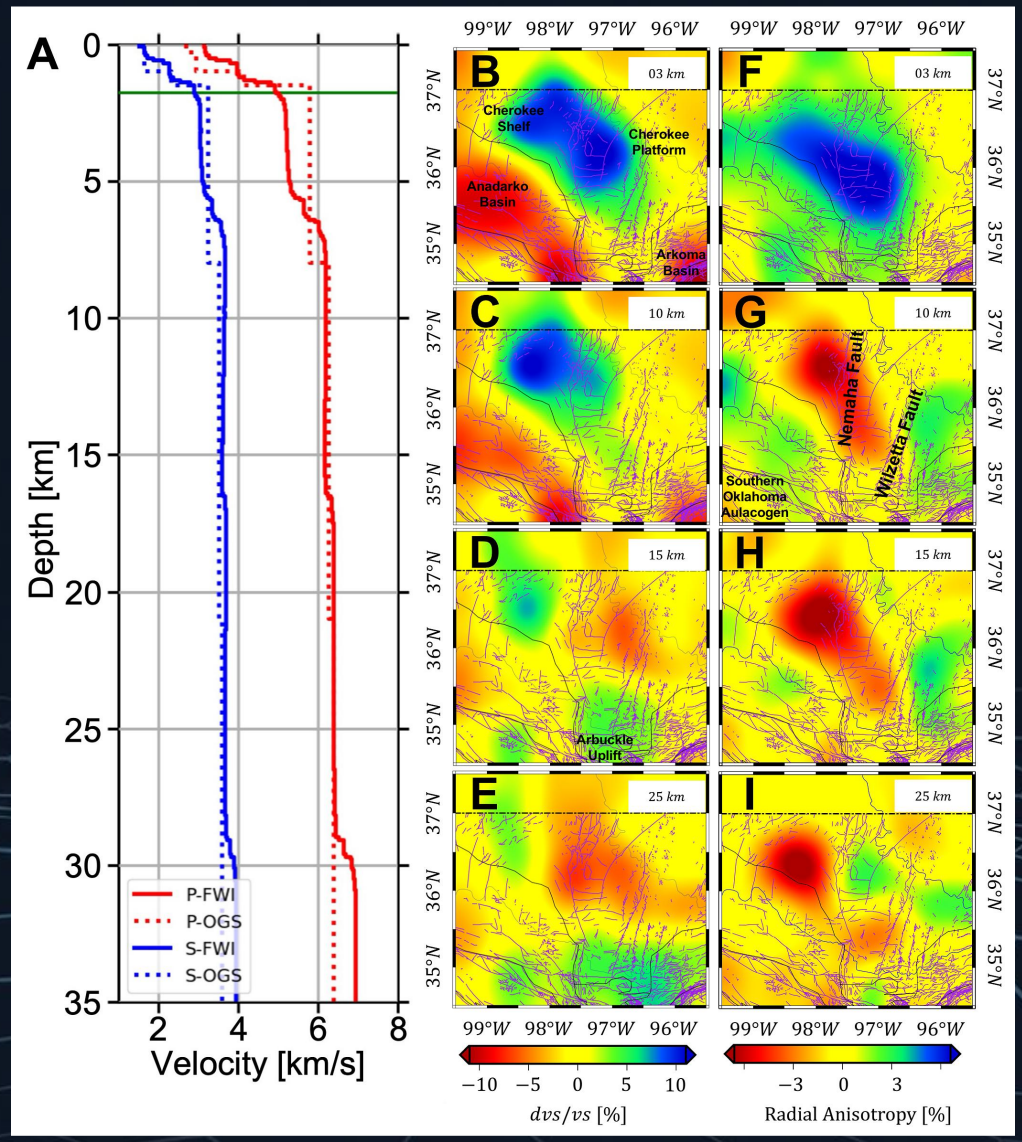


4. Case study 1. Oklahoma crustal model

SUSTech Southern University of Science and Technology

Oklahoma Data and Inversion Results





157 earthquakes and 176 seismic stations

(Zhang et al., JGR, 2023)

SUSTech Southern University of Science and Technology

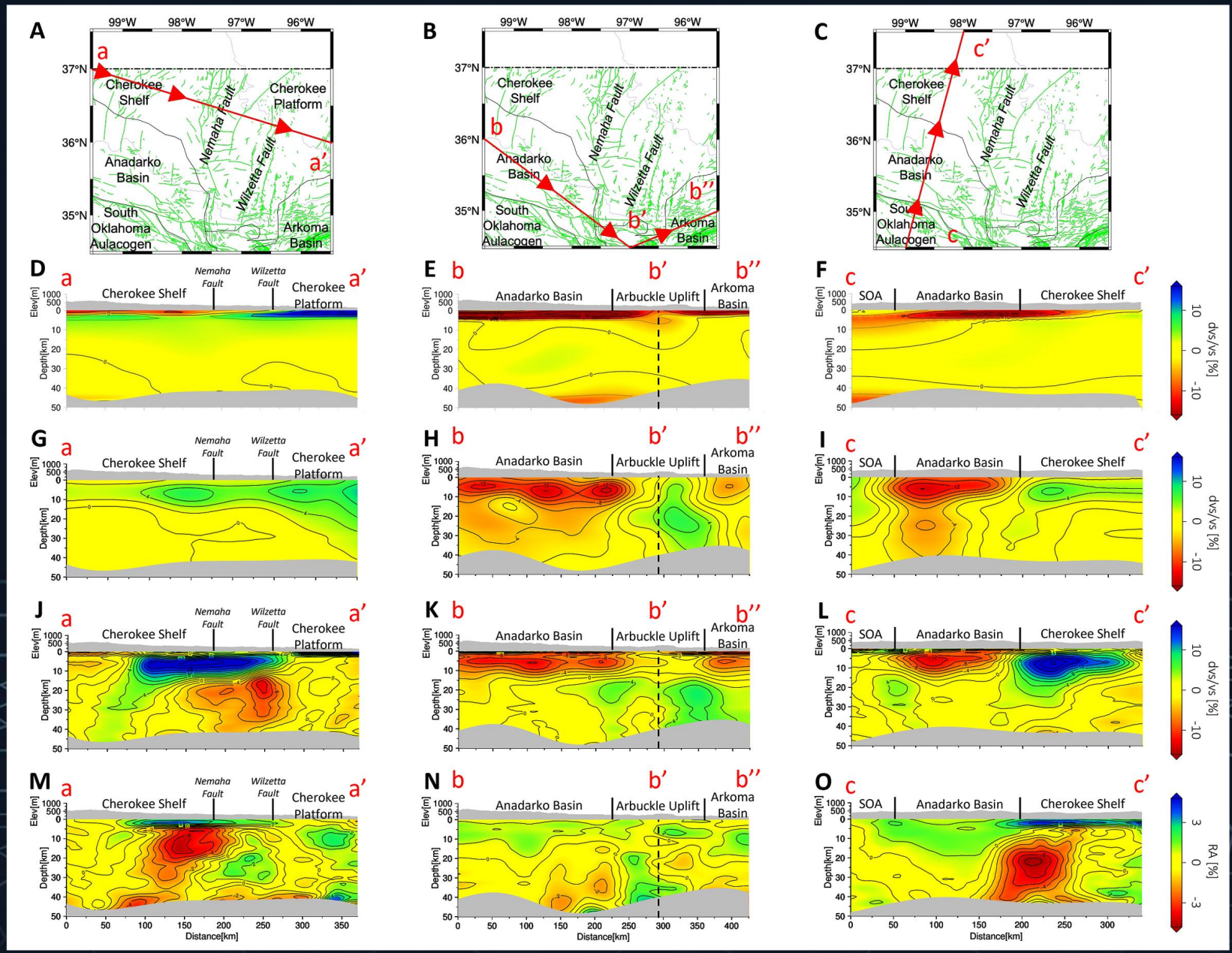
Comparison of Velocity Models

US2016
(Shen and Ritzwoller, JGR, 2016)

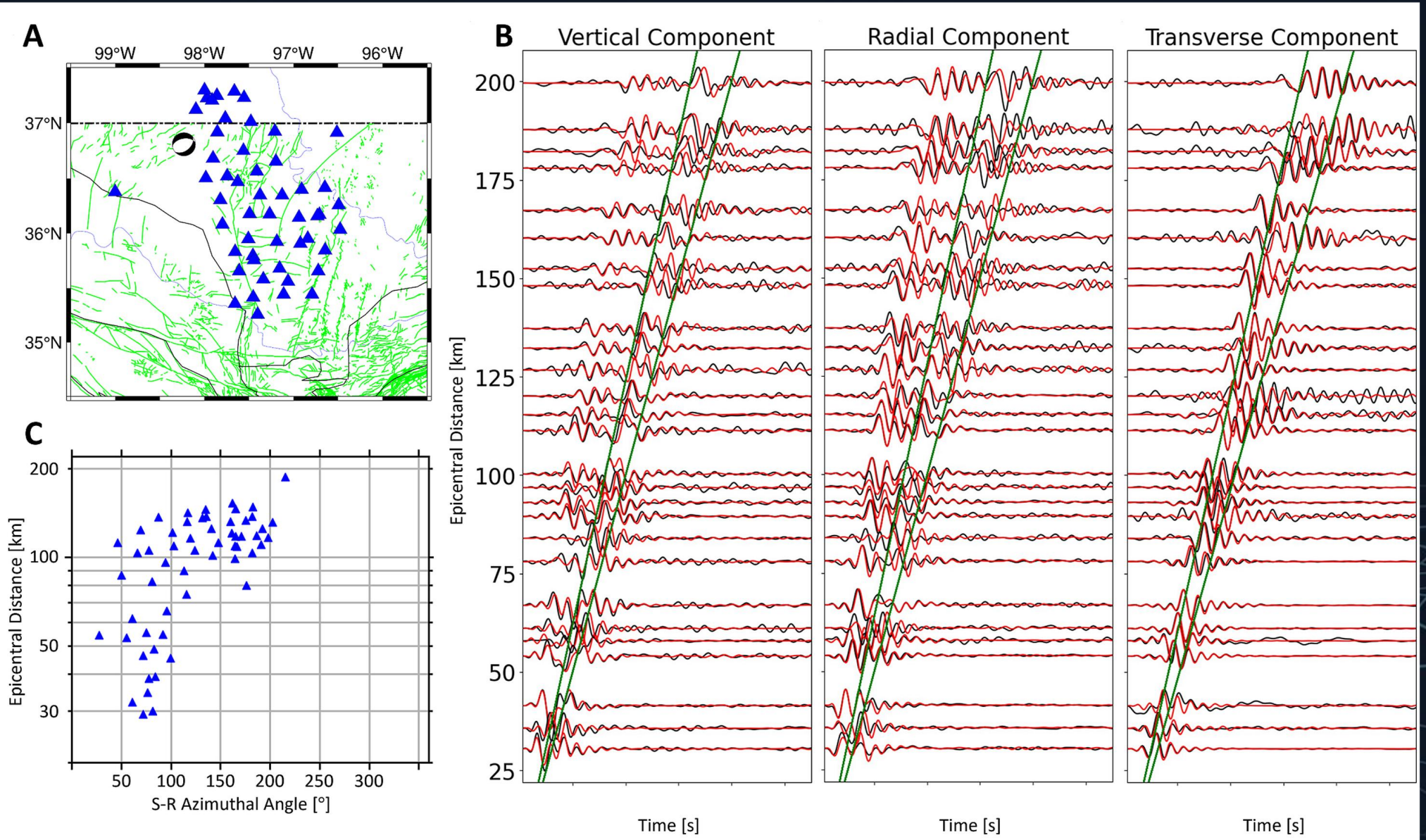
Starting model
(Zhu, GJI, 2018)
Ambient-noise FWI

New model
(Zhang et al., JGR, 2023)

Radial anisotropy



Comparison of Three-Component Seismograms



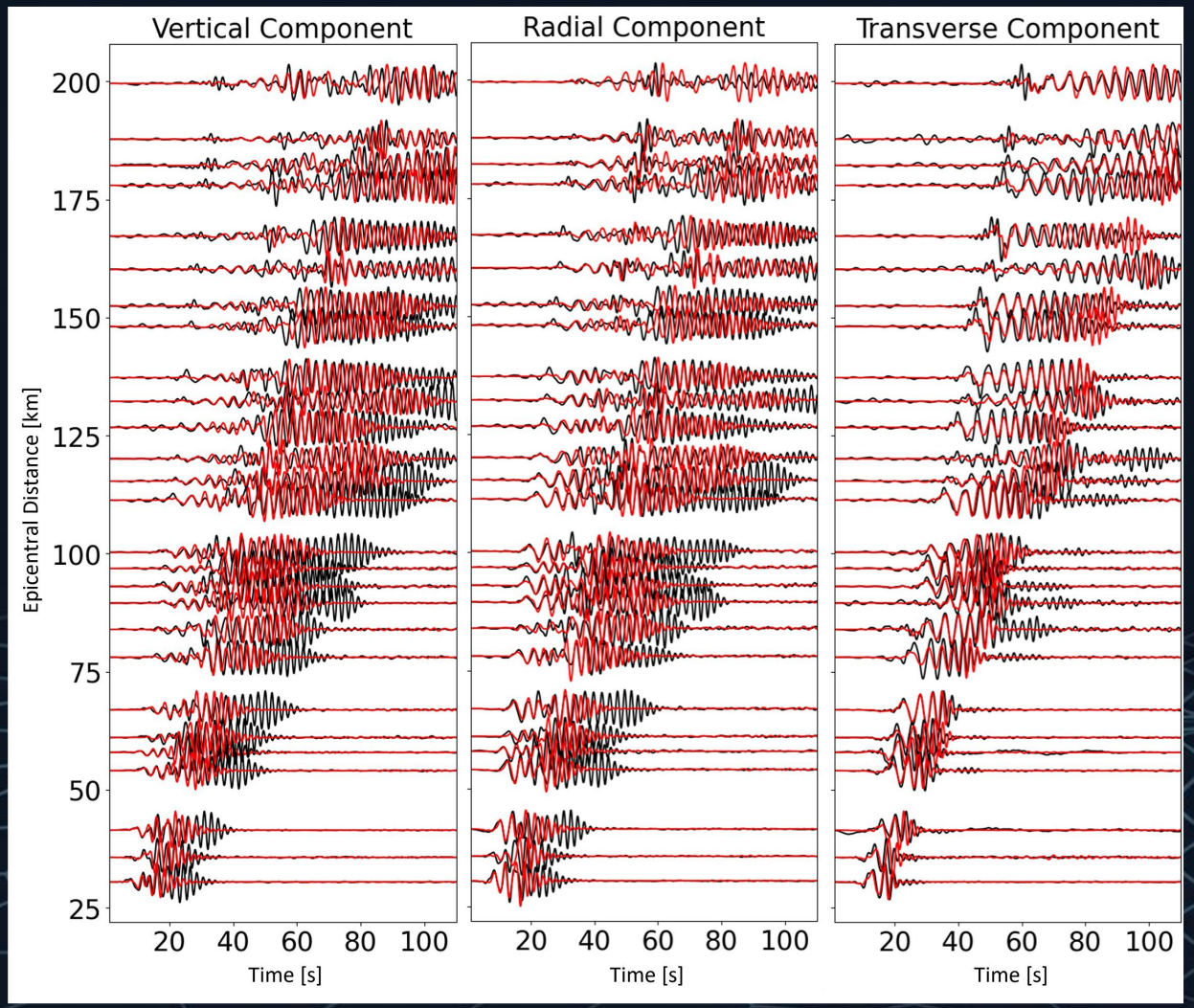
5–30 s bandpass

Red: synthetic

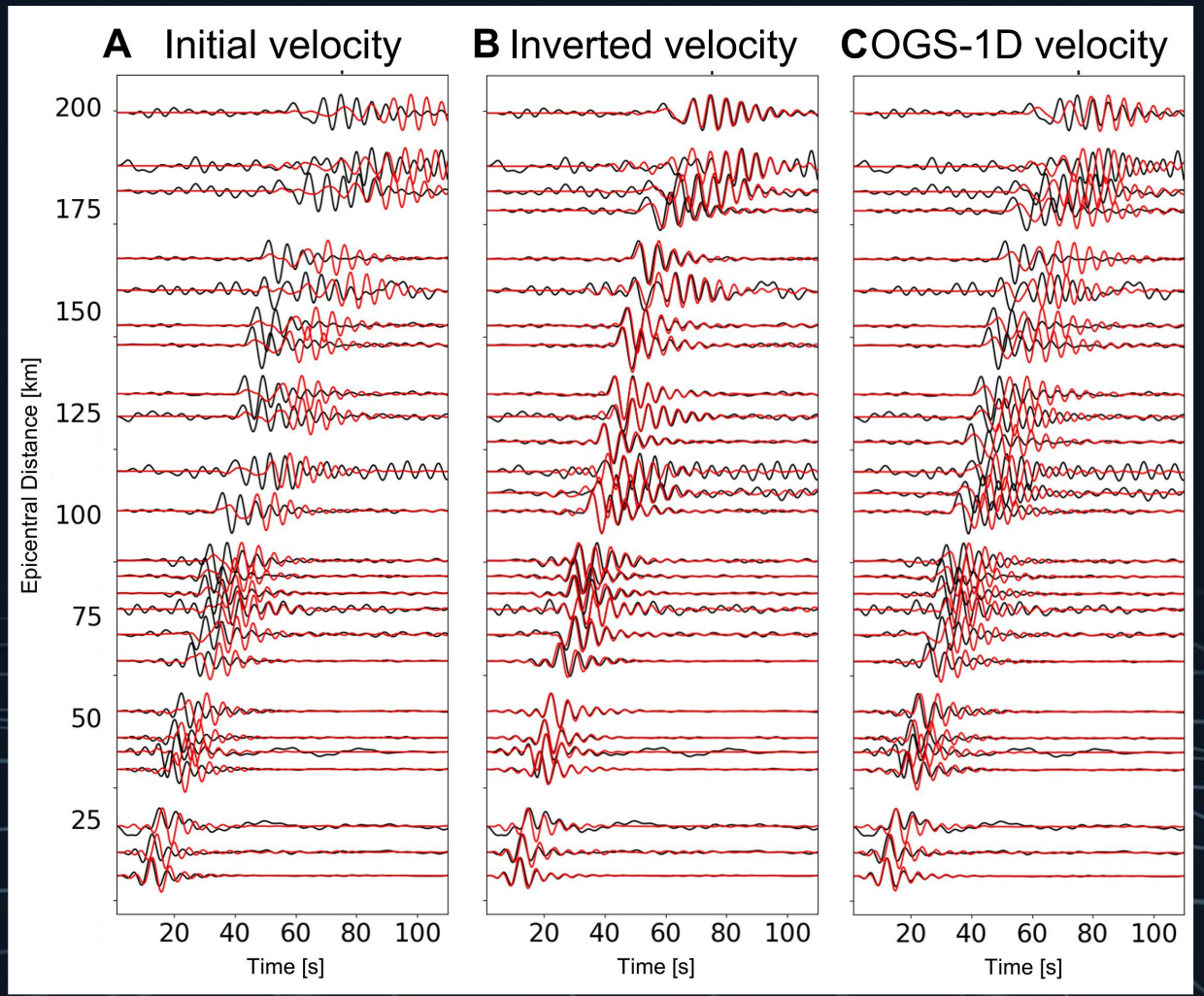
Black: observed

SUSTech Southern University of Science and Technology

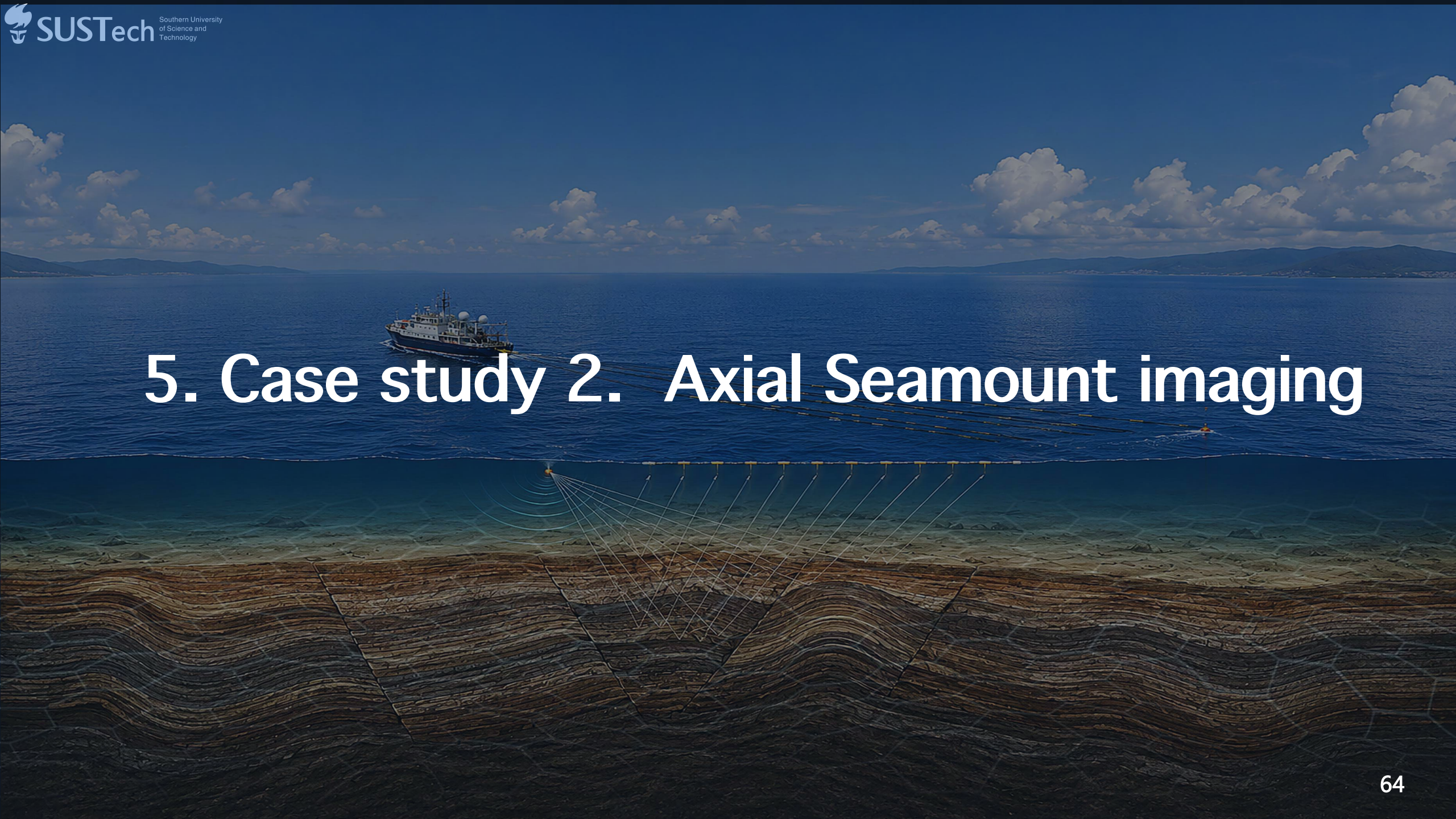
Seismogram Comparison



Higher-frequency band (2–30 s)



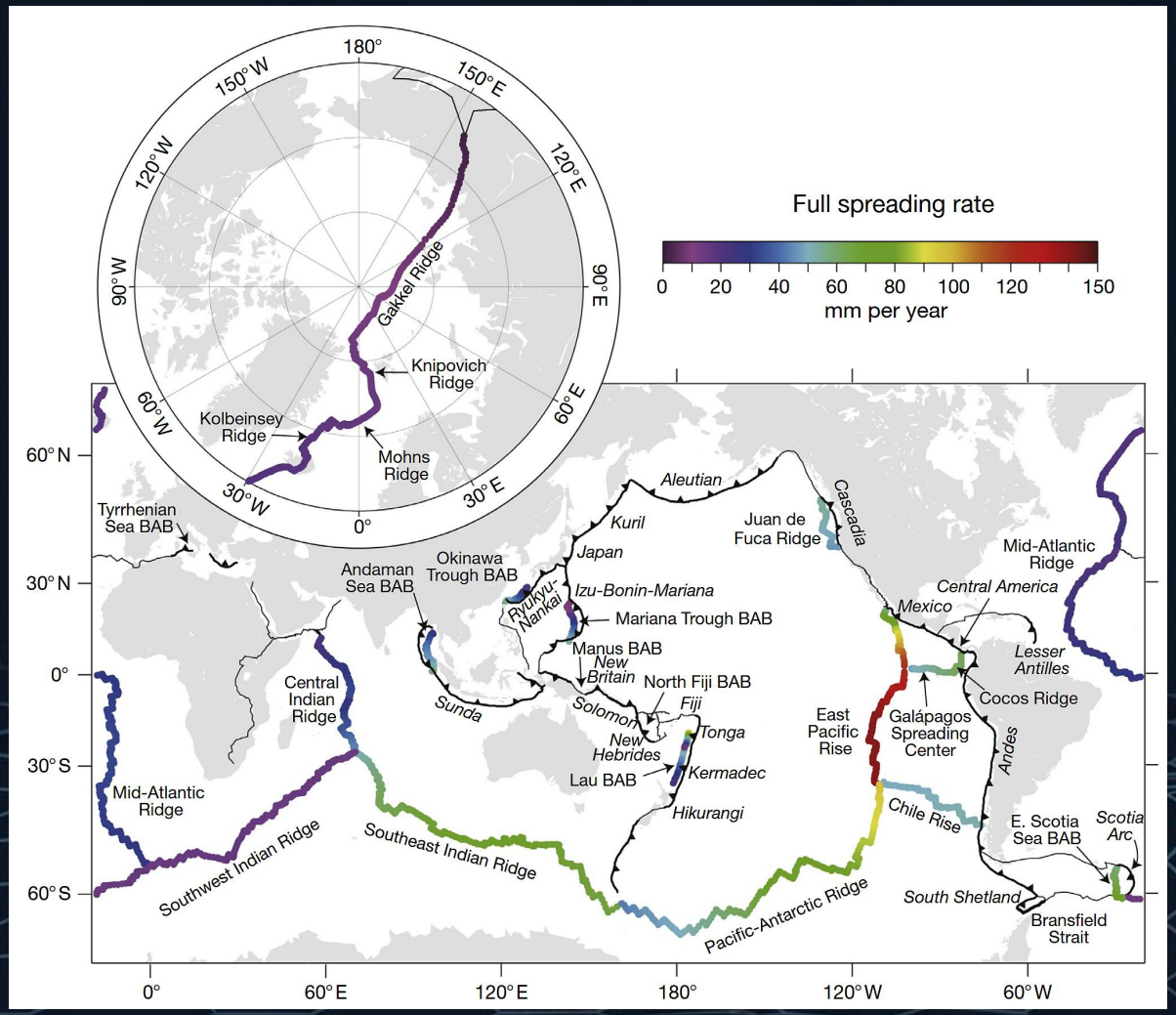
Different models



5. Case study 2. Axial Seamount imaging

SUSTech Southern University of Science and Technology

Why Study Mid-Ocean Ridges



Global distribution of mid-ocean-ridge spreading rates

R. Dunn, Treatise on Geophysics, 2015

- Mechanisms of oceanic crust formation
- Magma system evolution and hydrothermal circulation
- Mantle melting processes
- Seafloor spreading
- Global material cycling

➢ **Fast-spreading (>90 mm/year)**

East Pacific Rise

➢ **Intermediate-spreading (55-85 mm/year)**

Juan de Fuca Ridge

Southeast Indian Ridge

➢ **Slow-spreading (20-50 mm/year)**

Mid-Atlantic Ridge

➢ **Ultraslow-spreading (<20 mm/year)**

Southwest Indian Ridge

Gakkel Ridge

SUSTech Southern University of Science and Technology

Magma Plumbing at Mid-Ocean Ridges

- **Where does magma come from?**

How mantle melts focus and form efficient transport pathways

- **How is magma transported upward?**

Continuous melt channels, dikes or sills, or diapirs

- **Where is magma stored?**

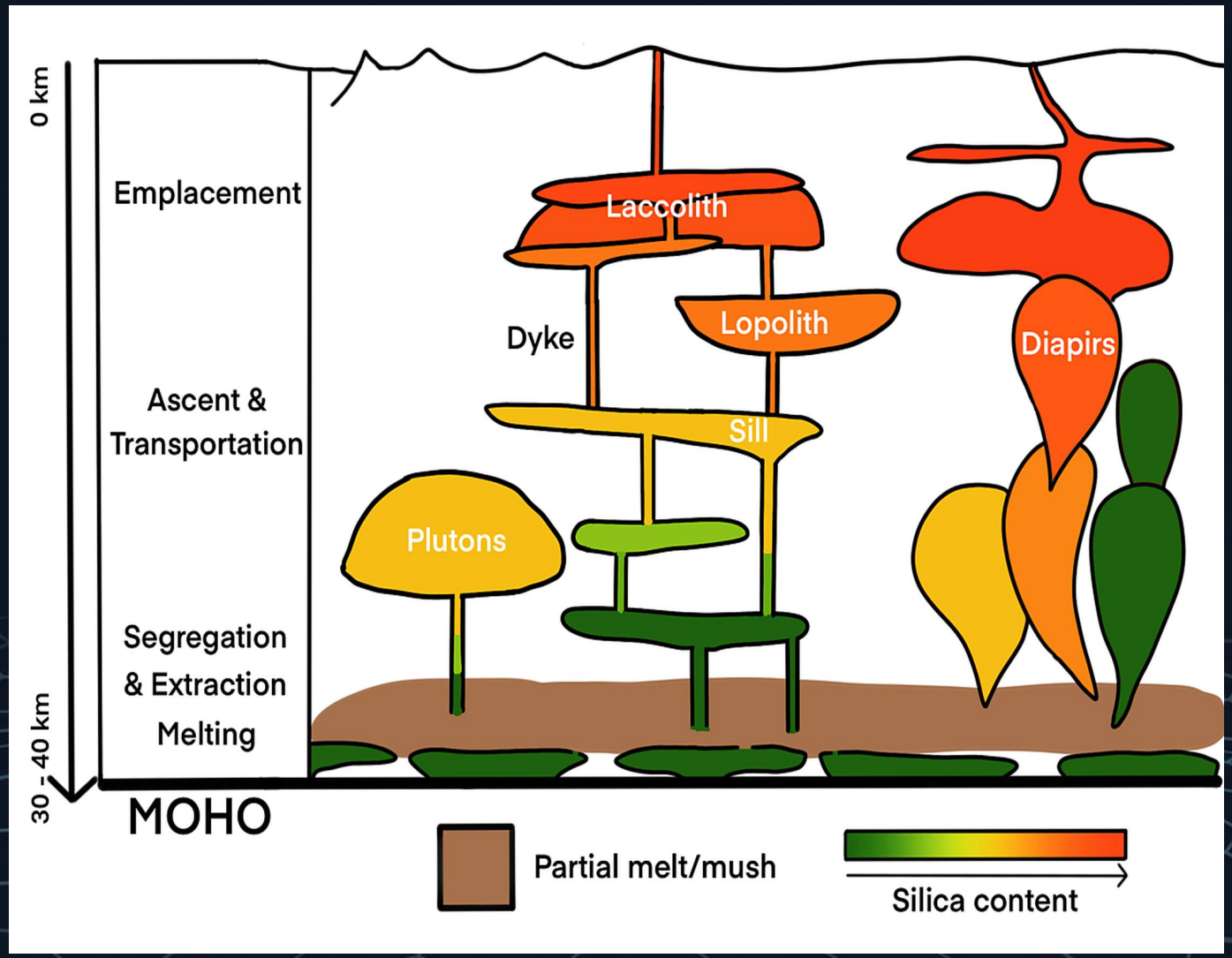
Magma chamber or crystal mush

Mush fraction and connectivity

- **How does magma form new oceanic crust?**

Lower-crust formation mechanism

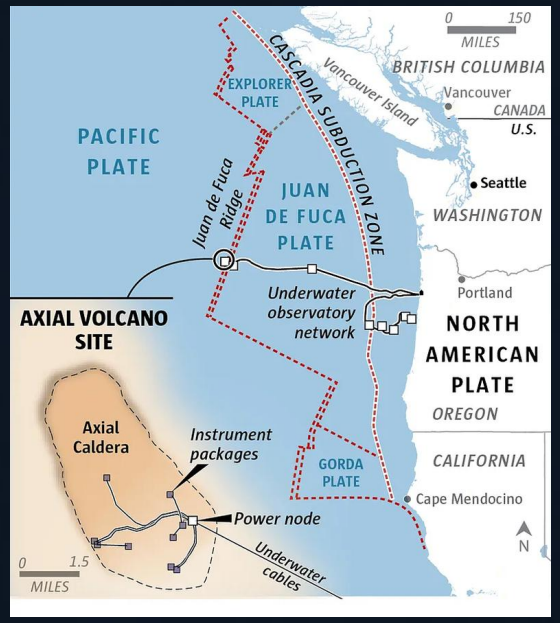
gabbro glacier v.s. sheet sill

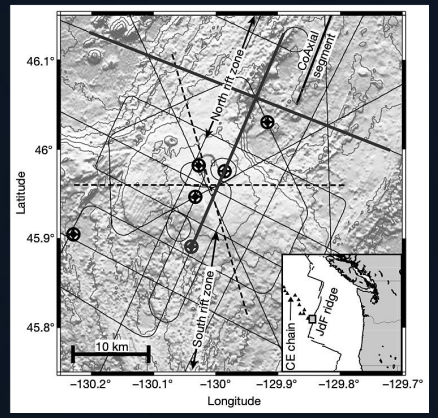


Volcanic magma plumbing
(Burchardt, Volcanic and Igneous Plumbing Systems, 2018)

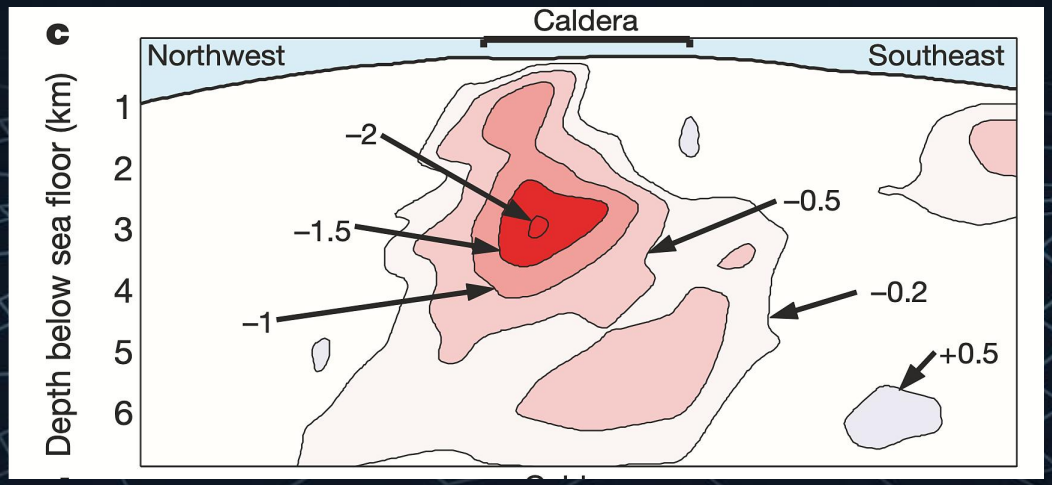
SUSTech Southern University of Science and Technology

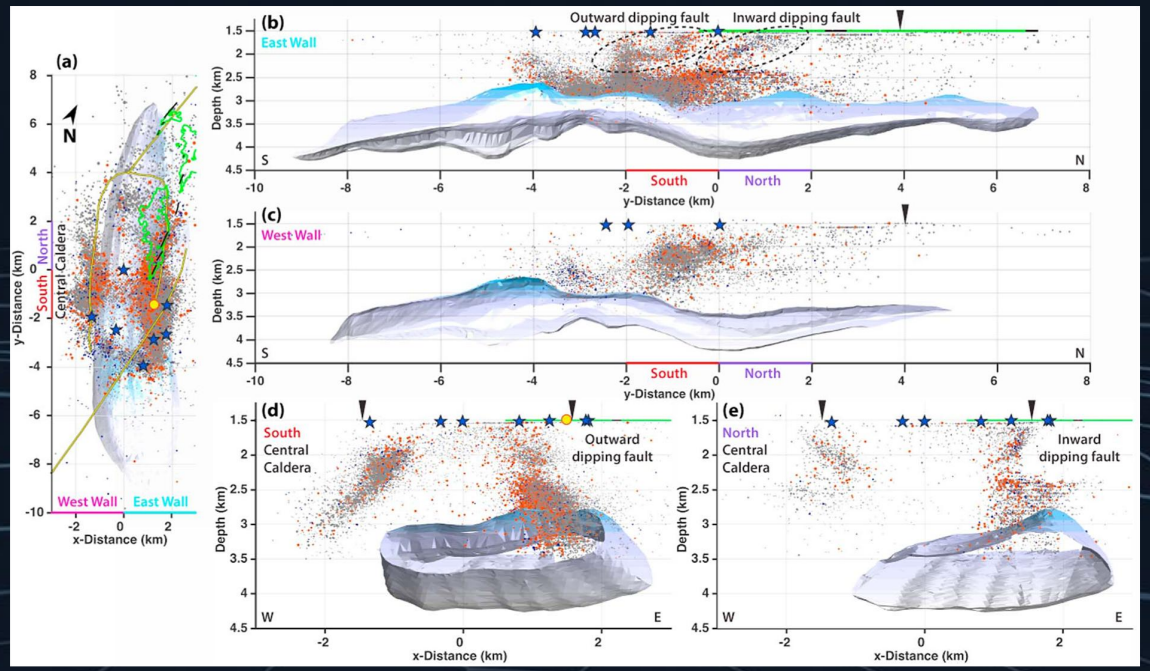
Axial Seamount





- Axial Seamount is an active submarine volcano located at the intersection between the Juan de Fuca ridge and Cobb hotspot
- One of the best monitored submarine volcanoes worldwide
- A key window into mid-ocean ridge accretion processes
- Active source traveltime tomography has revealed the approximate structure of its main magma reservoir structure

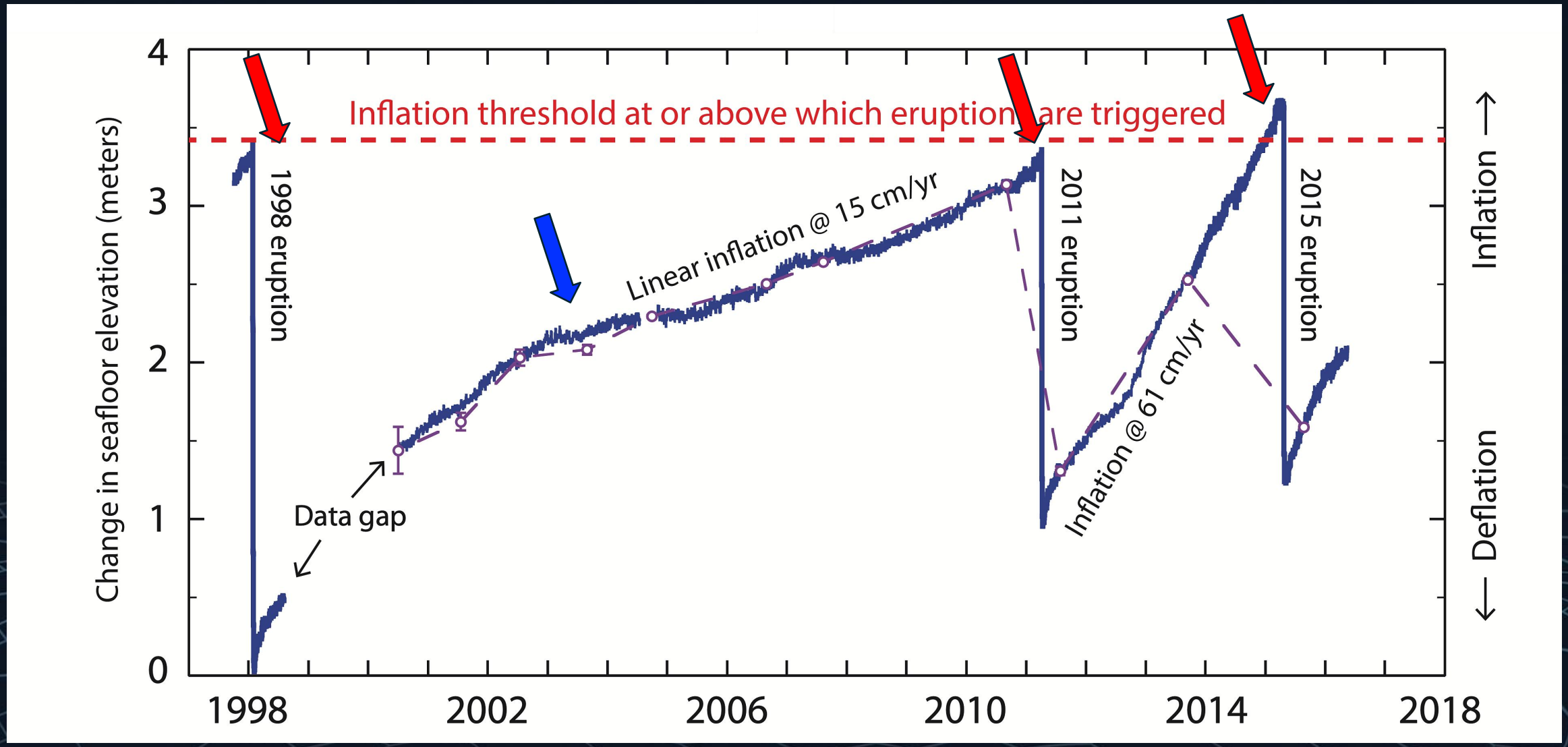




OBS Traveltime tomography (West et al, Nature, 2001)

MCS result (Arnulf et al, JGR, 2018)

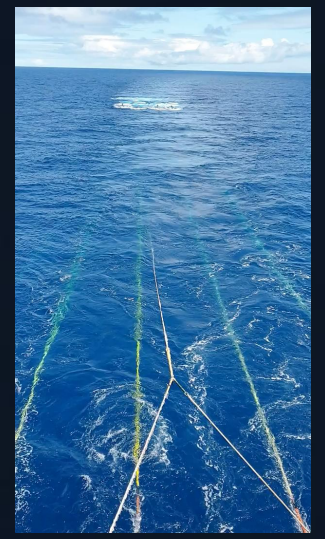
Axial Seamount: Inflation and Eruptions



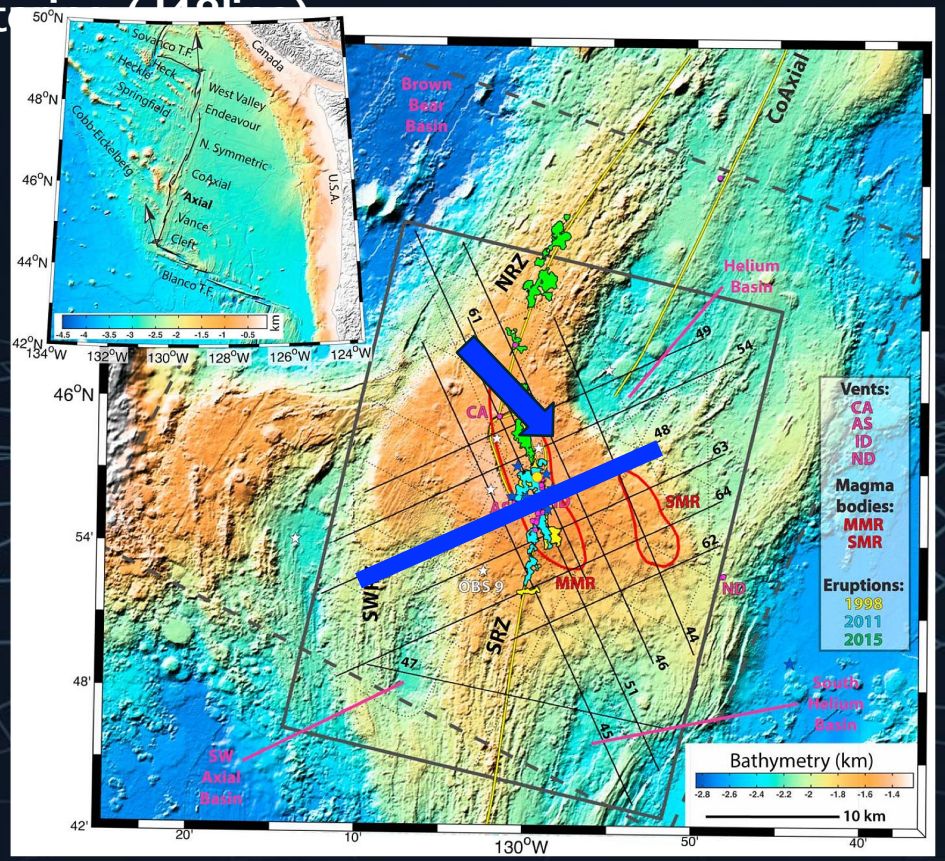
Frequent eruptions with clear recurrence cycles recorded by seafloor pressure gauges
Nooner and Chadwick, Science, 2016

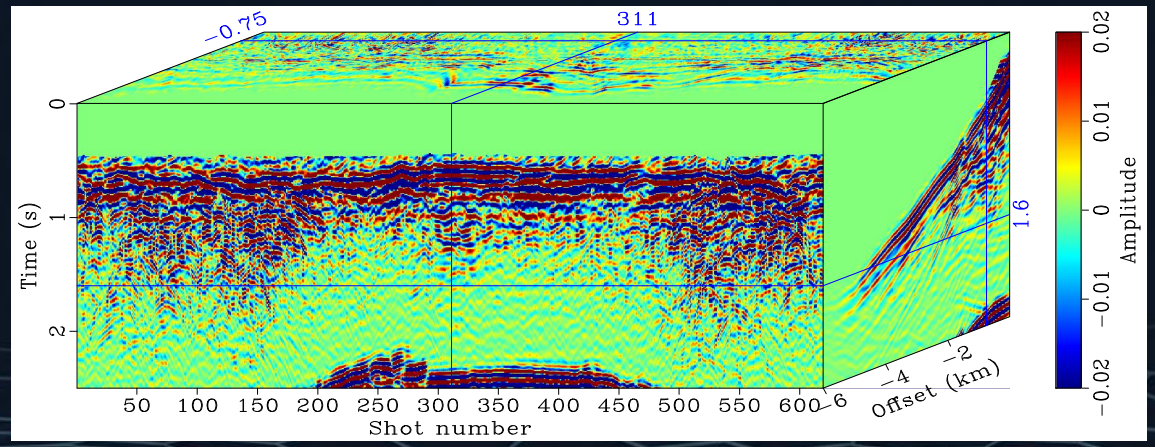
SUSTech Southern University of Science and Technology

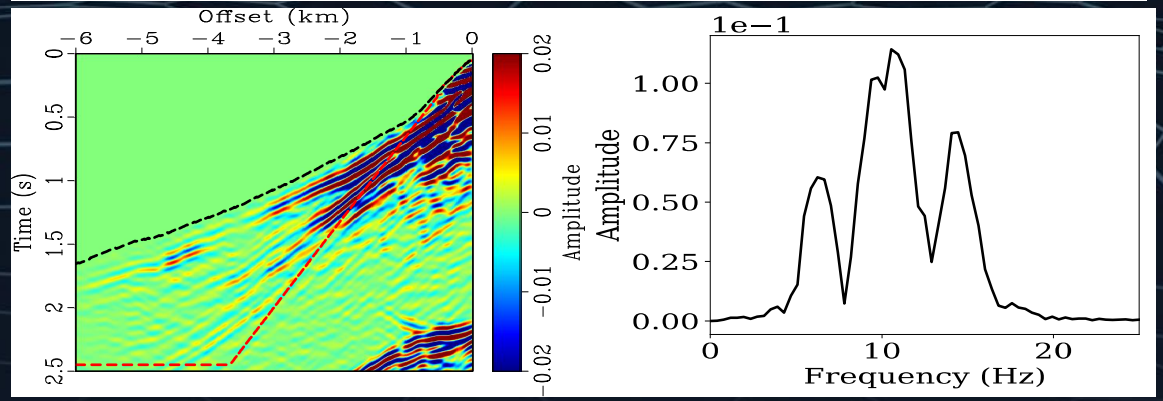
Active Source Data from Axial Seamount



- Multichannel seismic data were acquired in 2002 (EW0207 cruise)
- Air gun sources were towed at 7.5 m depth with 37.5 m shot spacing
- The receiver system used 480 hydrophone channels with 12.5 m spacing, streamer length 6 km
- Processing included denoising, amplitude correction, true-amplitude relocation, and band-pass filt[illegible]







A Time Domain Viscoacoustic Wave Equation

$$\begin{cases} -c_1 \dfrac{\partial^2 p}{\partial t^2} + i c_2 \dfrac{\partial p}{\partial t} - c_3 p + c_4 q + \nabla^2 p = f \\ q = \sqrt{-\nabla^2}\, \dfrac{\partial p}{\partial t} \end{cases}$$

$$\begin{cases} c_1 = \dfrac{1}{v_0^2}\left(1 - \dfrac{2a}{\pi Q}\right); \quad c_2 = \dfrac{2b}{\pi Q v_0^2} \\ c_3 = \dfrac{2c}{\pi Q v_0^2}; \quad c_4 = \dfrac{1}{Q v_0} \end{cases}$$

- The time domain equation can be solved using finite differences
- Quality factor Q appears explicitly in the equation
- Allows flexible combinations of amplitude attenuation and dispersion
- Complex partial differential equation
- Pseudo-differential operator

$$K_v(\mathbf{x}) = \mathrm{Re}\int_0^T \left\{ -\frac{1}{\rho_0(\mathbf{x}) v_0^2(\mathbf{x})}\left(C_1^0(\mathbf{x})\frac{\partial^2}{\partial t^2} - iC_2^0(\mathbf{x})\frac{\partial}{\partial t} + C_3^0(\mathbf{x})\right) p(\mathbf{x},t) p^\dagger(\mathbf{x},T-t) + C_4^0(\mathbf{x})\sqrt{-\nabla^2}\frac{\partial p(\mathbf{x},t)}{\partial t} p^\dagger(\mathbf{x},T-t)\right\} dt$$

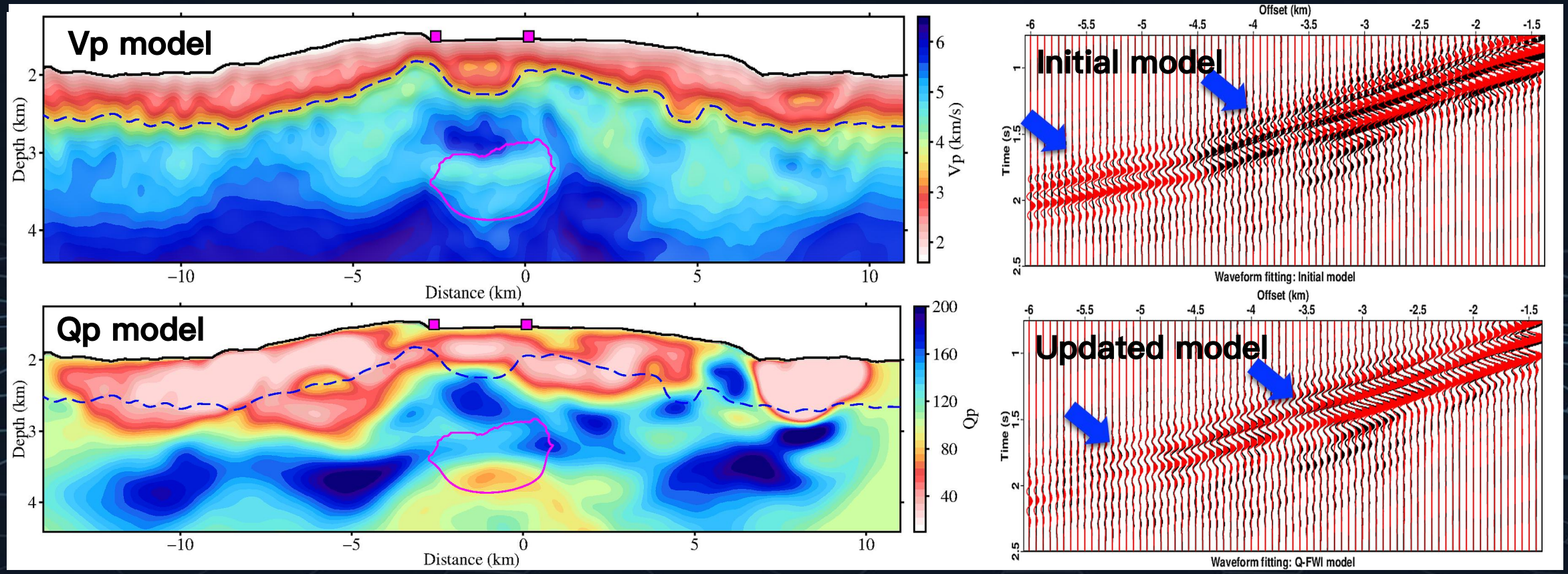
$$K_Q(\mathbf{x}) = \mathrm{Re}\int_0^T \left\{ \frac{1}{\rho_0(\mathbf{x}) v_0^2(\mathbf{x})}\left(\frac{2a}{\pi Q_0(\mathbf{x})}\frac{\partial^2}{\partial t^2} + iC_2^0(\mathbf{x})\frac{\partial}{\partial t} - C_3^0(\mathbf{x})\right) p(\mathbf{x},t) p^\dagger(\mathbf{x},T-t) + C_4^0(\mathbf{x})\sqrt{-\nabla^2}\frac{\partial p(\mathbf{x},t)}{\partial t} p^\dagger(\mathbf{x},T-t)\right\} dt.$$

(Yang et al, GJI, 2018; Yang et al, JGR, 2020)

Velocity and Attenuation Inversion Results

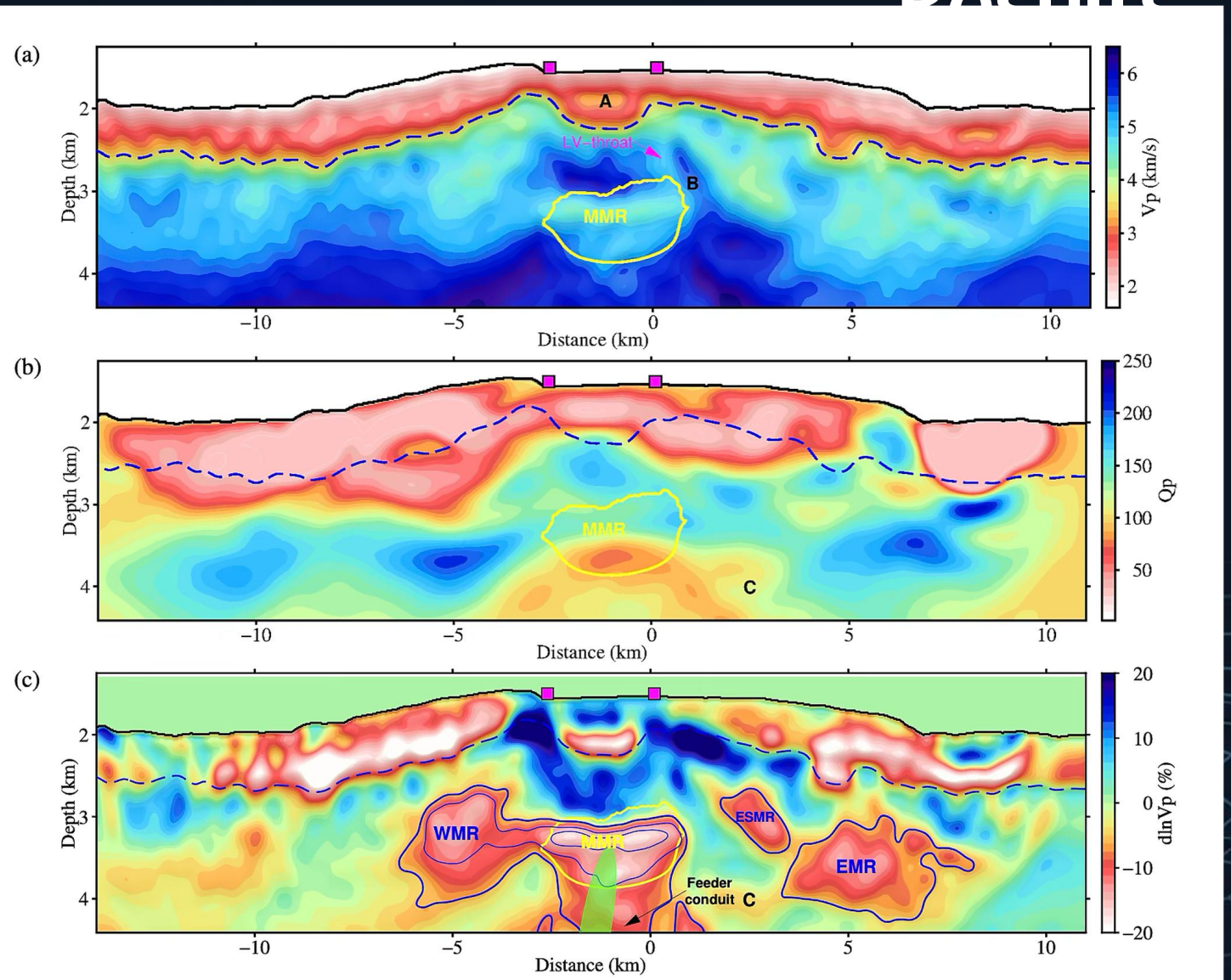
- FWI can produce high resolution P wave velocity and quality factor models
- It achieves good data fitting, especially at far offsets
- Multiscale inversion, frequency band 3-9 Hz

Black: data; red: synthetic



SUSTech Southern University of Science and Technology

Interpretation of Velocity and Attenuation Results

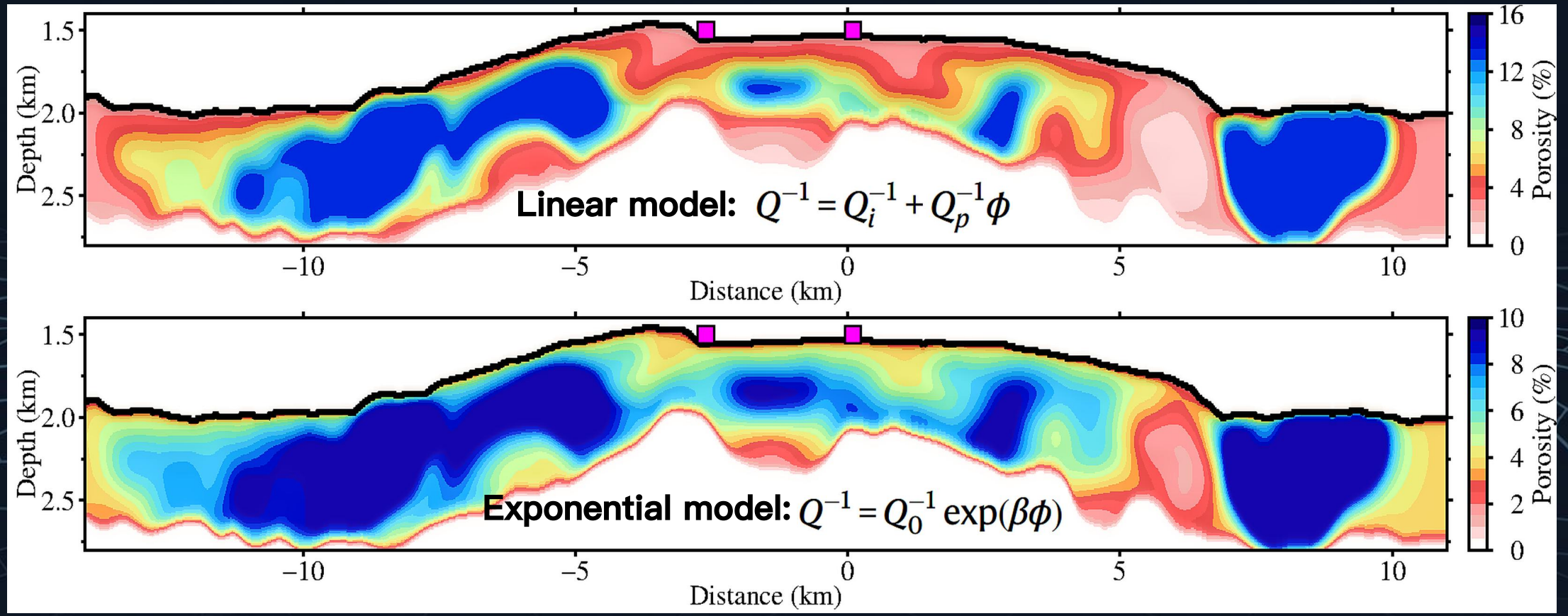


- Shallow high velocity cap or valve
- Upper main magma reservoir: −18% Vp reduction, higher melt fraction
- Lower MMR Vp decreases by about −12%, melt fraction decreases with depth
- At previously identified secondary reservoirs, two separate low velocity anomalies are resolved: SSMR and SMR
- A previously unidentified low velocity zone, with Vp reduced by about −12%, connects to the main magma reservoir and represents a third magma region with relatively high melt fraction

SUSTech Southern University of Science and Technology

Layer2A Porosity

- Layer2A high attenuation
- Based on the empirical relation between Qp and basalt porosity, the maximum porosity is estimated at about 10—16%
- This result is consistent with the measured porosity range(4—12%) of the Oman ophiolite



From Velocity to Temperature Structure

- **Temperature calculation:**

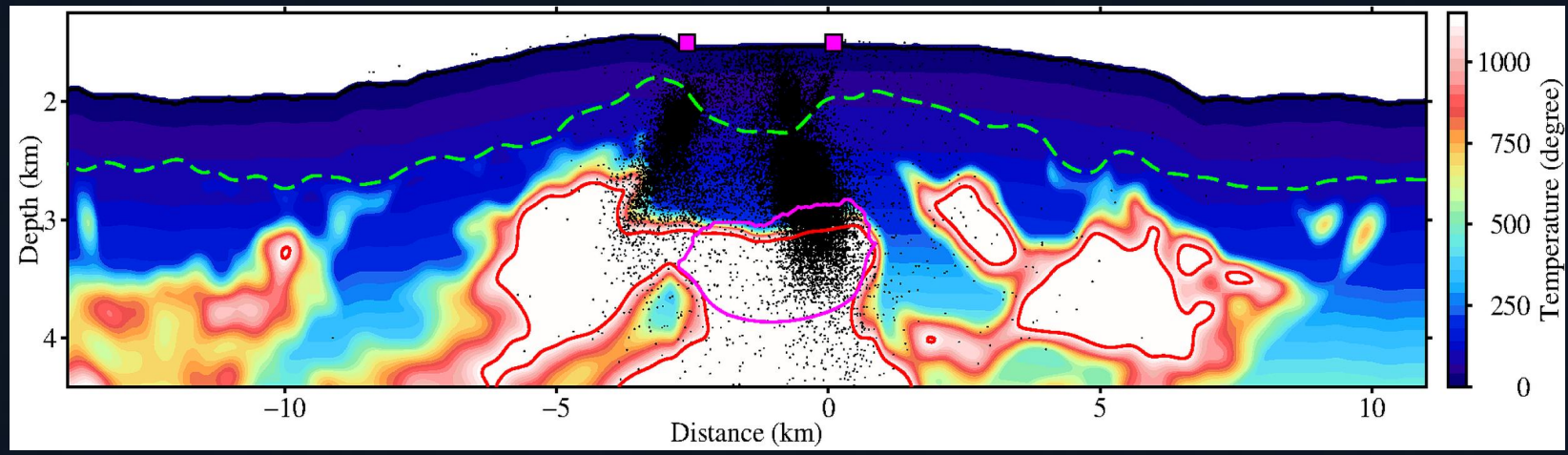
$$T(\mathbf{x}) = T_0(\mathbf{x}) + \delta \ln V_p(\mathbf{x}) / \frac{\partial \ln V_p(\mathbf{x})}{\partial T}$$

$$\frac{\partial \ln V_p(\mathbf{x})}{\partial T} = \frac{\partial \ln V_p}{\partial T}\bigg|_{anhar} - \frac{F(\kappa)}{\pi Q_p(\mathbf{x})} \frac{H^*}{RT^2(\mathbf{x})}$$

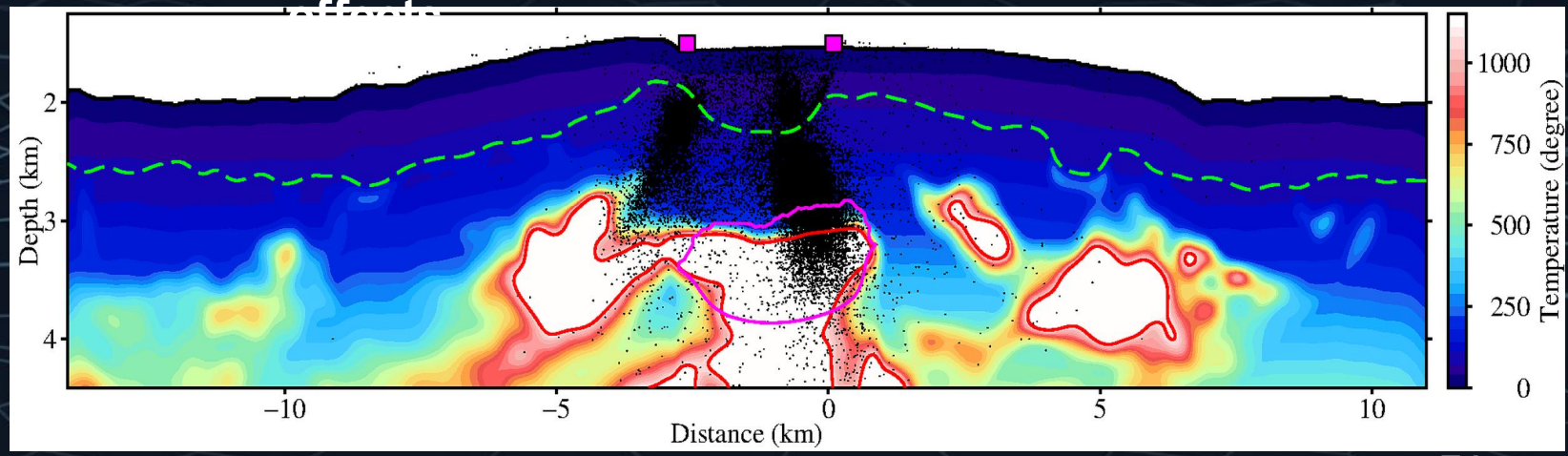
T_0: Reference off-axis temperature
Qp : FWI Qp model
R : the universal gas constant
H*: the activation enthalpy
κ: the power law exponent

- **Strong attenuation makes anelastic effects important in constraining temperature; the area enclosed by the 1150 degrees isotherm is narrower than the model that only considers anharmonic effects**

Considering only anharmonic effects



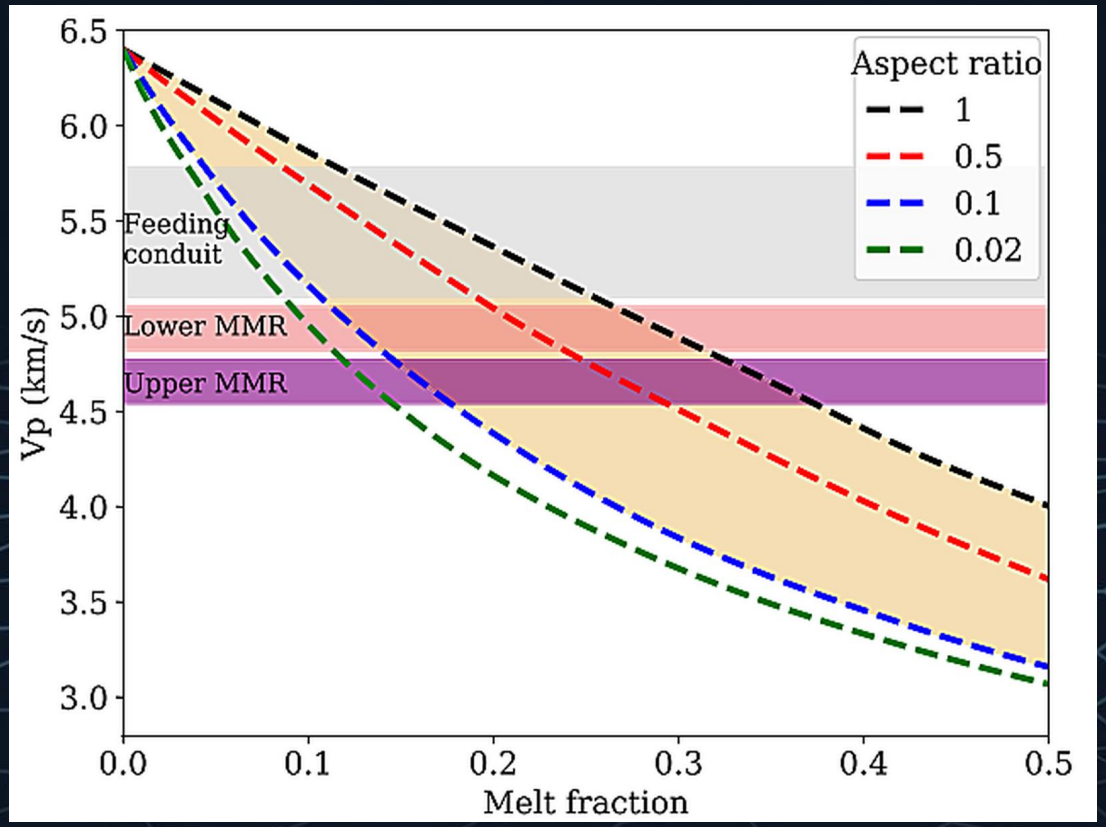
Considering both anharmonic and anelastic effects



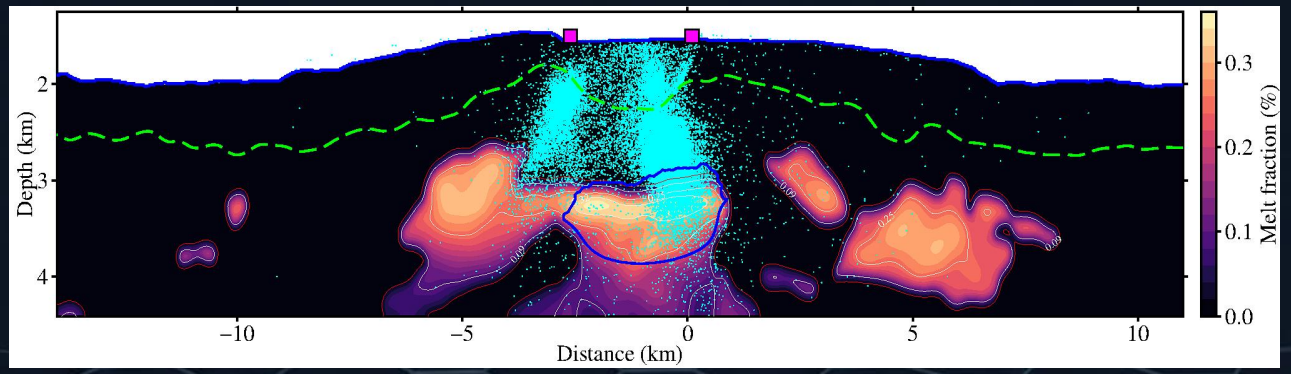
SUSTech Southern University of Science and Technology

Estimated Partial Melt Distribution

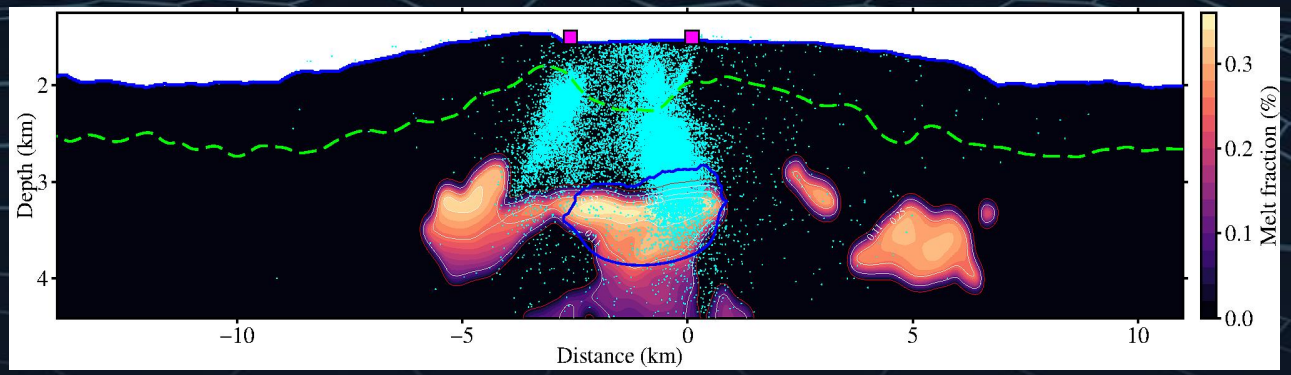
- For regions with temperatures above 1150 degrees, partial melt is calculated using a two–phase effective–medium model of solid rock and molten basalt
- As with the temperature results, including anelastic effects yields a much narrower partial–melt zone than considering anharmonic effects alone



Considering only anharmonic effects



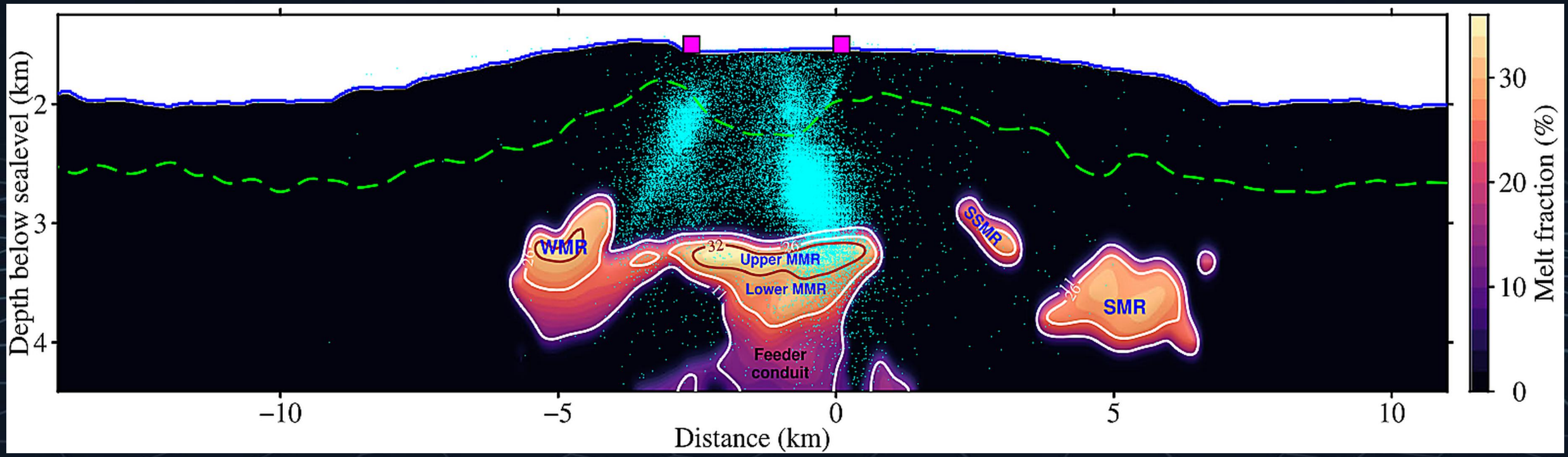
Considering both anharmonic and anelastic effects



SUSTech Southern University of Science and Technology

Interpretation of Partial Melt Results

- The upper main magma reservoir has the highest melt fraction, about 15%—37%, and is likely the magma source for the three most recent eruptions (1998,, 2011 and 2015)
- In the SMR, WMR, and lower MMR, the estimated melt fractions are lower, about 10%—26%
- The total magma volume in the upper and middle crust is estimated to be 12.38—29.60 km3, consistent with travel time tomography estimates based on OBS and MCS data



SUSTech Southern University of Science and Technology

地球与空间科学系
DEPARTMENT OF EARTH AND SPACE SCIENCES

Thanks!

SIML
SEISMIC IMAGING AND MONITORING LABORATORY